MODELLING SEISMIC RESPONSE OF UNREINFORCED MASONRY INFILLED REINFORCED CONCRETE MOMENT-RESISTING FRAMES

by

Amit Nagar

CE
1995
M
NAG
MOD

DEPARTMENT OF CIVIL ENGINEERING
INDIAN INSTITUTE OF TECHNOLOGY KANPUR
JANUARY, 1995

MODELLING SEISMIC RESPONSE OF UNREINFORCED MASONRY INFILLED REINFORCED CONCRETE MOMENT-RESISTING FRAMES

A Thesis Submitted

in Partial Fulfillment of the Requirements

for the Degree of

Master of Technology

by

Amit Nagar

to the

DEPARTMENT OF CIVIL ENGINEERING

INDIAN INSTITUTE OF TECHNOLOGY KANPUR

JANUARY, 1995

2 2 APR 1996

CENTRAL LIBRARY
I I T, KANPUR
No. A 121353

CE-1995-M-NAG-MOD

A121353

DEDICATED TO MY PARENTS ...

CERTIFICATE

It is certified that the work contained in the thesis entitled "MODELLING SEISMIC RESPONSE OF UNREINFORCED MASONRY INFILLED REINFORCED CONCRETE MOMENT-RESISTING FRAMES", has been carried out under my supervision and that this work has not been submitted elsewhere for a degree.

Murty CVR

(C.V.R.Murty)

Assistant Professor

Department of Civil Engineering

I.I.T.Kanpur

January, 1995

ACKNOWLEDGEMENTS

I express my sincere gratitude to my advisor, Dr. C V.R Murty for his spirited guidance, and continued support during the course of my Masters' programme. His help, both on academic as well as on the personal front has enabled me to cope with many a problem His continuous encouragement on all fronts is gratefully acknowledged.

I express my gratitude to Dr Sudhir K Jain for his continued guidance and moral support throughout my association with him This has been instrumental in developing my personality He has been most helpful in my times of need I have learnt a lot of things, academic and non-academic, from Dr. Murty and Dr. Jain. The same will be inculcated in my life and career.

I thank my parents for their love and affection, and the hardships that they have undertaken to enable me to study at the best of schools. I thank my sisters for their love and tender care My deepest thanks are due to my wife Anjali, for her warm support, care, and concern for me.

Special thanks are due to my friends, S. S. Kumar and Raj Kumar Singh, who have constantly helped me during the course of my work, as well as on the personal front. Many a late hours that they devoted to me are gratefully acknowledged.

I wish to thank all my friends - Chuphal, Botke, Abhishek, Tyagi, Sujit, Vishnu, Dheeraj, Akhilesh, Seth, Neeraj, Raman, Shekhar, Aparna, Gehad, Manoj, and others, for their distractions which added a spice to life at IITK. I am also grateful for the warm friendship and extensive support of Major Devesh Chaturvedi and Capt. Sanjay Sharma and their families during the course of my Masters' programme. Thanks are also due to Moti Lal and Ashok Tiwari for their continuous help over the years

ABSTRACT

An attempt has been made to model the hysteretic characteristics of unreinforced masonry infilled reinforced concrete moment-resisting frames for the first time. The difficulties encountered in the modelling are discussed and a new model, The Trilinear Hysteresis Model has been proposed for capturing the hysteretic response of infilled frames This model incorporates the stiffness and strength contributions of the masonry infill to the overall response of the frame

The critical parameters influencing the behaviour of masonry infill frames are identified, and a parametric study is conducted to study the affects of the same. The inelastic response spectra, and from those the ductility reduction factor spectra, are obtained for the Uttarkashi earthquake strong motion data and some other strong ground motions widely used in seismic analysis.

Based upon the results of the study, it has been concluded that the presence of the infill significantly reduces the ductility demand on the frame members. The infill-to-bare frame stiffness ratio is observed to be the most influential parameter governing the response of infilled frames. The masonry infill continues to govern the overall response of the infilled frame through the unloading stiffness even after it has cracked. Thus, it is essential to consider the influence of the infill in the seismic response of infilled frames. A few simple examples are provided to demonstrate the same. Design spectra valid for the Himalayan region are also proposed

TABLE OF CONTENTS

Acknowledgements iv

Abstract v

Table of Contents vi

List of Figures viii

List of Tables xiii

List of Notations xiv

1 · Introduction

1.1 General 1
1.2 Objectives of Present Study.... 2
1.3 Organization of the Thesis. 3
1.4 Sign Convention, Notation and Units.... 3

2 : Effect of Masonry Infills on RC Moment Resisting Frames :: A Review of Literature

2 1 General.... 5
2.2 Effect of Infills.... 5
2.3 Modes of Failure.... 8
2.4 Review of Literature.... 9
2.5 Summary.... 13

3 : Trilinear Hysteresis Model

3.1 General 18
3.2 Inelastic Response Spectrum.... 19
  3.2.1 Numerical Implementation for Obtaining Inelastic Response Spectrum.... 21
3.3 Modelling Load-Deformation Characteristics of Infilled Frames.... 22
3.4 Trilinear Hysteresis Model.... 23
  3 4.1 Monotonic Load-Deformation Curve 24
  3.4.2 Hysteresis Behaviour.... 24

3 5 Derivation of Ductility Reduction Factor . . . 27

4 : Parametric Study

4.1 General . . . 40
4 2 Ground Motion Considered . . . 40
4 3 Range and Choice of Parameters . . . 41
  4.3 1 Stiffness Ratio, $\mathcal{K}$ . . . 41
  4 3 2 Strength Ratio, σ . . . 42
  4 3 3 Slope Ratio, η . . . 42
4.4 Results and Discussions . . . 43
  4 4.1 Uttarkashi Earthquake . . . 43
  4.4.2 US Earthquakes . . . 47
4 5 Design Implications . . . 47
4.6 Examples . . . 49
4 7 The Role of Infills . . . 55
4 8 Design Spectra . . . 56

5 : Summary and Conclusions

5.1 Summary of the Study . . . 88
5 2 Conclusions . . . 89
5.3 Recommendations for Future Work . . . 90

List of References 92

LIST OF FIGURES

Figure	Caption	Page No
1 1	Schematic diagram of an infilled frame.	4
2 1	Monotonic load-deflection curves of bare and infilled frames showing increased strength and stiffness in the latter	14
2 2	Strut action in the infill and separation between infill and RC frame members under lateral force [Paulay and Priestly, 1992].	14
2 3	Eccentricity developed due to non-uniform location of infills	15
2.4	Increased shear forces in columns due to partial masonry infill in concrete frames [Paulay and Priestly, 1992]	15
2.5	Typical failure mechanism developed in masonry infilled RC frames [Mehrabi and Shing, 1994].	16
2.6	Actual and idealized monotonic load-deflection curves for brick masonry, bare frame and infilled frame.	17
3.1	Derivation of inelastic response spectra from elastic spectrum [Riddell *et al*, 1989].	29
3 2	Definition of ductility reduction factor, R_μ, and overstrength factor, Ω.	29
3.3	Definition of ductility reduction factor, R_μ, for systems with (a) elasto-plastic, and (b) trilinear backbone curves.	30
3.4	Trilinear backbone curve used in the Trilinear Hysteresis Model for URM RC infilled frames.	31
3.5	Translation of virgin curves and destination points of hysteresis loops in the Trilinear Hysteresis Model for (a) frame with low stiffness ratio, and (b) frame with high stiffness ratio.	32
3.6	Typical hysteresis loops as predicted by Trilinear Hysteresis Model for URM RC infilled frames.	33
3.7	Comparison of Load-deflection curves for URM RC infilled frames, (a) Experimental - test specimen 2 [Brokken and Bertero, 1981], (b) Analytical as predicted by Trilinear Hysteresis Model.	34
3.8	Comparison of Load-deflection curves for URM RC infilled frames, (a) Experimental - test specimen 7 [Brokken and Bertero, 1981], (b) Analytical as predicted by Trilinear Hysteresis Model.	35

3 9 Normalized yield displacement *versus* ductility curves for different natural periods, systems with EPP backbone curves 36

3 10 Normalized yield displacement *versus* ductility curves for different natural periods, systems with trilinear backbone curve. 36

3 11 Derivation of DRF from normalized yield displacement *versus* ductility curves 37

3 12 DRF spectra proposed in the literature, (a) Newmark and Hall, 1973, (b) Lai and Biggs, 1980 38

3.13 DRF spectra proposed in the literature, (a) Riddell *et al*, 1989 (b) Chandak and Jain, 1994. 39

4.1 Mean DRF spectra of Uttarkashi earthquake strong motion records, for URM RC infilled frame with stiffness ratio, $\mathcal{K}$ $(=E_{if}/E_b)=2$, and slope ratio, η $(=E_n/E_p)=1000$, for different values of strength ratio, σ $(=P_y/P_u)$. Mean DRF spectra of bare frame also shown. 59

4 2 Mean DRF spectra of Uttarkashi earthquake strong motion records, for URM RC infilled frame with stiffness ratio, $\mathcal{K}$ $(=E_{if}/E_b)=2$, and slope ratio, η $(=E_n/E_p)=2$, for different values of strength ratio, σ $(=P_y/P_u)$ Mean DRF spectra of bare frame also shown. 60

4 3 Mean DRF spectra of Uttarkashi earthquake strong motion records, for URM RC infilled frame with stiffness ratio, $\mathcal{K}$ $(=E_{if}/E_b)=2$, and slope ratio, η $(=E_n/E_p)=1$, for different values of strength ratio, σ $(=P_y/P_u)$. Mean DRF spectra of bare frame also shown 61

4.4 Mean DRF spectra of Uttarkashi earthquake strong motion records, for URM RC infilled frame with stiffness ratio, $\mathcal{K}$ $(=E_{if}/E_b)=2$, and slope ratio, η $(=E_n/E_p)=0.2$, for different values of strength ratio, σ $(=P_y/P_u)$. Mean DRF spectra of bare frame also shown. 62

4.5 Mean DRF spectra of Uttarkashi earthquake strong motion records, for URM RC infilled frame with stiffness ratio, $\mathcal{K}$ $(=E_{if}/E_b)=5$, and slope ratio, η $(=E_n/E_p)=1000$, for different values of strength ratio, σ $(=P_y/P_u)$. Mean DRF spectra of bare frame also shown. 63

4.6 Mean DRF spectra of Uttarkashi earthquake strong motion records, for URM RC infilled frame with stiffness ratio, 64

$\mathcal{K}$ $(=E_{if}/E_b)=5$, and slope ratio, η $(=E_n/E_p)=2$, for different values of strength ratio, σ $(=P_y/P_u)$ Mean DRF spectra of bare frame also shown

4.7 Mean DRF spectra of Uttarkashi earthquake strong motion records, for URM RC infilled frame with stiffness ratio, $\mathcal{K}$ $(=E_{if}/E_b)=5$, and slope ratio, η $(=E_n/E_p)=1$, for different values of strength ratio, σ $(=P_y/P_u)$. Mean DRF spectra of bare frame also shown 65

4.8 Mean DRF spectra of Uttarkashi earthquake strong motion records, for URM RC infilled frame with stiffness ratio, $\mathcal{K}$ $(=E_{if}/E_b)=5$, and slope ratio, η $(=E_n/E_p)=0.2$, for different values of strength ratio, σ $(=P_y/P_u)$ Mean DRF spectra of bare frame also shown 66

4.9 Mean DRF spectra of Uttarkashi earthquake strong motion records, for URM RC infilled frame with stiffness ratio, $\mathcal{K}$ $(=E_{if}/E_b)=10$, and slope ratio, η $(=E_n/E_p)=1000$, for different values of strength ratio, σ $(=P_y/P_u)$ Mean DRF spectra of bare frame also shown. 67

4.10 Mean DRF spectra of Uttarkashi earthquake strong motion records, for URM RC infilled frame with stiffness ratio, $\mathcal{K}$ $(=E_{if}/E_b)=10$, and slope ratio, η $(=E_n/E_p)=2$, for different values of strength ratio, σ $(=P_y/P_u)$. Mean DRF spectra of bare frame also shown. 68

4.11 Mean DRF spectra of Uttarkashi earthquake strong motion records, for URM RC infilled frame with stiffness ratio, $\mathcal{K}$ $(=E_{if}/E_b)=10$, and slope ratio, η $(=E_n/E_p)=1$, for different values of strength ratio, σ $(=P_y/P_u)$. Mean DRF spectra of bare frame also shown 69

4.12 Mean DRF spectra of Uttarkashi earthquake strong motion records, for URM RC infilled frame with stiffness ratio, $\mathcal{K}$ $(=E_{if}/E_b)=10$, and slope ratio, η $(=E_n/E_p)=0.2$, for different values of strength ratio, σ $(=P_y/P_u)$. Mean DRF spectra of bare frame also shown. 70

4.13 Mean-minus-one standard deviation DRF spectra of Uttarkashi earthquake strong motion records, for URM RC infilled frame with stiffness ratio, $\mathcal{K}$ $(=E_{if}/E_b)=2$, and slope ratio, η $(=E_n/E_p)=1000$, for different values of strength ratio, σ $(=P_y/P_u)$. Mean DRF spectra of bare frame also shown. 71

4 14 Mean-minus-one standard deviation DRF spectra of Uttarkashi earthquake strong motion records, for URM RC infilled frame with stiffness ratio, $\mathcal{K}$ $(=E_{if}/E_b)=2$, and slope ratio, η $(=E_n/E_p)=2$, for different values of strength ratio, σ $(=P_y/P_u)$ Mean DRF spectra of bare frame also shown 72

4 15 Mean-minus-one standard deviation DRF spectra of Uttarkashi earthquake strong motion records, for URM RC infilled frame with stiffness ratio, $\mathcal{K}$ $(=E_{if}/E_b)=2$, and slope ratio, η $(=E_n/E_p)=1$, for different values of strength ratio, σ $(=P_y/P_u)$. Mean DRF spectra of bare frame also shown. 73

4 16 Mean-minus-one standard deviation DRF spectra of Uttarkashi earthquake strong motion records, for URM RC infilled frame with stiffness ratio, $\mathcal{K}$ $(=E_{if}/E_b)=2$, and slope ratio, η $(=E_n/E_p)=0\ 2$, for different values of strength ratio, σ $(=P_y/P_u)$ Mean DRF spectra of bare frame also shown. 74

4 17 Mean-minus-one standard deviation DRF spectra of Uttarkashi earthquake strong motion records, for URM RC infilled frame with stiffness ratio, $\mathcal{K}$ $(=E_{if}/E_b)=5$, and slope ratio, η $(=E_n/E_p)=1000$, for different values of strength ratio, σ $(=P_y/P_u)$ Mean DRF spectra of bare frame also shown. 75

4.18 Mean-minus-one standard deviation DRF spectra of Uttarkashi earthquake strong motion records, for URM RC infilled frame with stiffness ratio, $\mathcal{K}$ $(=E_{if}/E_b)=5$, and slope ratio, η $(=E_n/E_p)=2$, for different values of strength ratio, σ $(=P_y/P_u)$. Mean DRF spectra of bare frame also shown 76

4.19 Mean-minus-one standard deviation DRF spectra of Uttarkashi earthquake strong motion records, for URM RC infilled frame with stiffness ratio, $\mathcal{K}$ $(=E_{if}/E_b)=5$, and slope ratio, η $(=E_n/E_p)=1$, for different values of strength ratio, σ $(=P_y/P_u)$. Mean DRF spectra of bare frame also shown. 77

4 20 Mean-minus-one standard deviation DRF spectra of Uttarkashi earthquake strong motion records, for URM RC 78

infilled frame with stiffness ratio, $\mathcal{K}$ (=E_{if}/E_b)=5, and slope ratio, η (=E_n/E_p)=0.2, for different values of strength ratio, σ (=P_y/P_u) Mean DRF spectra of bare frame also shown

4 21 Mean-minus-one standard deviation DRF spectra of Uttarkashi earthquake strong motion records, for URM RC infilled frame with stiffness ratio, $\mathcal{K}$ (=E_{if}/E_b)=10, and slope ratio, η (=E_n/E_p)=1000, for different values of strength ratio, σ (=P_y/P_u). Mean DRF spectra of bare frame also shown. 79

4 22 Mean-minus-one standard deviation DRF spectra of Uttarkashi earthquake strong motion records, for URM RC infilled frame with stiffness ratio, $\mathcal{K}$ (=E_{if}/E_b)=10, and slope ratio, η (=E_n/E_p)=2, for different values of strength ratio, σ (=P_y/P_u). Mean DRF spectra of bare frame also shown 80

4 23 Mean-minus-one standard deviation DRF spectra of Uttarkashi earthquake strong motion records, for URM RC infilled frame with stiffness ratio, $\mathcal{K}$ (=E_{if}/E_b)=10, and slope ratio, η (=E_n/E_p)=1, for different values of strength ratio, σ (=P_y/P_u). Mean DRF spectra of bare frame also shown. 81

4 24 Mean-minus-one standard deviation DRF spectra of Uttarkashi earthquake strong motion records, for URM RC infilled frame with stiffness ratio, $\mathcal{K}$ (=E_{if}/E_b)=10, and slope ratio, η (=E_n/E_p)=0.2, for different values of strength ratio, σ (=P_y/P_u). Mean DRF spectra of bare frame also shown. 82

4.25 DRF spectra of EL Centro strong motion record. 83

4.26 DRF spectra of Pacoima Dam strong motion record. 84

4.27 DRF spectra of Taft strong motion record 85

4 28 Additional energy dissipated in a URM RC infilled frame from monotonic considerations 86

4.29 Proposed design DRF spectra for the Himalayan region 87

LIST OF TABLES

Table No.	Caption	Page No.
4 1	Strong ground motion data recorded during the Uttarkashi earthquake, 1991 used in this study	57
4.2	Strong ground motion data recorded during the earthquakes, in US, used in this study	58
4 3	Different values of the parameters chosen in the current study.	58

LIST OF NOTATIONS

c	Damping value
E_b	Initial stiffness of bare frame
E_{if}	Initial stiffness of infilled frame
E_n	Negative slope on the trilinear backbone curve
E_p	Positive slope on the trilinear backbone curve
f	Inertial force
F^{el}_{max}	Maximum elastic lateral force
k_e	Initial elastic stiffness
m	Mass
p	Stiffness force
R_μ	Ductility reduction factor
T_b	Natural period of bare frame
T_{if}	Natural period of infilled frame
u, x, Δ	Lateral displacement
$V_{y,b}$	Yield force for the bare frame
$V_{y,if}$	Yield force for the infilled frame
$\dot{x}(t)$	Velocity at time t
$\ddot{x}(t)$	Acceleration at time t
$x_g(t)$	Ground acceleration at time t
β, γ	Newmark's parameters
$\Delta_{max,b}$	Maximum displacement of bare frame
$\Delta_{max,if}$	Maximum displacement of infilled frame
Δt	Time step
$\Delta_{y,b}$	Yield displacement of bare frame

$\Delta_{y,if}$	Yield displacement of infilled frame
η	Positive slope to negative slope ratio
$\mathcal{K}$	Infilled frame stiffness to bare frame stiffness ratio
μ	Displacement ductility
σ	Infilled frame strength to bare frame strength ratio
ζ	Damping ratio

CHAPTER 1

INTRODUCTION

1.1 GENERAL

In the analysis and design of building frames it is commonly assumed that non-structural elements do not contribute to their strength and stiffness The usual practice is to design building frames as "bare (skeletal) frames", wherein only the presence of beams and columns and sometimes also of the slabs, is accounted for Unfortunately, the list of non-structural elements also includes, among others, filler walls, staircases, canopies & other projections. While a mathematical model is required to design structures, such over-simplifications of their behaviour lead to the simulated behaviour being radically different from the actual one The deficiencies in the current approach of modelling are more pronounced during dynamic response, such as in the event of an earthquake Thus, the contributions of some of these structural elements, which are *considered* to be non-structural, need to be accounted for realistically This study is focused on the urgency to include filler walls in the design of frame buildings

An infilled frame building is one having in-plane walls in between the frame members, namely beams and columns, as shown in Figure 1 1. These filler walls may or may not occupy the full panel area between the beams and columns These infill panels could be made of clay brick masonry, reinforced or unreinforced, or of reinforced concrete. In developing countries, like India, unreinforced masonry (URM) infills are most commonly used In general, Reinforced Concrete (RC) *Moment Resisting Frame* (MRF) buildings with infill wall panels are widely used Detailed research in the past has established that analyses of RC MRFs based on the bare frame approach lead to significantly lower level of lateral stiffnesses, and hence larger fundamental natural periods, than the actual values obtained through experimental measurements

1.2 OBJECTIVES OF PRESENT STUDY

This study aims to critically review the implications of considering URM infills in the seismic design of planar RC MRFs. The following are the salient objectives of this study ·

(i) Review the existing formulations for modelling the response of RC masonry infilled frames. Propose a cyclic constitutive law based on experimental hysteretic data for the overall load-deformation behaviour of masonry infilled frames

(ii) Develop a computer program for obtaining the inelastic response spectrum using the proposed hysteresis model

(iii) Study the inelastic response spectrum of certain strong ground motion records in light of the proposed hysteretic model for RC MRFs with masonry infills. Critically study ductility reduction factors

(iv) Identify critical issues affecting the seismic behaviour of existing buildings, and hence the seismic design of buildings.

1.3 ORGANIZATION OF THE THESIS

The contention of this thesis is presented in five relatively independent chapters Chapter 1 introduces the subject matter of this study and the need for it thereof. The objectives of the study are also outlined Chapter 2 presents the various issues involved in a realistic modelling of infilled frames and reviews the associated literature

The details relating to the inelastic response spectrum of strong ground motion for masonry infilled RC MRFs is presented in Chapter 3. A simple model for the cyclic constitutive load-deformation relationship of masonry infilled RC MRFs is presented. The set of simple hysteresis rules governing the cyclic behaviour of infilled frames is listed Chapter 4 presents the results of a limited parametric study carried out to establish the effect of the different parameters governing the constitutive law. Some new issues in the design of frames are highlighted with the help of examples

Finally, the summary of the work done and contentions of this thesis are listed in Chapter 5. Recommendations are made for possible future work in this area.

1.4 SIGN CONVENTION, NOTATION AND UNITS

Consistent sign convention and notations have been adopted throughout this work. Scalars are indicated by their variable names, *e g.,* u The time derivative of any quantity is indicated with a dot over the variable name, *e.g.,* x

All dimensions are referred to in SI units Linear dimension is expressed in *millimeters* (mm), while force is expressed in *kilo-Newton* (kN) The unit of time is *second* (sec)

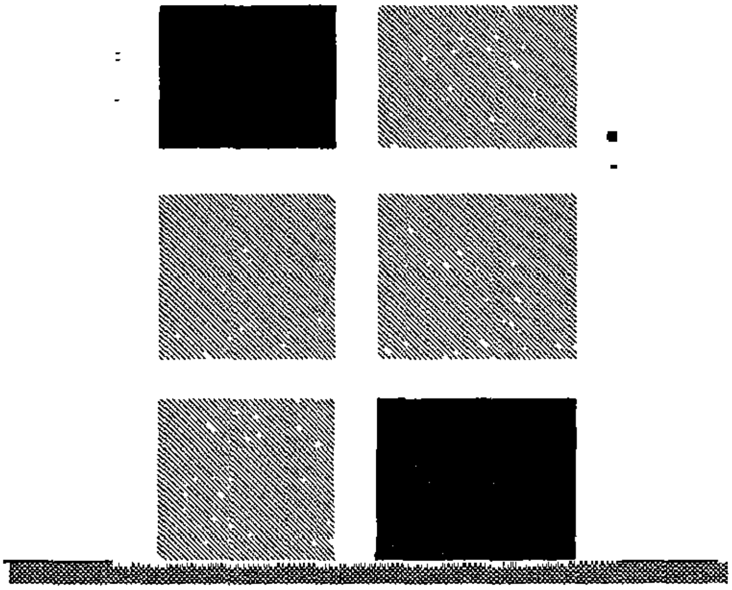

Figure 1.1 . Schematic diagram of an infilled frame

CHAPTER 2

EFFECT OF MASONRY INFILLS ON RC MOMENT RESISTING FRAMES :: A REVIEW OF LITERATURE

2.1 GENERAL

Ambient vibration measurements of existing buildings indicate that the actual stiffness of an RC MRF building is much more than that perceived by the bare frame analysis [Jain, *et al*, 1995]. Also, in some cases, the contribution of the infill walls to the lateral strength of the building is experimentally recorded to be very significant. Thus, an infilled frame, in general, exhibits both higher lateral stiffness and larger maximum lateral load capacity than that estimated from the analysis of bare frames. This has far reaching consequences in the seismic design of buildings, which is critically dependent on both their strength and their stiffness.

2.2 EFFECT OF INFILLS

The infill imparts a significantly higher initial in-plane stiffness to the bare frame. This increase may typically be about ten times. Extreme values as high as 50-100 times have also been reported in cases [Pires and Carvalho, 1992] where the infills were constructed first and the frame was later cast all around.

The infill also imparts a higher lateral load capacity to the frame. However, with increased cracking and progressive yielding of the masonry, this maximum lateral load capacity drops down to that of the bare frame for large values of lateral displacements The drop is relatively gradual in the case of reinforced brick masonry as there is a possibility of the development of both shear and flexural failure modes However in the case of URM panels, only shear failure mode is developed, resulting in a sudden brittle failure Consequently, a rather sudden drop in the load-deformation relationship is observed The maximum lateral load capacity of frames with URM infills may be upto about two times that of a bare frame [Brokken and Bertero, 1981; Pires and Carvalho, 1992]. The above two characteristic changes, namely increased strength and stiffness, in the load-deformation relation of building frames with infills are schematically shown in Figure 2 1.

In an infilled frame, the lateral shear is resisted primarily through strut action This involves a separation between the infill and beam/column ends along the unloaded diagonal [Paulay and Priestley, 1992], as shown in Figure 2 2 Along the loaded diagonal, there is an extra rigid zone near the beam/column ends

In actual buildings, not all panels are infilled, some are left without filler walls depending on functional requirements. This random location of infills and of openings for doors/windows lead to a complex distribution of mass in the infilled frame. Also, the sudden stiffness changes due to missing/partial infills cause uneven seismic shear distribution Further, the non-uniform use of infills in the three dimensions of buildings (see Figure 2.3) may lead to eccentric distribution of stiffness which attracts large torsional moment. The presence of partial infills can lead to higher values of shear forces in individual frame members, as shown in Figure 2.4. Hence, the inadequacy of a design based on the bare frame approach is obvious

Increased stiffness and enhancement in strength cause larger dissipation of input seismic energy with progressive cracking of infills Also, the infilled frame exhibits an increased shear capacity for ground shaking upto moderate levels. Infill panels, however, also have some undesirable consequences on the overall behaviour of the frame. Under strong ground shaking, the failure of the strong infills may lead to sudden transfer of shear forces to columns, thereby exerting a significantly higher ductility demand on columns If not provided for, the columns may demonstrate brittle shear failure. Needless to say, the presence of infills attracts more earthquake forces to the structure

The extent of the influence of infill panels on the overall building behaviour depends on a number of factors. These factors are primarily owing to the material used as well as the construction methodology adopted. Some of them are .

a) initial gaps between the infill and the frame members,

b) the choice of reinforced/unreinforced masonry used,

c) the properties of the mortar used,

d) the column to infill stiffness ratio,

e) strength of the infill,

f) slip of masonry during the cyclic loading,

g) extent of cracking in the masonry,

and h) out-of-plane instability due to separation of wythes.

2 3 MODES OF FAILURE

The primary modes of failure of infilled frames are

a) Tensile failure of the tension column, attributable to the presence of large overturning moments,

b) Sliding shear failure manifested in the form of a horizontal crack in the panel, caused due to the relatively weak mortar,

c) Compression failure of the diagonal strut,

d) Flexural or shear failure of the columns,

and e) Diagonal cracking of the infilled panel Since additional load can be taken upto the compression failure mode of the diagonal strut and the flexural or shear failure modes of the columns, this is not considered as a strict failure condition

The other failure modes for the infill frames include horizontal slip and out-of-plane instability. Some of the failure modes mentioned above are schematically shown in Figure 2.5

The load-deformation relationship of a reinforced concrete bare frame has been well established by experimental researchers. The behaviour of reinforced masonry is also relatively well documented. However, the behaviour of unreinforced masonry has not drawn much attention. Its load-deformation relation is taken to be linear for relatively low values of loads with a sudden brittle failure. The little experimental data available for masonry infilled frames [Brokken and Bertero, 1981, Gergely, *et al*, 1994, Klinger and Bertero, 1976; Kwan, *et al*, 1990, Liauw, 1979] indicate a load-deformation relationship of the type shown in Figure 2.6. The figure also shows a comparison with the characteristics of URM and the bare frame The load-deformation characteristics of the infilled frame may be thought of as a superposition of those of URM infills and the bare frame. Figure 2 6 also *qualitatively shows these components* as parts of the· net characteristics of infilled frames, and their idealized representations thereof.

2.4 REVIEW OF LITERATURE

Efforts for a realistic analysis of infilled frames started in the late 1950's The initial contributions were largely limited to the modelling of lateral stiffness of infills. And, most of this work focused on the static behaviour of RC infills. This led to the *development of the diagonal strut* analogy, in *which the infill stiffness* was estimated based on an equivalent diagonal strut in the panel [Polyakov, 1952]. The mechanism of load transfer in an infilled frame is primarily through strut action. The strut is itself formed when flexural deformations in the beams and columns cause their separation from the infill along the unloaded diagonal. This subjects the infill to a compressive loading along the loaded diagonal Extensive work has been reported [Flanagan, *et al*, 1994; Gergely, *et al*, 1994] on the modelling of the stiffness through this concept of the equivalent diagonal strut analogy

The equivalent strut approach was later extended to also include the influence of infill-to-frame stiffness ratio and multi-panel interaction [Smith, 1962; Smith, 1966]. Based on this extension, design curves for infilled frames were proposed [Smith and Carter, 1969] Later, an expression for the width of the equivalent strut as a function of column-to-infill relative stiffness and panel geometry, was proposed [Mainstone, 1971]

In the 1970's, a formulation based on the Airy's stress function approach was proposed [Lai and Biggs, 1980] to compute the stress distribution in the infilled frame. This was used to later propose an approximate method of analysis for the infilled frame.

Extensive work on the application of the finite element method to investigate the static as well as dynamic behaviour of infilled frames is available in the literature [Ali and Page, 1987, Girish, *et al*, 1992; King and Pandey, 1978; Liauw and Lee, 1977; Liauw and Lo, 1988, Samarasinghe and Hendry, 1982; Youssef, 1994] Initially, the infill was idealized as a plane stress element, considering the frame members to be axially rigid [Mallik and Severn, 1967, Mallik and Severn, 1968] This analysis was further extended [Mallik and Garg, 1971] to include the axial effects in the windward column. In this, approximate pre-determined contact lengths along the interfaces between the infill and the frame members were used. The effect of openings on overall behaviour of infilled frame was also investigated.

Cracking and slipping in the infill panel have been simulated through the use of short, stiff linking members between nodes on the interface [Riddington and Smith, 1977]. Friction elements have also been successfully used to model the interaction between the frame and the infill [King and Pandey, 1978].

Separation, slip and friction between infill and frame members have been incorporated in a non-linear modelling of infilled frames [Liauw and Kwan, 1982]. Flexural and flexural-cum-membrane type analysis using a super-masonry element has been proposed in a recent study [Bhandari and Trikha, 1988] Flexural analysis was observed to give better results.

In the recent past, tests have been conducted to investigate the influence of initial gaps on the behaviour of infilled frames [Riddington, 1984]. Results from these tests indicate that initial gaps should be avoided as they lead to undesirable effects Tests to study the influence of infill properties on the overall infill frame behaviour, have also been reported [Dhanasekar and Page, 1986; Grimm, 1975; Jagadish, *et al*, 1992, Rahman and Reddy, 1992; Sawko and Rouf, 1984; Schuller, *et al*, 1994].

Plastic theory has also been employed to model the behaviour of infilled frames A unified plastic theory has been proposed for analysis and design of infilled frames [Liauw and Kwan, 1984]. In a recent study, model tests have been conducted and plastic analysis has been applied to study the behaviour of infilled frames [Kwan, *et al*, 1990].

In another recent study [Altin, *et al*, 1991], tests were conducted to understand the effect of infill on the stiffness, strength, energy dissipation, lateral drift and ductility characteristics of infilled frames The study leads to interesting and important conclusions towards a better understanding of the behaviour of the infilled frame. However, the tests were restricted to frames with RC infills only.

Extensive work has been done on the behaviour of brick infilled steel frames However, since the infill-to-column stiffness ratio is much higher for infilled steel frames, their overall behaviour is significantly different from that of infilled RC frames However, in a recent study on infilled steel frames [Chrysostomou, *et al*, 1992], a new multi-strut model is proposed as an extension of the equivalent diagonal strut approach. This is basically a compression-only six strut model which is capable of simulating plastic hinge formation in frame members

The current thinking amongst researchers on the design of a RC building with infills, clearly reflects the need for including the contribution of infills to its overall lateral strength and stiffness A rational approach is now available [Rashad, 1993] for incorporating the properties of infills in the design procedure However, this is based on *monotonic* behavioural *consideration only*

Experimental data on URM infilled RC MRFs is scanty. Moreover, clay brick masonry being a grossly heterogeneous material, the experimental results indicate a very wide range of scatter [Brokken and Bertero, 1981, Klinger and Bertero, 1976; Liauw, 1979] While most of the results are for monotonic load conditions, some are also available for reversed cyclic load conditions. Hardly any work has been reported on the modelling of the hysteretic response of masonry infilled frames

2.5 SUMMARY

Masonry infill panels contribute significantly to the strength and stiffness of frame buildings. The current approach of modelling infilled frame buildings as elastic perfectly-plastic systems is inadequate There is an urgent need to include the effect of infill panels in the lateral load-deformation characteristics of building frames Analytical models are required to describe the hysteretic behaviour of masonry infilled RC MRFs

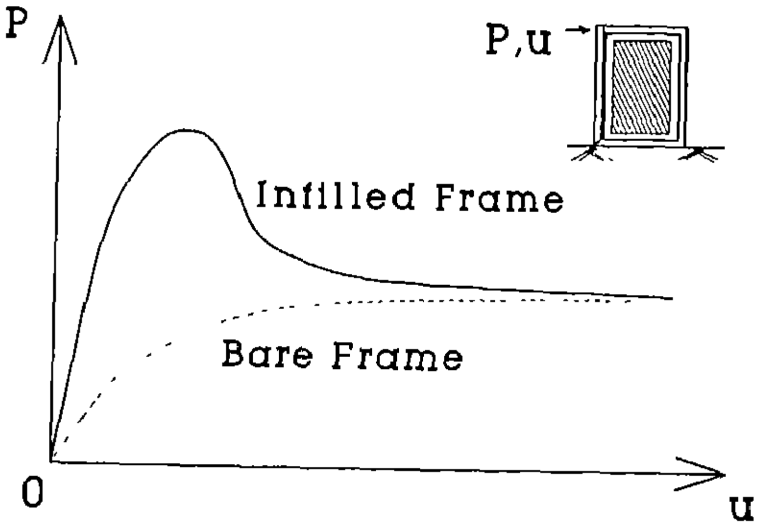

Figure 2 1 Monotonic load-deflection curves of bare and infilled frames showing increased strength and stiffness in the latter

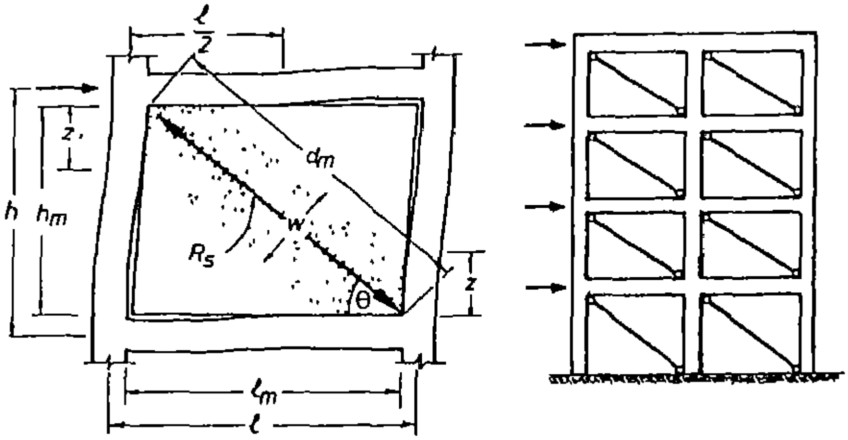

Figure 2.2 : Strut action in the infill and separation between infill and RC frame members under lateral force [Paulay and Priestley, 1992]

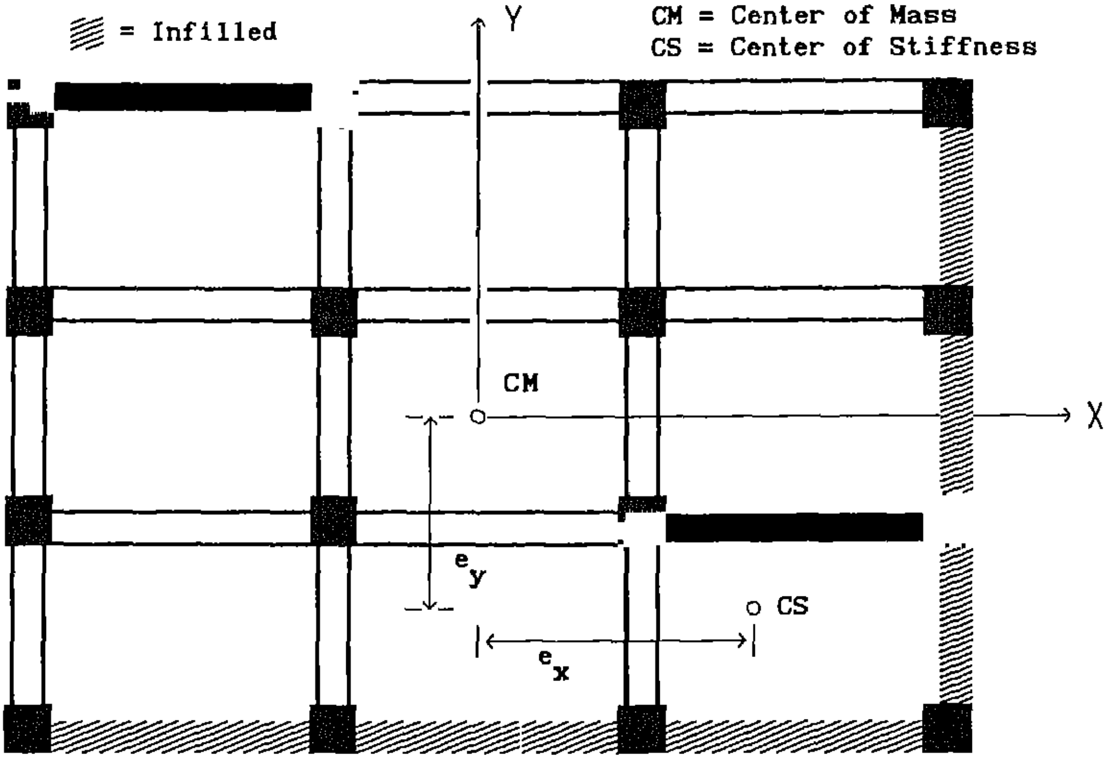

Figure 2.3 . Eccentricity developed due to non-uniform location of infills.

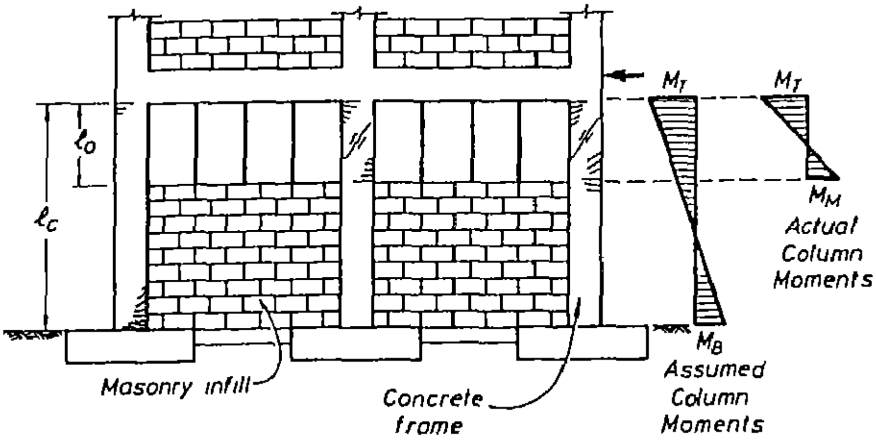

Figure 2.4 . Increased shear forces in columns due to partial masonry infill in concrete frames [Paulay and Priestley, 1992].

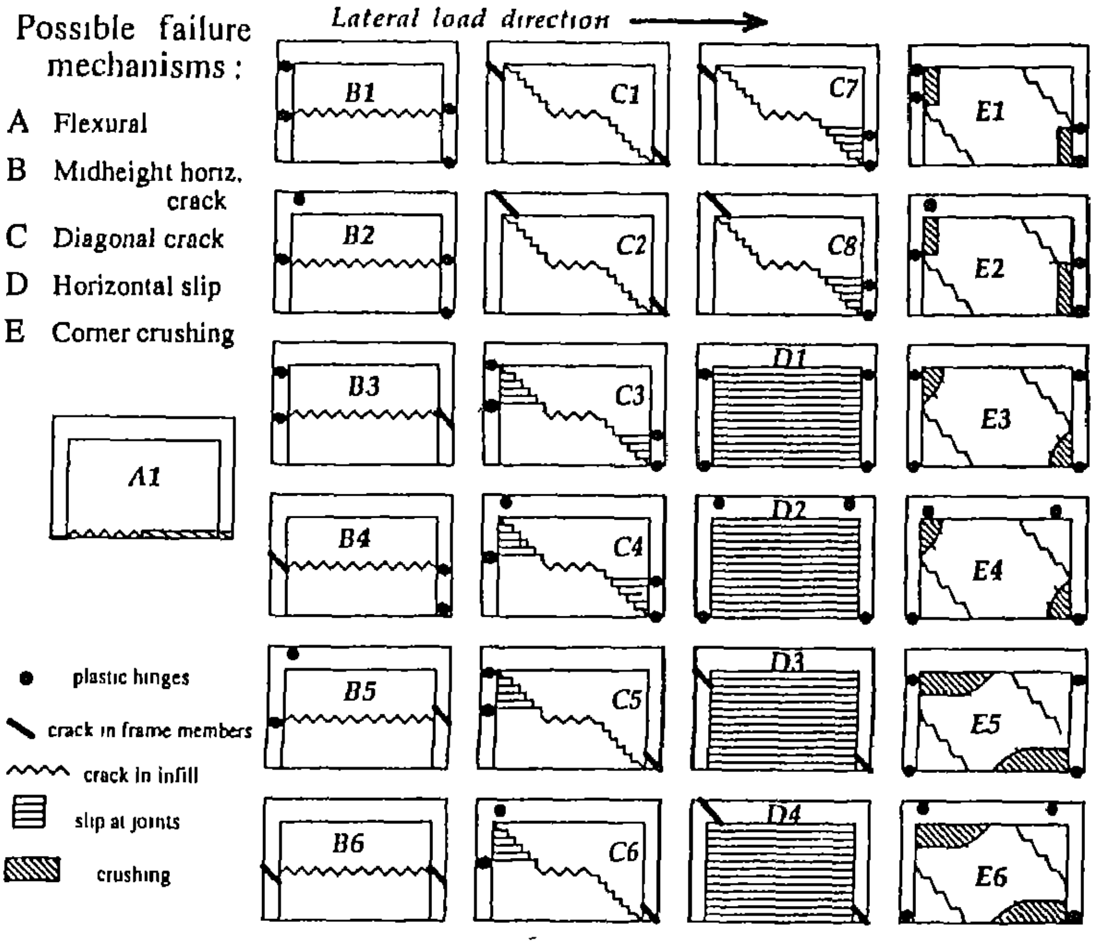

. Failure Mechanisms

Figure 2.5 : Typical failure mechanism developed in masonry infilled RC frames [Mehrabi and Shing, 1994].

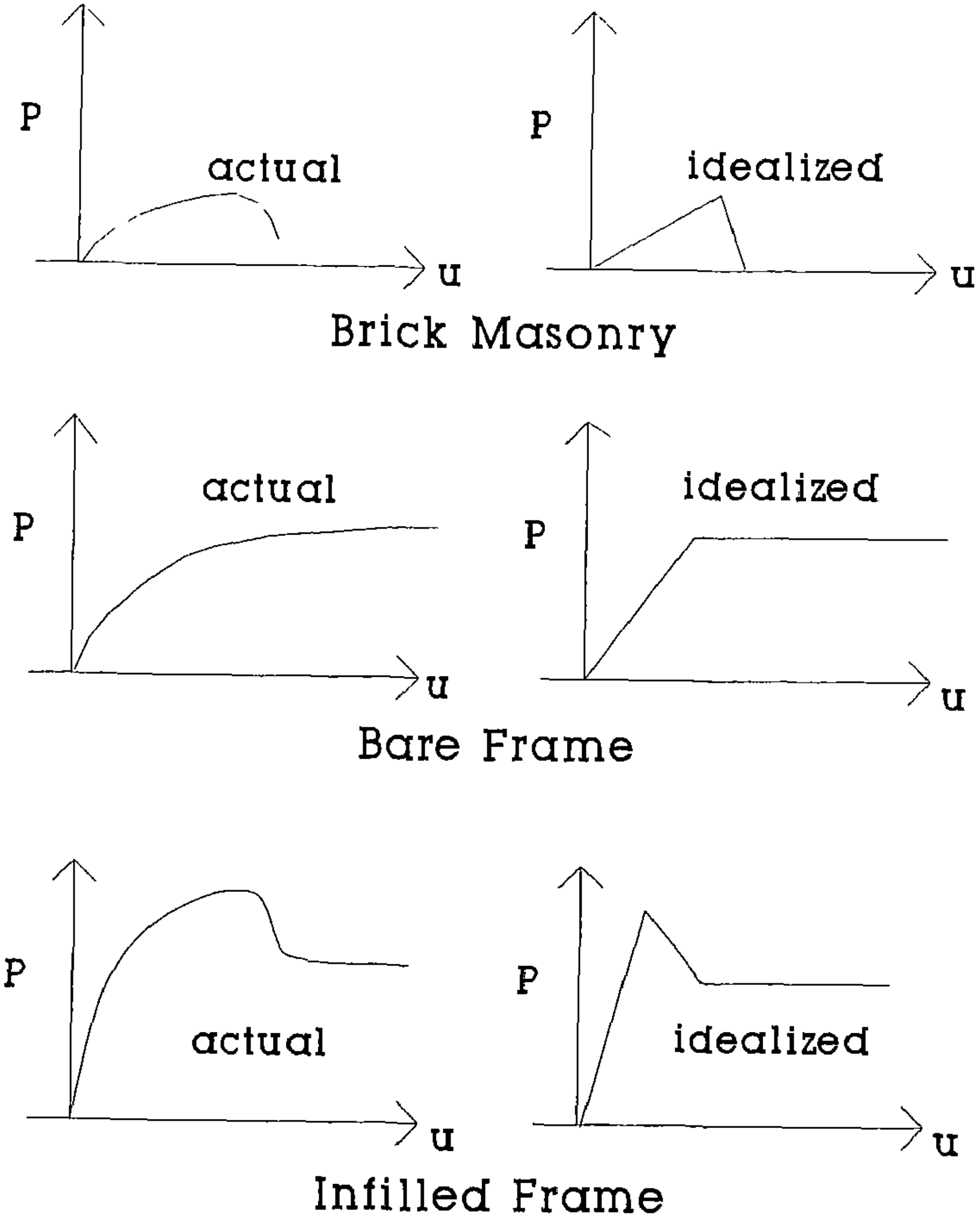

Figure 2.6 Actual and Idealized monotonic load-deflection curves for brick masonry, bare frame and infilled frame

CHAPTER 3

TRILINEAR HYSTERESIS MODEL

3.1 GENERAL

The earthquake-resistant design philosophy currently in practice, requires that a structure should be able to resist (a) minor levels of earthquake ground motion without damage, (b) moderate levels of earthquake ground motion without structural damage, but possibly with some non-structural damage, and (c) major levels of earthquake ground motion without collapse, but possibly with some structural as well as non-structural damage. Most design codes fulfill the first two requirements directly, while the third is implicitly accounted for through sufficient ductility and strength provisions

In accordance with the above philosophy, a well designed building frame is expected to behave inelastically under strong ground shaking, thereby dissipating the input seismic energy without collapse. The nonlinear behaviour in buildings can arise from its components, namely beams, columns, joints, slabs and walls, either individually or collectively. The nonlinearity stems from both material as well as geometric nonlinearities. Hence the true behaviour of an infilled frame building can be studied through nonlinear dynamic analysis, which realistically incorporates both the above types of nonlinearities. It is uneconomical to design a structure to remain elastic during severe ground motions of rare occurrence. But if it is ensured that the building is capable of undergoing inelastic deformations in a stable manner through adequate ductility features built into it, it can be designed for a much lower seismic force than the maximum force experienced by it if it were to remain elastic. Thus, its inelastic response is an important input to the design process

3.2 INELASTIC RESPONSE SPECTRUM

An estimate of the maximum inelastic seismic response during a particular ground motion is possible through the inelastic response spectrum (IRS) The structure is considered to be a single degree of freedom system, the natural period of which is the fundamental natural period of the structure. The IRS is a plot of the maximum pseudo spectral acceleration (PSA) experienced by a SDOF system of natural period T, normalized with peak ground acceleration (PGA), for a specified value of ductility, μ The derivation of the design inelastic response spectrum from the design elastic response spectrum of a system is shown in Figure 3.1 [Riddell, *et al*, 1989]. The IRS provides a quick preliminary estimate of the maximum expected response of a structure given its fundamental natural period and expected ductility, under a given ground motion However, this method implicitly assumes that only the first fundamental mode of vibration contributes to the response This assumption is reasonable for most regular building frames which behave primarily in lateral shear, but may be unacceptable in case of irregular building frames, in which other modes also contribute significantly to their response In the latter case, a detailed dynamic analysis becomes necessary.

In the current trend of design, the design seismic lateral force is obtained by dividing the realistic level of elastic base shear force corresponding to a design ground motion by a factor R, called the response reduction factor [Murty and Jain, 1994, ATC-1978; UBC-1994] This factor, R, stems from two factors, and is given by,

$$R = R_{\mu}\ \Omega, \tag{3 1}$$

where R_{μ} is the ductility reduction factor and Ω, the overstrength factor R_{μ} represents the reduction in the elastic force to the level of the yield strength of the structure This depends on the ductility of the structure, and hence on its energy dissipation capacity. Ω represents the overstrength inherent in the code-designed structures, and is defined as the ratio of the maximum lateral strength of the structure to the code-prescribed design base shear. These factors are schematically shown in Figure 3 2

The inelastic response spectrum is commonly re-cast as the plot of the ductility reduction factor (DRF), R_{μ} *versus* the natural period of the single degree of freedom system [Gupta, 1990]. The DRF is the ratio of the maximum elastic response (PSA) to the maximum inelastic response (PSA) for a ductility of μ, with say 5% damping, *i.e.*,

$$R_{\mu}(T,\mu) = \frac{\mathrm{PSA}(T,\ \zeta=5\%,\ \mu=1)}{\mathrm{PSA}(T,\ \zeta=5\%,\ \mu)}\ , \tag{3 2}$$

where μ represents the displacement ductility. μ is the ratio of maximum displacement response, u_{max}, to yield displacement, u_y, of the structure, *i.e.*,

$$\mu = \frac{u_{max}}{u_y}\ . \tag{3.3}$$

The DRF depends on the natural period, damping, ductility and cyclic load-deformation characteristics of the structure, as well as on the ground motion characteristics. For the elastic perfectly-plastic (EPP) system, R_μ is obtained as shown in Figure 3.3(a).

3.2.1 Numerical Implementation for Obtaining Inelastic Response Spectrum

The equation of equilibrium of a nonlinear single degree of freedom system, with mass m, elastic stiffness k_e and damping c, is

$$m\,\ddot{x}(t) + c\,x(t) + p(x,t) = f(t), \tag{3.4}$$

where $\ddot{x}(t)$, $\dot{x}(t)$ and $x(t)$ are respectively the acceleration, velocity and displacement responses relative to the ground at time t. $p(x,t)$ is the nonlinear stiffness force generated in the system under the application of the external force $f(t)$. Under seismic conditions, $f(t)$ is owing to the inertial effects, and is given by

$$f(t) = -\,m\,\ddot{x}_g(t), \tag{3.5}$$

where $\ddot{x}_g(t)$ is the input ground acceleration. The nonlinear response quantities $\ddot{x}(t)$, $\dot{x}(t)$ and $x(t)$ are obtained by integration of Eq.(3.4) in the time domain.

Let Δt be the time step. Then, the equation of equilibrium at time, $(t+\Delta t)$, is

$$m\,\ddot{x}(t+\Delta t) + c\,\dot{x}(t+\Delta t) + p(x,(t+\Delta t)) = f(t+\Delta t)\ . \tag{3.6}$$

For iteration k within the time step, the incremental equilibrium equation is obtained from Eq (3.6) using Newmark's Gamma-Beta difference recipe and the Modified Newton Raphson Procedure, as

$$
\begin{aligned}
&[\beta\ k_e + \frac{\gamma}{\Delta t}\ c + \frac{1}{(\Delta t)^2}\ m]\ \Delta x^k \\
&\quad = \beta\ f(t+\Delta t) - \beta\ p^k(t+\Delta t) \\
&\quad - [\frac{\gamma}{\Delta t}\ c + \frac{1}{(\Delta t)^2}\ m]\ x^k(t+\Delta t) + [\frac{\gamma}{\Delta t}\ c + \frac{1}{(\Delta t)^2}\ m]\ x(t) \\
&\quad + [(\gamma-\beta)\ c + \frac{1}{\Delta t}\ m]\ \dot{x}(t) + [(\gamma-2\beta)\ \frac{\Delta t}{2}\ c + [(0.5-\beta)\ m]\ \ddot{x}(t)\ ,
\end{aligned}
\tag{3.7}
$$

where β and γ are Newmark's parameters. Within the load step from time t to time $(t+\Delta t)$, the initial estimates for $x^k(t+\Delta t)$ and $p^k(t+\Delta t)$ are taken as $x(t)$ and $p(t)$, respectively. Eq.(3.7) is then solved iteratively till Δx^k converges.

For linear problems, unconditional stability of the numerical scheme in the Newmark's γ-β Method is guaranteed, if $\gamma \geq 0.5$ and $\beta \geq 0.25(0.5+\gamma)^2$. The values $\beta=0.25$ and $\gamma=0.5$ have been used in the analysis. This particular choice for the parameters β and γ, called the *Constant Average Acceleration Method* or the *Trapezoidal Method*, has the advantage of not introducing any artificial damping through the numerical scheme.

The stiffness force $p^{k+1}(t+\Delta t)$, is obtained by applying the cumulative incremental deformation within the time step to the state of the system at the end of the previous time step. The hysteresis rules described in the preceding section are employed to ascertain the new state.

3.3 MODELLING LOAD-DEFORMATION CHARACTERISTICS OF INFILLED FRAMES

Building frames are usually modelled on the basis of bilinear load-deformation characteristics. Of these, the elastic perfectly-plastic (EPP) model has been the most popular choice of researchers. However, this model is inadequate to reflect the true characteristics of infilled frames discussed in Chapter 2. A better model is required for the study of these frames

From the various experiments reported in the literature [Brokken and Bertero, 1981, Gergely, *et al*, 1994, Klinger and Bertero, 1976; Kwan *et al*, 1990, Liauw, 1979], the actual behaviour of the infilled frames can be summarized as follows

a) The initial stiffness of the infilled frame is much higher than that of the corresponding bare frame

b) The presence of unreinforced masonry infills leads to a higher maximum lateral load capacity for the frame The behaviour is almost linear upto the maximum load, when sudden cracking of the brittle masonry leads to a sharp drop in the load carrying capacity of the frame At large lateral displacements, it reaches that of the corresponding bare frame

c) Once the masonry has cracked, the frame behaves just like a bare frame, except that the unloading stiffness remains at the level of the infilled frame initial stiffness.

3 4 TRILINEAR HYSTERESIS MODEL

Based on observations made in Section 3.3, an analytical model, called Trilinear Hysteresis Model, is proposed to capture the hysteretic response of URM infilled RC MRFs This hysteresis model, is motivated by the experimental data, though limited, collected from the literature

3.4.1 Monotonic Load-deformation Curve

The infilled frames demonstrate a very distinct backbone curve The monotonic load-deformation curve, also called the *virgin curve,* for a single-storey single-bay URM infilled frame can be idealized by the trilinear curve shown in Figure 3.4 The various parameters that control the characteristics are, yield strength, P_y, ultimate strength, P_u, initial stiffness, E_p, and negative slope, E_n, in the unstable region Although, much analytical work has been done on the behaviour of infilled frames, only a few experimental tests are reported. The highly heterogeneous properties of masonry and the lack of adequate data make it impractical to correctly quantify the above parameters using the material properties and the geometric dimensions

In this study, the yield displacement, u_y, on the trilinear load-deformation curve is defined as displacement corresponding to maximum load carrying capacity of infilled frame (see Figure 3.4). For the Trilinear Hysteresis Model, R_μ is obtained as in Figure 3.3(b)

3.4.2 Hysteresis Behaviour

The cyclic behaviour of infilled frames is captured from the experimental data The phenomenological model for the cyclic hysteretic response of frames proposed in this study is discussed below. It is primarily based on a set of hysteresis rules

Hysteresis Rules -

Hysteresis rules are the most important inputs to nonlinear analysis for reversed cyclic loading. The proposed rules resemble the

Extended Masing's Hypothesis [Jayakumar, 1987] relevant for metals A close observation of the available scanty data from infill frames made of heterogeneous materials, namely reinforced concrete and masonry, provide some broad guidelines to form the hysteresis rules

The hysteresis rules formulated for the proposed model are

(1) The virgin curves are identical for both directions of loading

(2) The virgin curve is linearly elastic upto the yield point, beyond which the curve drops off linearly to the ultimate capacity, which is assumed to remain constant with displacement

(3) Plastic strains accumulate only by progressing along the virgin curves and not by progressing along the branch curves. When plastic strains are added in one direction, the virgin curve in the other direction is translated along the deformation axis. This translated virgin curve is called the backbone curve.

(4) The branch curve originating from the virgin curve is the first branch curve The destination of this first branch curve leaving a positive virgin curve is a symmetric force point on the translated negative virgin curve. Similarly, the destination of the first branch curve leaving a negative backbone curve is a symmetric force point on the translated positive backbone curve.

(5) Under force reversals, the first branch curve is linearly elastic, with initial stiffness, until zero force is reached. Thereafter, the curve heads linearly, at a reduced stiffness, to its destination point. However, this reduced stiffness has a lower bound corresponding to the initial stiffness of the bare frame. If

lower bound governs, the curve follows the slope given by the initial stiffness of the corresponding bare frame, till the target force level is reached, and proceeds horizontally thereafter, until it reaches the destination point (Figure 3 5)

(6) All subsequent branch curves originating from the first branch curve are linearly elastic, with initial stiffness, till zero force is reached Thereafter, the curves head linearly towards the last turning point on the other side, until either all the nested loops are closed, or the destination point on the virgin curve is reached.

Comparison -

Typical hysteretic loops of URM infilled frames predicted by the Trilinear Hysteresis Model, based on the above set of hysteresis rules, are shown in Figure 3.6. Further, the hysteresis rules are validated by comparing the simulated response with the experimental response of two infilled frames [Brokken and Bertero, 1976] Figures 3 7 and 3.8 show the experimental and the simulated cyclic load-deformation curves for the same. The simulated response based on the Trilinear Hysteresis Model seems to compare reasonably well, considering the simplicity of the model. The experimental curves show some deviation from the simulated response, and it is not very clear whether the actual specimen show some relaxation effects near the yield region, or some strain hardening at moderate levels of displacement. More work is required to study these aspects and to reduce the ambiguity in the interpretations of . such results.

The proposed Trilinear Hysteresis Model is only a first attempt towards a more realistic modelling of infilled frames. It does not incorporate the effects of relaxation, strain hardening, stiffness degradation, *etc.* However, the Trilinear Hysteresis Model incorporates a gradual reduction in the loading stiffness of the infilled frame to the level of that of the bare frame.

3.5 DERIVATION OF DUCTILITY REDUCTION FACTOR

The procedure for obtaining the inelastic response spectrum of a ground motion for single-degree-of-freedom (SDOF) systems with EPP characteristics is very well established [Riddell and Newmark, 1979] SDOF systems with different natural period and yield force are subjected to the chosen ground motion and the maximum responses recorded are used to evaluate the ductility demand, μ Maximum acceleration *versus* natural period curves are drawn for fixed values of μ In case of EPP systems, as the yield force level is gradually reduced, the ductility demand μ gradually increases. Figure 3.9 shows the typical yield displacement *versus* ductility relationship of the EPP system for a given natural period.

However, in systems with trilinear monotonic curves, even if the yield force is gradually reduced, there is a sudden jump in the ductility demand for short period systems, as shown in Figure 3.10. The natural periods indicated are those corresponding to the initial stiffness of the infilled frames. The physical reasoning for this is as follows. The sudden cracking of the masonry leads to a sudden transfer of shear forces to the frame members, particularly for very stiff structures. Consequently, there is a sudden, sharp increase in the displacement of the structure The variation of ductility with yield displacement need not necessarily be monotonic. For intermediate natural period range, multiple solutions often exist for the yield displacement of a system to produce a fixed ductility [Riddell and Newmark, 1979] Figure 3 11 shows that in case of a non-monotonic variation of ductility with yield displacement, the lowest value of yield displacement for a given ductility gives the largest reduction factor, and *vice versa*. This is reflected in the ductility reduction factor (DRF) spectrum, a plot of R_μ *versus* T for a given μ, which has a fan-like shape in the intermediate natural period range, as shown in Figure 3.10 This fan region in the DRF spectrum can be considered as a zone of severe inelasticity. It is interesting to note that different shapes for the DRF spectra of systems with EPP characteristics proposed by different researchers correspond to either the lower limit of the fan [Newmark and Hall, 1973, Lai and Biggs, 1980], or to the upper bound of the fan [Riddell *et al*, 1989; Chandak and Jain, 1994] Figures 3.12 and 3 13 show the mean DRF spectra as proposed by some researchers. In the current study the lowest value of the yield displacement is chosen

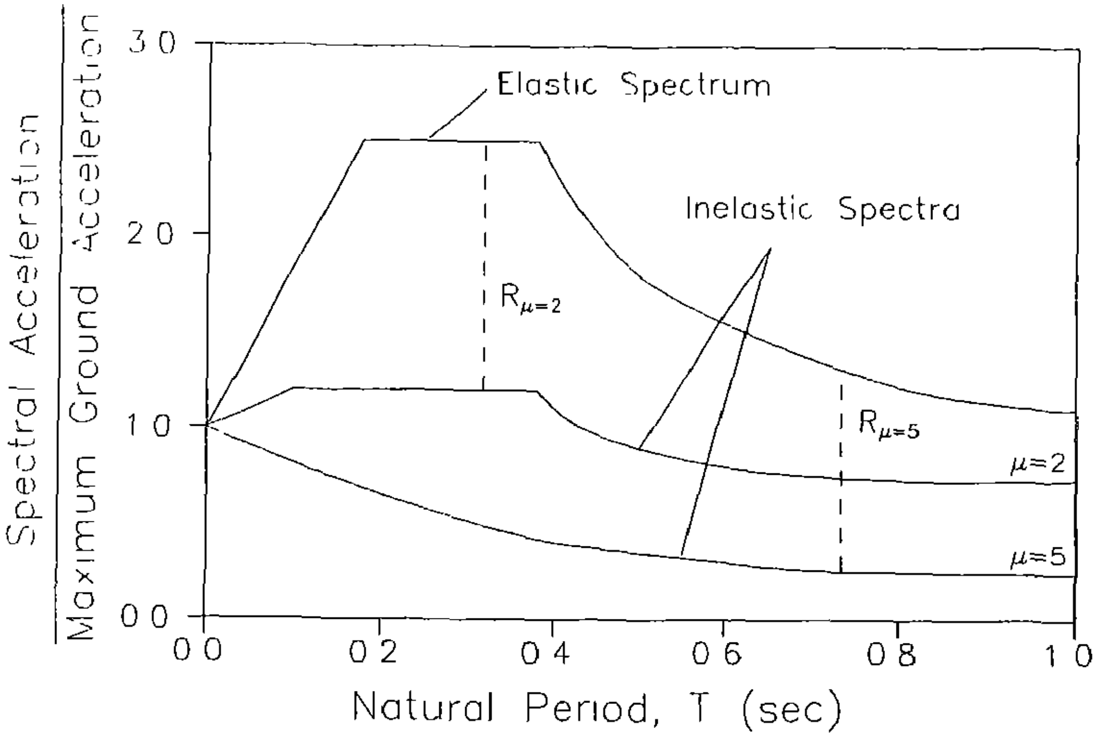

Figure 3 1 : Derivation of inelastic response spectra from elastic spectrum [Riddell *et al*, 1989]

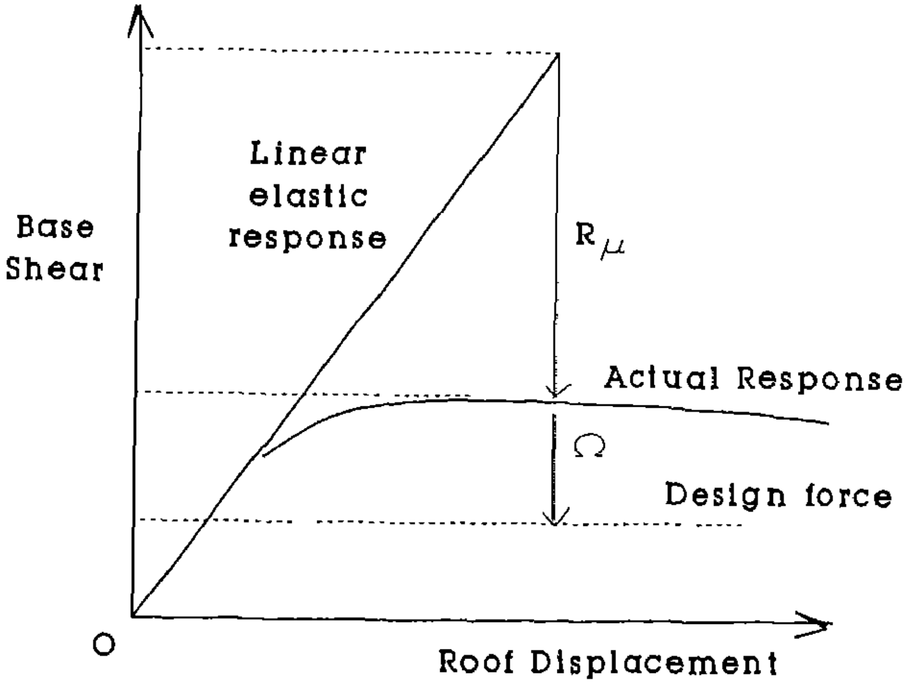

Figure 3.2 . Definition of ductility reduction factor, R_{μ}, and overstrength factor, Ω.

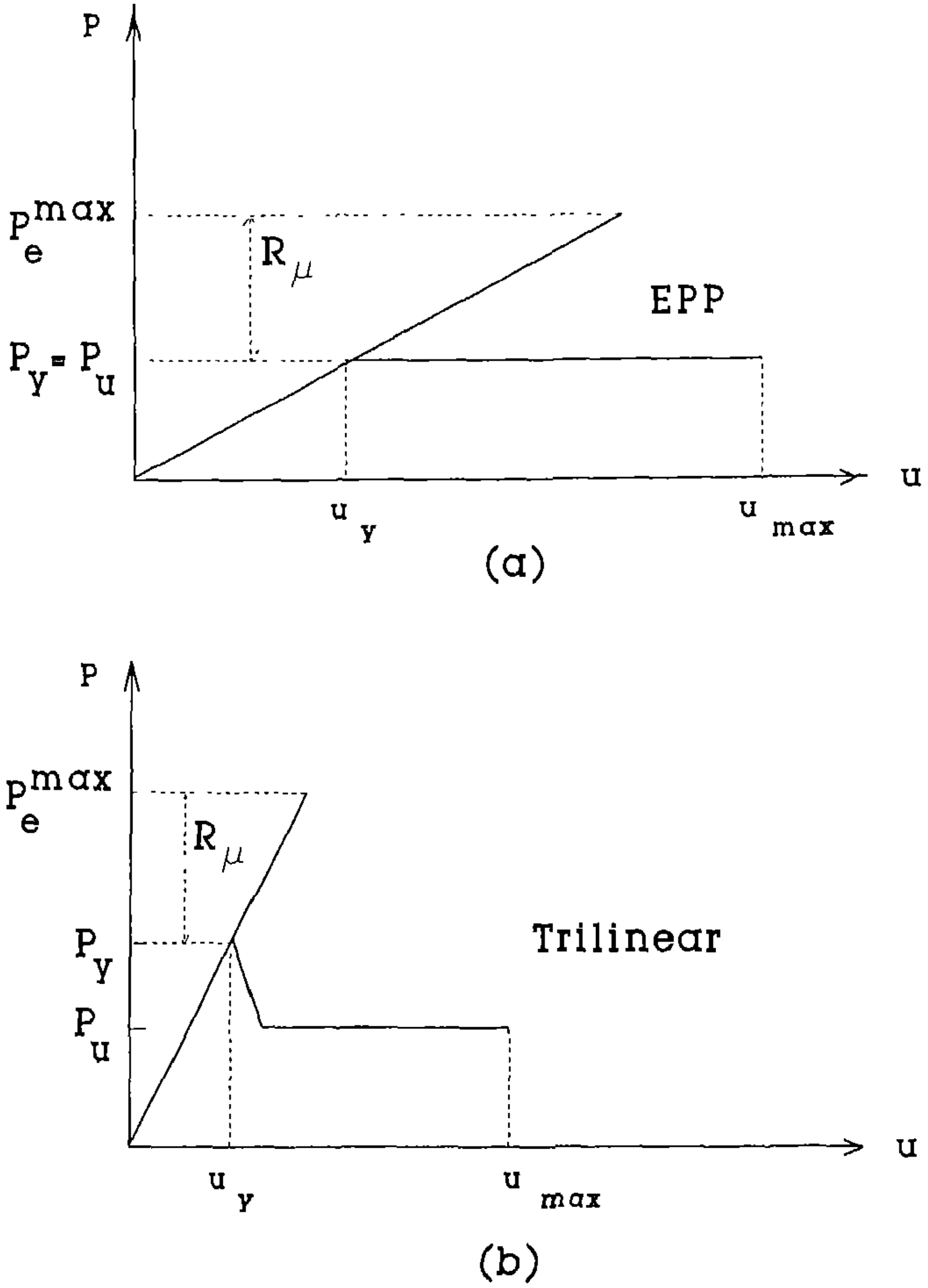

Figure 3.3 · Definition of ductility reduction factor, R_μ, for systems with (a) elasto-plastic, and (b) trilinear backbone curves.

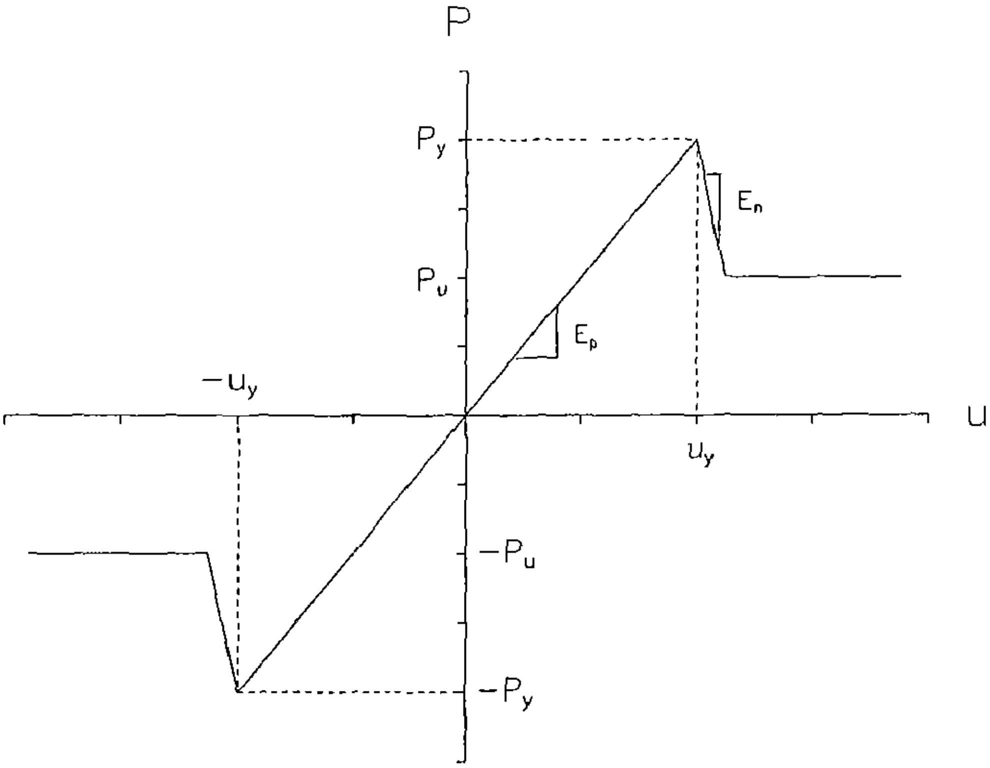

Figure 3 4 . Trilinear virgin curve used in the Trilinear Hysteresis Model for URM RC infilled frames.

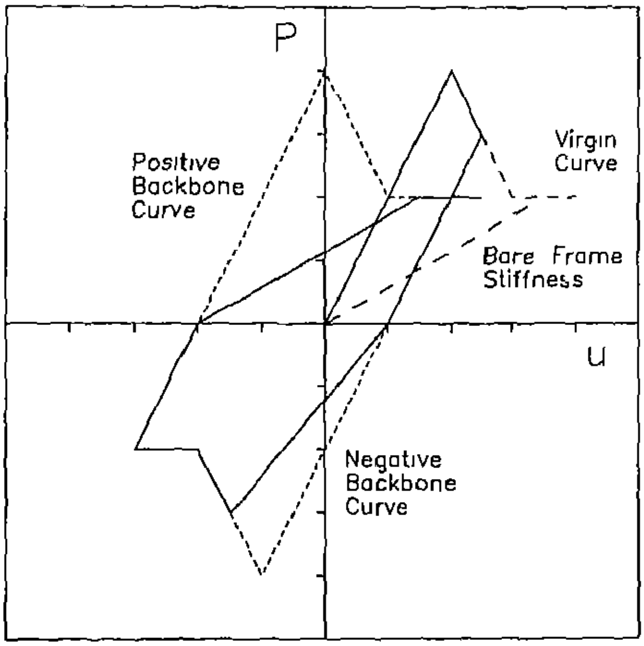

(a)

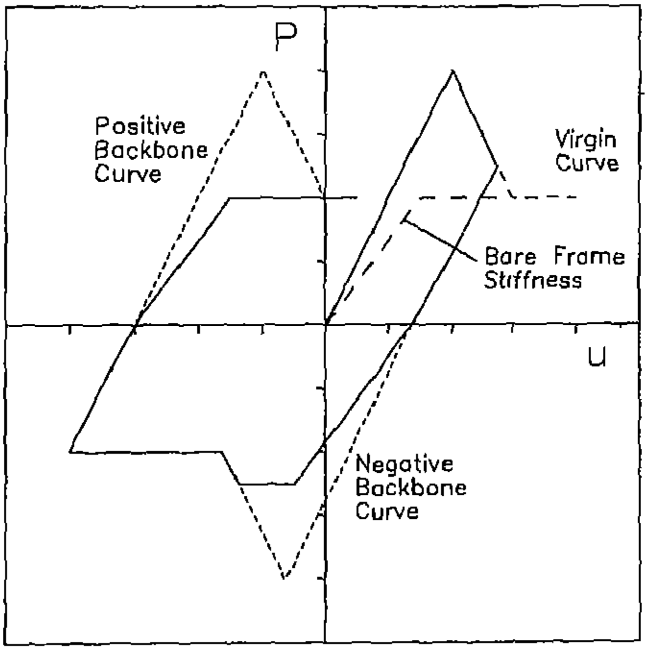

(b)

Figure 3.5 : Translation of virgin curves and destination points of hysteresis loops in the Trilinear Hysteresis Model for (a) frame with low stiffness ratio, and (b) frame with high stiffness ratio

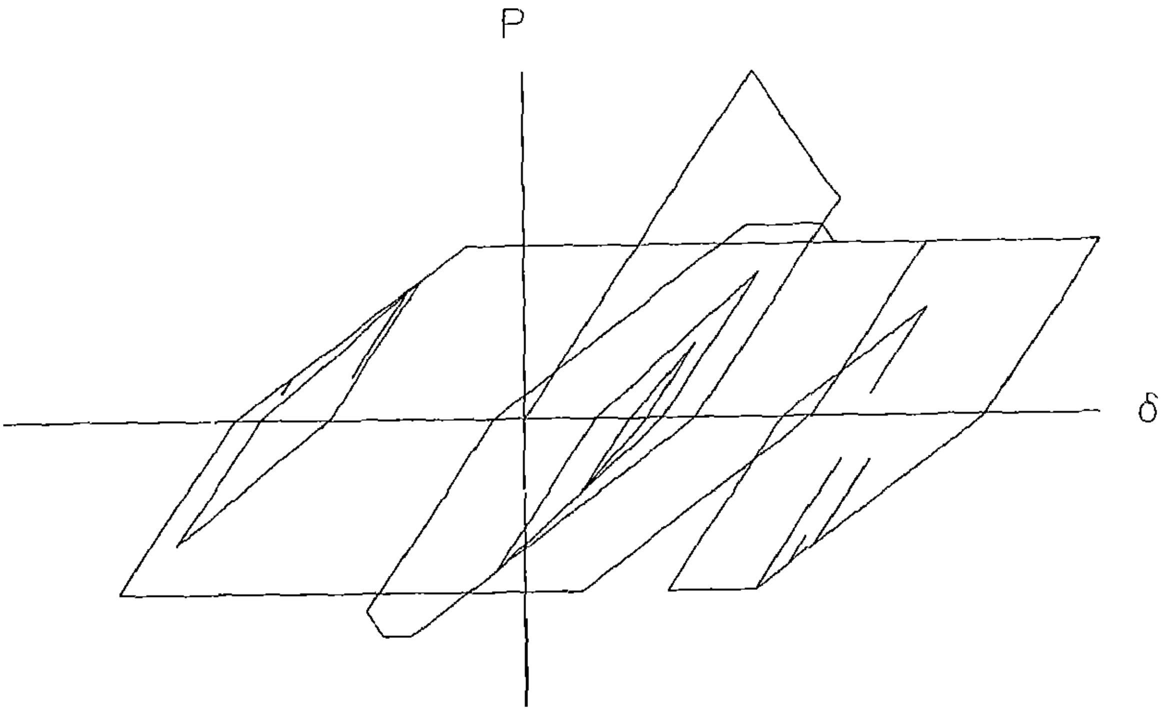

Figure 3.6 . Typical hysteresis loops as predicted by Trilinear Hysteresis Model for URM RC infilled frames

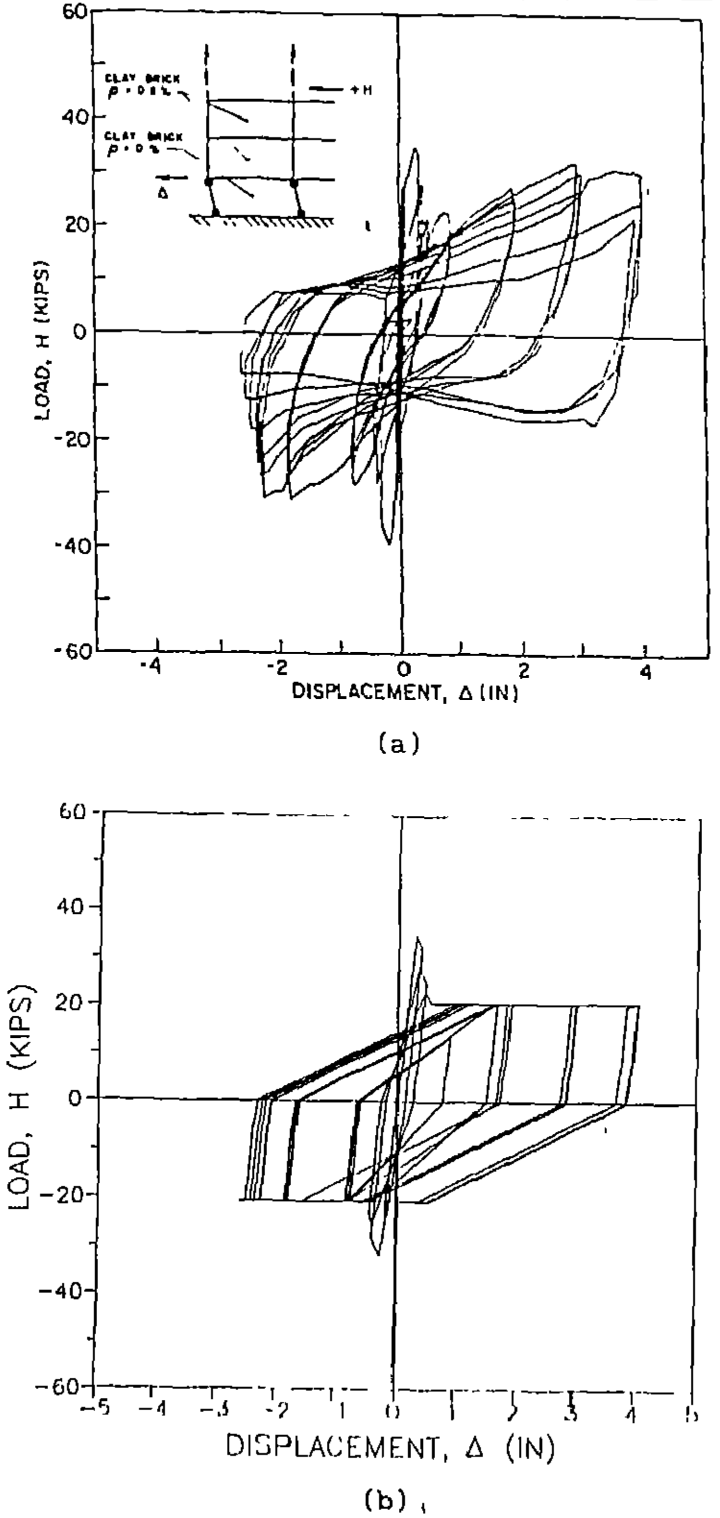

(a)

(b)

Figure 3.7 : Comparison of Load-deflection curves for URM RC infilled frames, (a) Experimental - test specimen 2 [Brokken and Bertero, 1981], (b) Analytical as predicted by Trilinear Hysteresis Model.

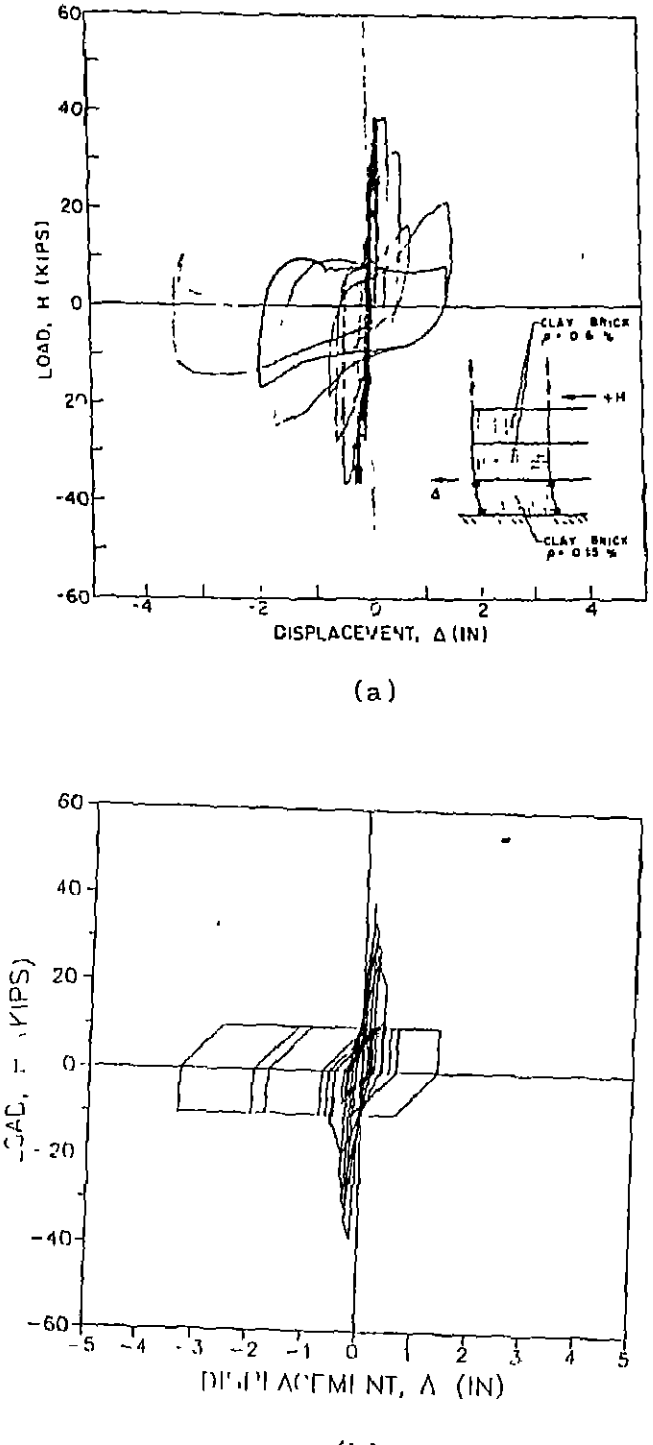

(a)

(b)

Figure 3.8 : Comparison of Load-deflection curves for URM RC infilled frames, (a) Experimental - test specimen 7 [Brokken and Bertero, 1981], (b) Analytical as predicted by Trilinear Hysteresis Model.

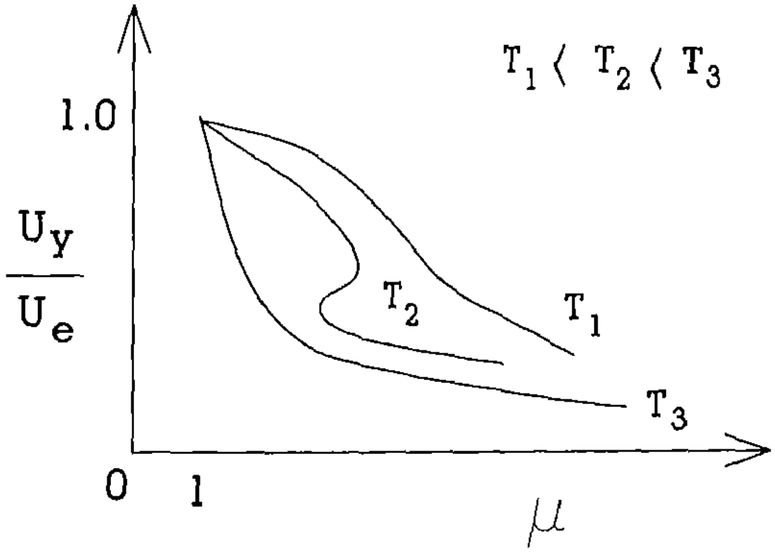

Figure 3.9 : Normalized yield displacement *versus* ductility curves for different natural periods, systems with EPP backbone curves

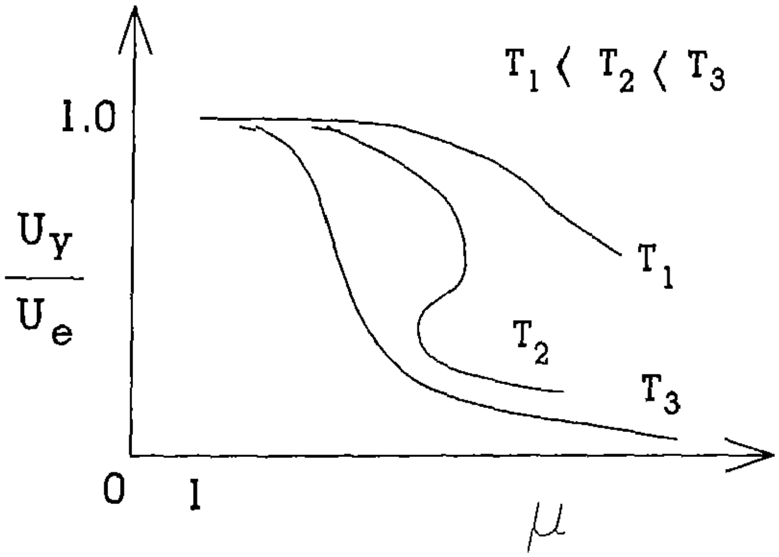

Figure 3.10 : Normalized yield displacement *versus* ductility curves for different natural periods, systems with trilinear backbone curve.

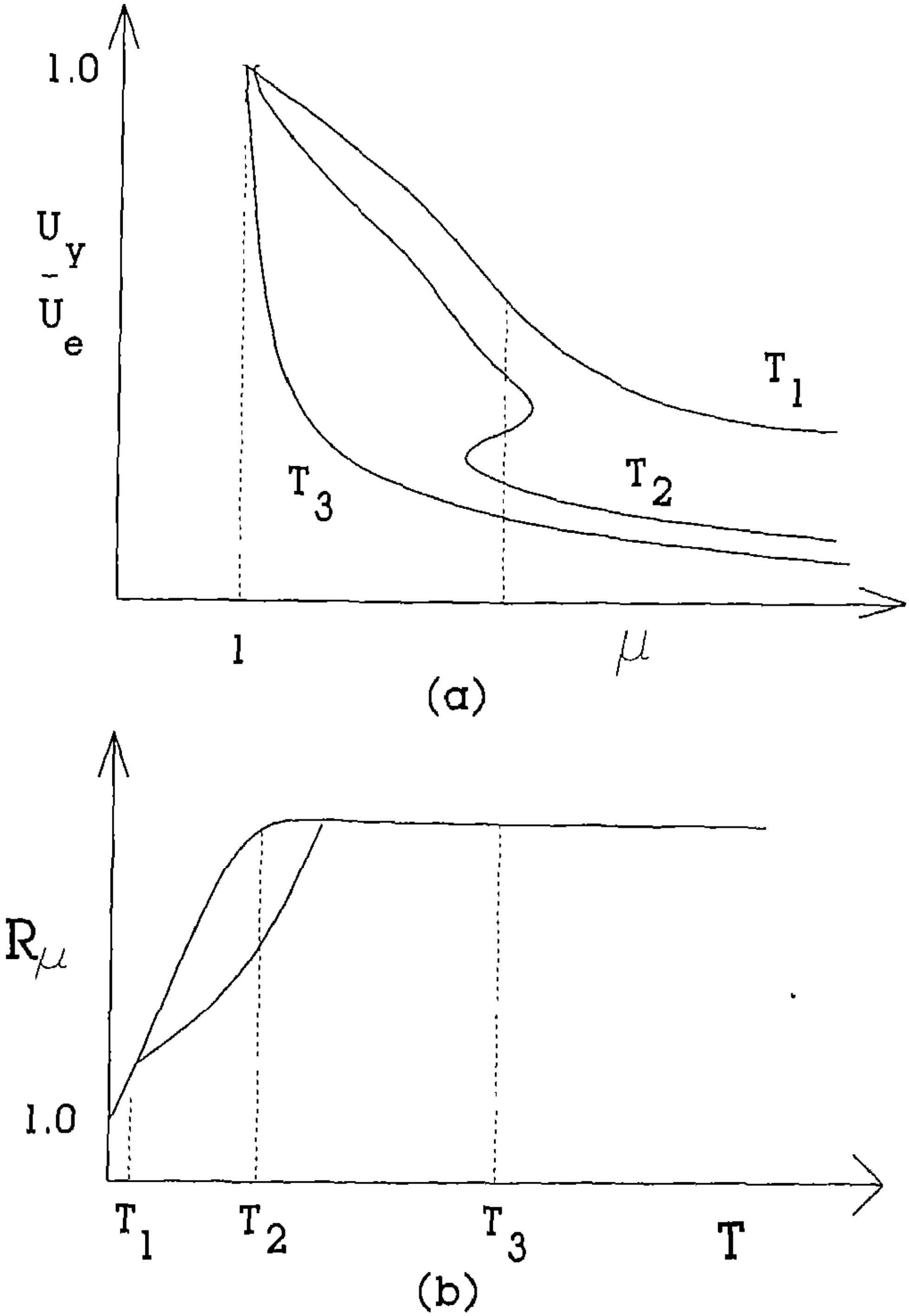

Figure 3.11 : Derivation of DRF from normalized yield displacement *versus* ductility curves

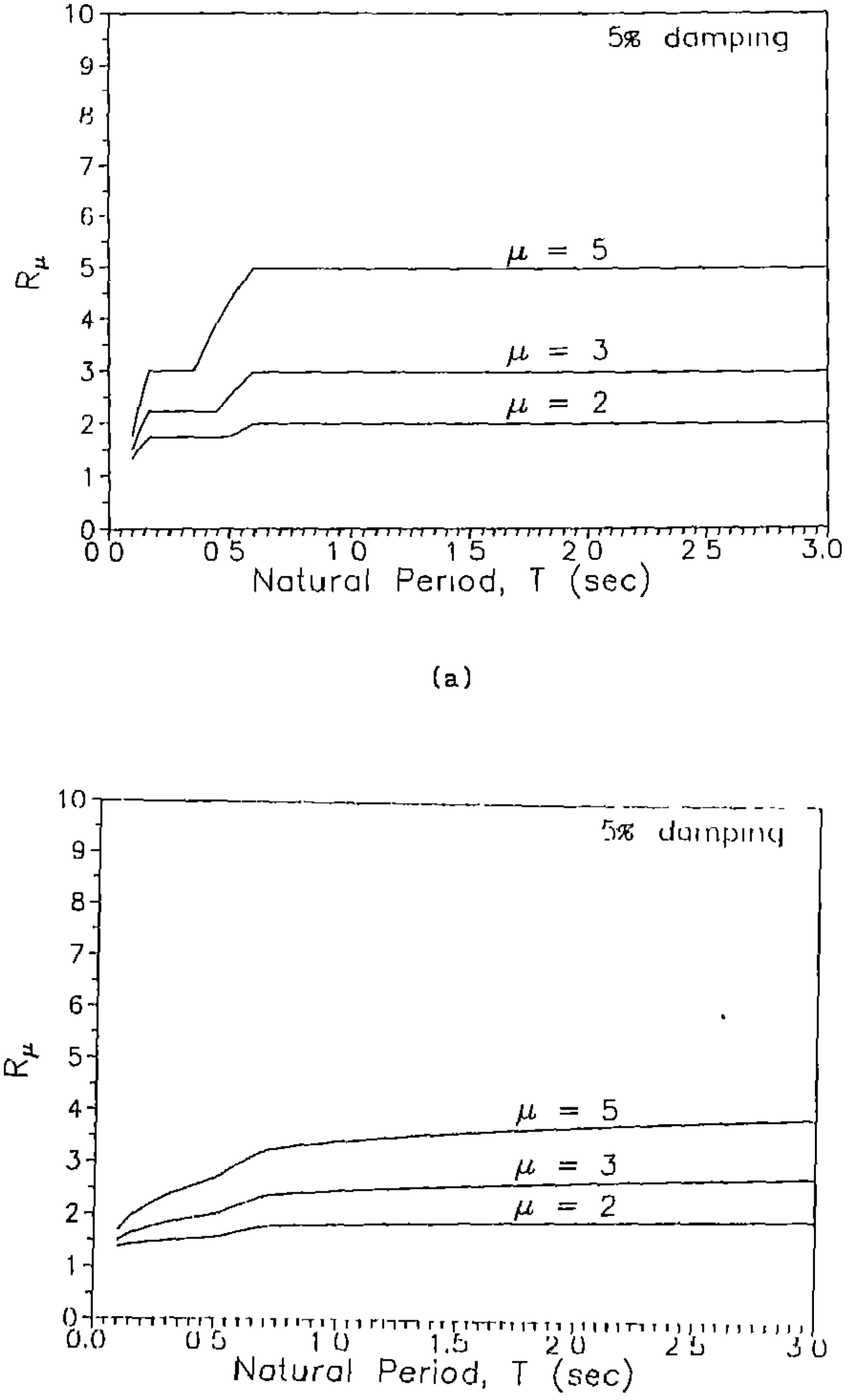

(b)

Figure 3.12 : DRF spectra proposed in the literature , (a) Newmark and Hall, 1973, (b) Lai and Biggs, 1980.

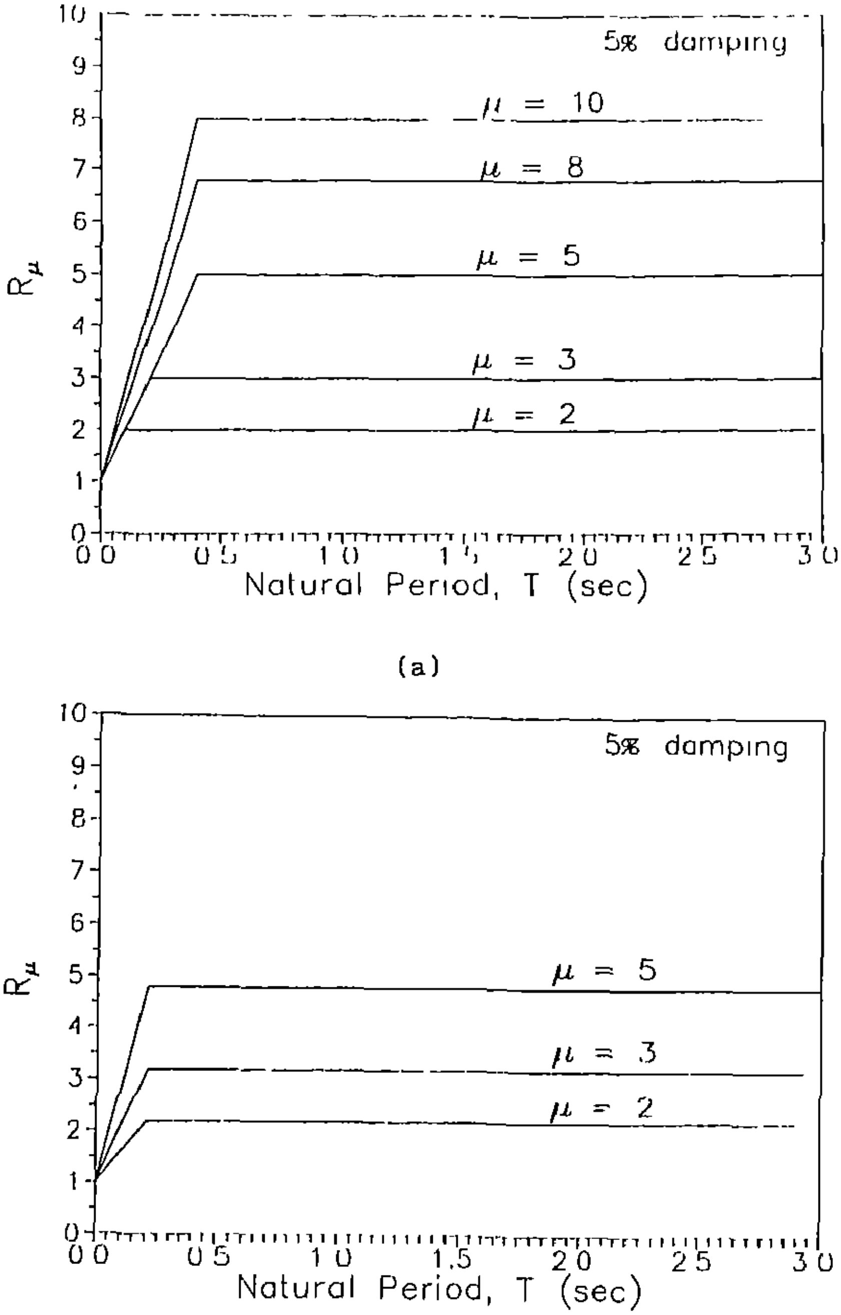

(a)

(b)

Figure 3.13 . DRF spectra proposed in the literature, (a) Riddell, *et al*, 1989 (d) Chandak and Jain, 1994

CHAPTER 4

PARAMETRIC STUDY

4.1 GENERAL

The properties of masonry are highly heterogeneous as discussed in Chapter 2. The exact stiffness and strength of the infilled frame depends on many uncertain factors. The available experimental data shows a large scatter. The difficulty is aggravated by the fact that even the different specimens tested as part of the same study, exhibit a large variation in properties. This is in some cases owing to the different specimens not being subjected to the same load-time history Also, under pseudo-static test conditions, affected due to slip, relaxation and strain-hardening seem to significantly influence the infilled frame characteristics. To overcome this difficulty, a parametric study is conducted with different values of the relevant parameters.

In this chapter, the conventional analysis based on the SDOF EPP system of the bare frame is compared with the analysis based on the Trilinear Hysteresis Model for the load-deformation characteristics of the RC infilled frame

4.2 GROUND MOTIONS CONSIDERED

The strong ground motions used in this study are chosen such that different features of the ground characteristics are well represented. The strong motion accelerograms recorded during the October 1991 Uttarkashi Earthquake in India are used to bring relevance to the study from the Indian context Twenty-four strong ground motion records collected from different stations during the Uttarkashi Earthquake are used in the analysis. The details of the same are listed in Table 4 1. The inelastic response spectra obtained from these ground motions are averaged and the standard deviations computed to extract meaningful trends The study also includes a few widely used earthquake strong ground motions recorded in US. These have markedly different characteristics, which help in drawing ground motion independent conclusions. The details of these ground motions are given in Table 4.2.

4.3 RANGE AND CHOICE OF PARAMETERS

In the absence of sufficient experimental data, selecting the ranges of the parameters is difficult. However, some typical representative values of each of them are selected. The parameters involved in this study are discussed below

4.3.1 Stiffness Ratio, $\mathcal{K}$

The experimental data available [Brokken and Bertero, 1981; Gergely *et al*, 1994; Klinger and Bertero, 1976; Kwan *et al*, 1990; Liauw, 1972] on URM infilled RC MRFs indicate that the ratio of stiffness of the infilled frame to that of the bare frame, hereinafter referred to as stiffness ratio, $\mathcal{K}$, may be about ten. This ratio varies with the characteristics of masonry, mortar, thickness of infill, frame member dimensions, presence and size of openings, and the prevalent construction practices. The presence of moderate-sized openings reduces this ratio by upto 50%, while bigger openings lead to an infilled frame stiffness which is only slightly higher than that of the bare frame Based upon the experimental results [Brokken and Bertero, 1981, Choubey, 1990, Klinger and Bertero 1976], three values of stiffness ratio, namely 2 0, 5.0 and 10 0 are selected for this study These are also listed in Table 4.3.

4.3.2 Strength Ratio, σ

The presence of the infill leads to a higher maximum load capacity for the frame. With reference to Figure 3 3, the ratio of this maximum load capacity, P_y, to the ultimate load capacity of the frame, P_u, hereinafter referred to as strength ratio, σ, has been found to vary with the type and size of infill and the openings present in it For the case of URM infilled RC MRFs, this ratio may be as high as two.
For investigating the effect of the variation in this parameter, five different values of this ratio, namely 1 0, 1.25, 1 5, 1.75 and 2.0 are considered in this study. These are also listed in Table 4.3

4.3.3 Slope Ratio, η

The third parameter defining the load-deformation characteristics of the infilled frames is the slope ratio, η, which is the ratio of the negative slope E_n, in the backbone curve, to the initial positive slope, E_p The value of E_n primarily depends on the type of masonry used. For brittle masonry, this is very high owing to a sudden drop in the load once the masonry fails. For ductile masonry, the slope is relatively much more gradual In line with these observations, four different values of slope ratio, namely 1000, 2, 1 and 0.2 have been used in this study. These are also listed in Table 4 3

4.4 RESULTS AND DISCUSSIONS

The results are shown in the form of mean DRF spectra for different values of the parameters. Each of these figures shows the plots of the DRF spectra with variation in one parameter only. The DRF spectrum for the bare frame is also included in each of these figures for comparison Similar figures showing the mean-minus-one standard deviation DRF spectra are also presented The natural period values on the horizontal axis of the DRF spectra for infilled frames correspond to their elastic stiffness. All the above figures correspond to a damping ratio of 5% The ductility values used are 1, 1.5, 2, 3, 5, 8, 10, 12 and 15

4.4.1 Uttarkashi Earthquake

The mean DRF curves for the Uttarkashi data, are shown in Figures 4 1 to 4.12. From these curves, the following conclusions are drawn ·

(1) The slope ratio η (=E_n/E_p) does not have any significant affect on the shape and values of the DRF spectra.

A marginal increase in the DRF values with increase in the slope ratio is noticed However, even this slight increase is observed only in the intermediate range of the natural period, and that too for higher values of strength ratio.

(2) The strength ratio σ (=P_y/P_u) also does not seem to significantly

influence the DRF spectra.

For higher values of σ, there is a slight reduction in the values of the DRF spectra. This reduction increases with increase in ductility The proportional reduction in the values is noticeable at very low natural periods.

(3) The stiffness ratio, $\mathcal{K}$ (=E_{if}/E_b), seems to significantly affect the shape and the values of the DRF spectra

This parameter influences the inelastic response of infilled frames most With increase in the stiffness ratio, $\mathcal{K}$, there is an increase in the value of the ductility reduction factor. The stiffness ratio, $\mathcal{K}$, directly governs the behaviour of infilled frames through the unloading stiffness, which remains at the level of the original elastic stiffness. Also, with increase in the stiffness ratio, $\mathcal{K}$, multiple peaks are observed in the intermediate natural period range.

(4) With increase in the stiffness ratio, $\mathcal{K}$, the DRF for infill frames curves for different ductility values converge to a value of unity, at non-zero, though very small, values of the natural period.

The above observation is in difference with the expected convergence to unity at zero natural period in case of bare frames The Trilinear Hysteresis Model for the infilled frame has an unstable negative slope. Here a marginal perturbation beyond the yield value, leads to a very sharp decline in the load carrying capacity, and consequently, to a relatively large value of displacement. This is very pronounced in the very short period systems. It leads to a sudden, sharp jump in the ductility value, and the smaller values of ductility are not at all achieved

Thus, with increase in K, a plateau is observed in the DRF spectra, with the DRF values remaining at unity till about 0.1 sec natural period for $K=10$.

From the mean-minus-one standard deviation curves shown in Figures 4.13 to 4 24 for the Uttarkashi data, the following conclusions can be drawn ·

(1) With increase in the K, the mean-minus-one standard deviation curves show a sharp V-notch in the intermediate natural period range, around a value of 0 3-0.4 secs

This v-notch is more pronounced for higher values of the stiffness ratio. The absence of this notch in the case of the bare frame suggests that this could be a characteristic of the infill properties However, it is also observed that the elastic spectra of the Uttarkashi earthquake ground motions exhibit a lull around the natural period of 0.3-0.4 secs [Das and Jain, 1993]. This suggests that the notch could well be a characteristic of the ground motion itself. Thus, in the intermediate natural period range corresponding to the location of this notch, there is a sharp, localized decrease in R_μ.

(2) It is noticed that the mean-minus-one standard deviation curves show a value less than unity for the short period range

For natural periods upto about 0 15 secs, the structure cannot be expected to realize the higher ductility levels for the extreme seismic shaking conditions. Since a value of less than unity for the DRF spectra is not meaningful, it can be taken as unity for this region.

(3) The DRF spectra for higher values of ductility exhibit a higher standard deviation

The above observation is also in line with those reported by other researchers for bilinear elasto-plastic systems [Chandak and Jain, 1993; Riddell *et al*, 1989]. Thus, for reliable estimates of the mean-minus-one standard deviation curves for higher ductility values, more data is required Moreover, these curves for the higher ductility values sometimes intersect those for the lower ductility values In such cases, the information presented by the mean-minus-one standard deviation curves do not follow the physically intuitive argument that the ductility reduction factor is always higher for systems with higher ductility Such crossing over of the m-σ curves have been observed [Chandak and Jain, 1994] in the very short natural period range for EPP systems for the Uttarkashi earthquake ground motions.

The crossing over of the m-σ curves as observed above may be a consequence of the inherent instability in the Trilinear Hysteresis Model owing to the presence of the negative slope The increase in the stiffness ratio, K, only adds to this instability Further, the complexity is increased by higher ductility values, which are already known to exhibit higher standard deviation values. This could also be due to high standard deviation for some stray points

4.4.2 US Earthquakes

The DRF spectra for each of these three strong ground motion records are computed separately. A few representative curves for a set of the parameters are given in Figure 4.25 to 4 27. These curves are for individual time histories. The trends shown by these are similar to those of the mean curves for the Uttarkashi Earthquake strong motion records

The conclusions derived from the Uttarkashi data also apply for these strong ground motion records. Since these strong ground motion records have widely different spectral characteristics, the results of this study seem to hold independent of the ground motion characteristics. However, a detailed study on this is required.

4.5 DESIGN IMPLICATIONS

In the light of the above limited parametric study, the following implications can be drawn for the design of infilled frames .

(a) The design DRF is inadequate for short buildings, *i.e.*, buildings with a low natural period value.

As is observed from the mean and the mean-minus-one standard deviation curves, the ductility reduction factor value is very close to unity till about 0.4 sec natural period. This implies that the design force cannot be reduced in the case of short period infilled frames. The DRF value being close to unity, the designer can only rely on the overstrength of the structure while reducing elastic force level through the use of response reduction factor.

(b) For infilled frames with high stiffness ratios, the DRF can be slightly increased over that of the corresponding bare frames

The DRF for infilled frames is slightly higher than that of the bare frames with the same natural period. This could be due to the stiffer and stronger initial characteristic upto yield of the infilled frames.

(c) The presence of the infill reduces the ductility demand on the frame members.

This conclusion has tremendous implications on the analysis and design of infilled frames. This study indicates that the DRF values are slightly higher for the infilled frames compared to that for bare frames, for a given ductility level Thus, the ductility demand on the building is lower However, the yield displacement is much smaller for the infilled frame building. Also, the increased strength of the building on account of the infills leads to a higher yield force level This implies that the maximum displacement of the infilled frame building is much smaller than that of the corresponding bare frame. This reduces the ductility demand on the RC frame members. The infilled frame dissipates more energy as compared to its bare frame for the same level of maximum displacement, provided the ultimate strengths of the two are same This is schematically shown in Figure 4.28

4.6 EXAMPLES

The examples below are intended to highlight the beneficial aspects of the presence of infills in RC MRFs. They also highlight the higher input seismic energy dissipation characteristics of infilled frames, whereby the infilled frames lead to lower maximum displacements, even after the infills have been completely damaged

In all the following examples, the subscripts "b" and "if" refer to bare frame and infilled frame, respectively

Example 1 : Frame with Large Natural Period

Let the bare frame have natural period, T_b, of 3 0 sec, yield displacement, $\Delta_{y,b}$, of 10 mm, and maximum elastic force, $F^{el}_{max,b}$, of 800 kN. Let the design ductility, μ, be 10 Therefore, the maximum displacement will be

$$\begin{aligned}\Delta_{max,b} &= \mu \times \Delta_{y,b}\\ &= 10 \times 10 = 100 \text{ mm}\end{aligned}$$

Then, ductility reduction factor, R_μ, [Riddell *et al*, 1989], is about 8 Thus, the yield base shear, $V_{y,b}$, of bare frame is

$$\begin{aligned}V_{y,b} &= \frac{F^{el}_{max,b}}{R_\mu}\\ &= \frac{800}{8} = 100 \text{ kN}\end{aligned}$$

Let the infilled frame corresponding to the same bare frame have a stiffness ratio, $\mathcal{K}$ (= E_{if}/E_b), of 10, and a strength ratio, σ (=P_y/P_u) of 2.0

$$\therefore \text{ Natural period, } \quad T_{if} = \frac{T_b}{\sqrt{E_{if}/E_b}}$$

$$= 0\ 95 \text{ sec}$$

Also, yield displacement, $\Delta_{y,b} = \frac{P_u}{E_{if}} = \frac{2P_u}{10E_b} = 0.2 \left(\frac{P_u}{E_b}\right) = 0.2\ \Delta_{y,b}$

$$= 0.2 \times 10 = 2 \text{ mm}$$

Assuming that the spectral acceleration due to the ground motion varies as 1/T between natural periods 0.5 sec, to 3 sec, the maximum elastic force $F^{el}_{max,if}$, is given by

$$F^{el}_{max,if} = F^{el}_{max,b} \times \frac{T_b}{T_{if}}$$

$$= 800 \times \frac{3}{0.95} = 2526 \text{ kN}$$

And, yield base shear, $V_{y,if} = \frac{P_y}{P_u} \times V_{y,b}$

$$= 2.0 \times 100 = 200 \text{ kN}$$

Thus, required value of ductility reduction factor, R_μ, for the infilled frame building is

$$R_\mu = \frac{2526}{200} = 12\ 6$$

From the results of current study (see Figure 4 9), the required ductility, μ, for the infilled frame building is about 15.

$$\therefore\ \Delta_{max,if} = \mu \times \Delta_{y,if} = 15 \times 2 = 30 \text{ mm}$$

Hence, the ductility demand on frame members is only 30/10 = 3.

The bare frame experiences a maximum displacement of 100mm. Its yield displacement is 10mm. However, the presence of infills reduces the maximum displacement to be experienced by the infilled frame building to 30mm. Insofar as the RC frame members are concerned, the ductility demand on them has been reduced. With respect to the yield displacement of the bare frame of 10mm, the maximum displacement of the infilled

ENTRAL LIBRARY
I I T KANPUR
No. A.121

frame building, and hence of the frame members, of 30mm implies a ductility demand of 3 on the RC frame members, as against 10 in case of bare frame members.

Example 2 : Frame with Intermediate Natural Period

Let the bare frame have natural period, T_b, of 0.5 sec, yield displacement, $\Delta_{y,b}$, of 4 mm, and maximum elastic force, $F^{el}_{max,b}$, of 3000 kN. Let the design ductility, μ, be 5. Therefore, the maximum displacement will be

$$\Delta_{max,b} = \mu \times \Delta_{y,b}$$
$$= 5 \times 4 = 20 \text{ mm}$$

Then, ductility reduction factor, R_μ, [Riddell *et al*, 1989], is about 5. Thus, the yield base shear, $V_{y,b}$, of bare frame is

$$V_{y,b} = \frac{F^{el}_{max,b}}{R_\mu}$$
$$= \frac{3000}{5} = 600 \text{ kN}$$

Let the infilled frame corresponding to the same bare frame have a stiffness ratio, $\mathcal{K}$ (= E_{if}/E_b), of 10, and a strength ratio, σ (=P_y/P_u) of 2.0.

$$\therefore \text{ Natural period, } \quad T_{if} = \frac{T_b}{\sqrt{E_{if}/E_b}}$$
$$= 0\ 16 \text{ sec}$$

$$\text{Also, yield displacement, } \Delta_{y,b} = \frac{P_u}{E_{if}} = \frac{2P_u}{10E_b} = 0.2\left(\frac{P_u}{E_b}\right) = 0\ 2\ \Delta_{y,b}$$
$$= 0.2 \times 4 = 0.8 \text{ mm}$$

Assuming that the spectral acceleration due to the ground motion is constant between natural periods 0 16 sec to 0.5 sec, the maximum elastic force $F^{el}_{max,if}$, is given by

$$F^{el}_{max,if} = F^{el}_{max,b}$$

$$= 3000 \text{ kN}$$

And, yield base shear, $V_{y,if} = \frac{P_y}{P_u} \times V_{y,b}$

$$= 2\ 0 \times 600 = 1200 \text{ kN}$$

Thus, required value of ductility reduction factor, R_μ, for the infilled frame building is

$$R_\mu = \frac{3000}{1200} = 2\ 5$$

From the results of current study (see Figure 4.9), the required ductility, μ, for the infilled frame building is about 3.

$$\Delta_{max,if} = \mu \times \Delta_{y,if} = 3 \times 0.8 = 2.4 \text{ mm}$$

Hence, the ductility demand on frame members is just 2 4/4 = 0 6.

The bare frame experiences a maximum displacement of 20 mm. Its yield displacement is 4 mm. However, the presence of infills reduces the maximum displacement to be experienced by the infilled frame building to 2.4 mm. *Insofar as the RC frame members are concerned,* the ductility demand on them has been reduced. With respect to the yield displacement of the bare frame of 4 mm, the maximum displacement of the infilled frame building, and hence of the frame members, of 2.4 mm implies a ductility demand of 0 6 on the RC frame members, as against 5 in case of bare frame members Thus, there is no ductility demand on the frame members. However, the ductility demand on the infilled frame as a whole is 5.

Example 3 : Frame with Low Natural Period

Let the bare frame have natural period, T_b, of 0.3 sec, yield displacement, $\Delta_{y,b}$, *of* 2 *mm*, and *maximum elastic force*, $F^{el}_{max,b}$, *of* 3000 kN. Let the design ductility, μ, be 2. Therefore, the maximum displacement will be

$$\begin{aligned} \Delta_{max,b} &= \mu \times \Delta_{y,b} \\ &= 2 \times 2 = 4 \text{ mm} \end{aligned}$$

Then, ductility reduction factor, R_μ, [Riddell *et al*, 1989], is about 2. Thus, the yield base shear, $V_{y,b}$, of bare frame is

$$\begin{aligned} V_{y,b} &= \frac{F^{el}_{max,b}}{R_\mu} \\ &= \frac{3000}{2} = 1500 \text{ kN} \end{aligned}$$

Let the infilled frame corresponding to the same bare frame have a stiffness ratio, $\mathcal{K}$ (= E_{if}/E_b), of 10, and a strength ratio, σ (=P_y/P_u) of 1.25.

$$\therefore \text{Natural period, } T_{if} = \frac{T_b}{\sqrt{E_{if}/E_b}} = 0.095 \text{ sec}$$

$$\text{Also, yield displacement, } \Delta_{y,if} = \frac{P_u}{E_{if}} = \frac{2P_u}{10E_b} = 0.2\left(\frac{P_u}{E_b}\right) = 0.2\,\Delta_{y,b} = 0.125 \times 2 = 0.25 \text{ mm}$$

Assuming that the spectral acceleration due to the ground motion is linear between natural periods 0.0 sec to 0.1 sec, the maximum elastic force $F^{el}_{max,if}$, is given by

$$F^{el}_{max,if} = F^{el}_{max,b} \times \left[2.5 - \left(\frac{2.5 - 1.0}{0.1 - 0.0}\right)(0.1 - T_{if})\right] / 2.5$$

$$= 2910 \text{ kN}$$

And, yield base shear, $V_{y,if} = \frac{P_y}{P_u} \times V_{y,b}$

$$= 1.25 \times 1500 = 1875 \text{ kN}$$

Thus, required value of ductility reduction factor, R_μ, for the infilled frame building is

$$R_\mu = \frac{2910}{1875} \approx 1.55$$

From the results of current study (see Figure 4.9), the required ductility, μ, for the infilled frame building is about 5.

$$\therefore \Delta_{max,if} = \mu \times \Delta_{y,if} = 5 \times 0.25 = 1.25 \text{ mm}$$

Hence, the ductility demand on frame members is just 1.25/2 = 0.625

The bare frame experiences a maximum displacement of 4 mm. Its yield displacement is 2 mm However, the presence of infills reduces the maximum displacement to be experienced by the infilled frame building to 1.25 mm. Insofar as the RC frame members are concerned, the ductility demand on them has been reduced. With respect to the yield displacement of the bare frame of 2 mm, the maximum displacement of the infilled frame building, and hence of the frame members, of 1.25 mm implies a ductility demand of 0.625 on the RC frame members, as against 2 in case of bare frame members Thus, there is no ductility demand on the frame members.

4 7 THE ROLE OF INFILLS

Based upon the current study, although the infilled frame loses strength and stiffness on cracking of the masonry infills, the initial stiffness and strength contribution of the infills significantly alters the overall behaviour of the frame during the later load cycles Also, it continues to govern the subsequent behaviour through the unloading stiffness, which is same as the initial infilled frame stiffness This reduces the ductility demand on the frame members Thus, the increased initial stiffness of the frame cannot be ignored and must be incorporated in the analysis and design of building frames with infills.

It has been noticed during the past earthquakes that in countries like India, where RC frame buildings are built with brick infills, many of these infilled frame buildings, constructed by local masons without any formal aseismic considerations, have performed well On the other hand, many formally constructed reinforced concrete frame structures without infills, even in countries with good aseismic construction, have performed poorly in the past earthquakes. The examples in the previous section clearly bring out the role of the infills in reducing the maximum displacement, and hence, the damage incurred by the frame. The role of the increased stiffness and strength contributions of the infills is, thus, not just limited to the initial response of the infilled frames, but does effect the hysteretic response even after the infills have been damaged.

4.8 DESIGN SPECTRA

The results of the study clearly indicate that the shape of the DRF spectra are affected severely by the ground motions considered The US ground motions are significantly different from the Indian ground motions and consequently, their DRF spectra are widely different in shape. Hence, the design spectra of other countries cannot be used as the design spectra in India Moreover, different sites within the country may have significantly different frequency contents Thus, site specific spectra need to be evolved. Towards this end, the average spectra of all the data and parameters considered in this study is relevant and meaningful. Figure 4.29 shows the average spectra for all the parameters considered in this study

The above figure is meaningful for the Uttarkashi data only. However, the Uttarkashi data is similar in content to other Himalayan ground motions [Chandak and Jain, 1994], and thus, the above figure may serve as a design spectrum for the Himalayan region. However, region specific design spectra still need to be evolved for other parts of the country.

Table 4.1 : Strong Ground Motion Data Recorded During the Uttarkashi Earthquake, 1991 Used in This Study.

Location	Distance	MMI	Dirn *	Peak ** Ground Accl (g)	Peak ** Ground Vel. (mm/ sec)	Peak ** Ground Accl (mm)	Spectral Inten- sity (mm)	A/V Ratio (sec^{-1})
Bhatwari	25	VIII	L T	0.253 0.247	178.73 207.78	37.54 53.23	709.73 1235.36	13.90 8.12
Uttarkashi	40	VIII$^-$	L T	0.242 0.310	169.56 194.68	21.15 19.85	448.86 579.36	13.99 15.61
Ghansali	41	VII	L T	0.118 0.117	80.44 78.21	13.57 13.37	317.02 300.50	14.37 14.69
Rudraprayag	54	VI$^+$	L T	0.053 0.052	20.70 27.06	7.85 4.01	77.61 75.30	25.26 18.76
Tehri	54	VI	L T	0.073 0.062	42.15 92.30	8.17 19.84	184.29 373.62	16.94 6.62
Barkot	63	VI$^+$	L T	0.095 0.082	57.87 44.84	10.93 6.98	183.37 148.44	16.10 17.95
Koteshwar	65	VI	L T	0.101 0.056	51.55 39.27	11.14 6.78	194.54 170.16	19.18 16.61
Karnaprayag	65	VI$^+$	L T	0.062 0.079	36.90 37.30	5.80 4.02	103.23 91.72	16.53 20.74
Purola	76	VI$^+$	L T	0.075 0.093	48.13 45.91	8.44 9.22	112.21 176.59	15.36 19.97
Koti	105	VI	L T	0.021 0.042	23.43 28.60	4.27 3.40	80.44 91.88	8.81 14.32
Kosani	144	V$^+$	L T	0.029 0.032	18.82 15.55	3.77 2.86	46.16 45.65	15.06 20.26
Almora	150	V$^+$	L T	0.018 0.021	13.32 12.62	3.42 4.50	45.44 46.77	13.07 16.66

* L - Longitudinal, T - Transverse

** Peak acceleration, velocity, and displacement values are from Chandrasekharan and Das, 1992.

Table 4.2 : Strong Ground Motion Data Recorded During the Earthquakes, in US, Used in This Study.

Strong Motion Records	Peak Ground Acceleration (PGA) (cm/s/s)
El Centro[1]	341.7
Taft[2]	152.7
Pacoima Dam[3]	1148 1

1. Imperial Valley Earthquake, 1940, El Centro Site Imperial Valley Irrigation District.
2. Kern County Earthquake 1952, Taft Lincoln School Tunnel.
3 San Fernando Earthquake 1971, Pacoima Dam Abutment

The data has been taken from Hudson, *et al,* 1976

Table 4.3 : Different values of the parameters chosen in the current study.

Stiffness Ratio $\mathcal{K} = E_{lf}/E_b$	2.0, 5.0, 10.0
Slope Ratio $\eta = E_n/E_p$	1000, 2, 1, 0.2
Strength Ratio $\sigma = P_y/P_u$	1.0, 1.25, 1.5, 1.75, 2.0

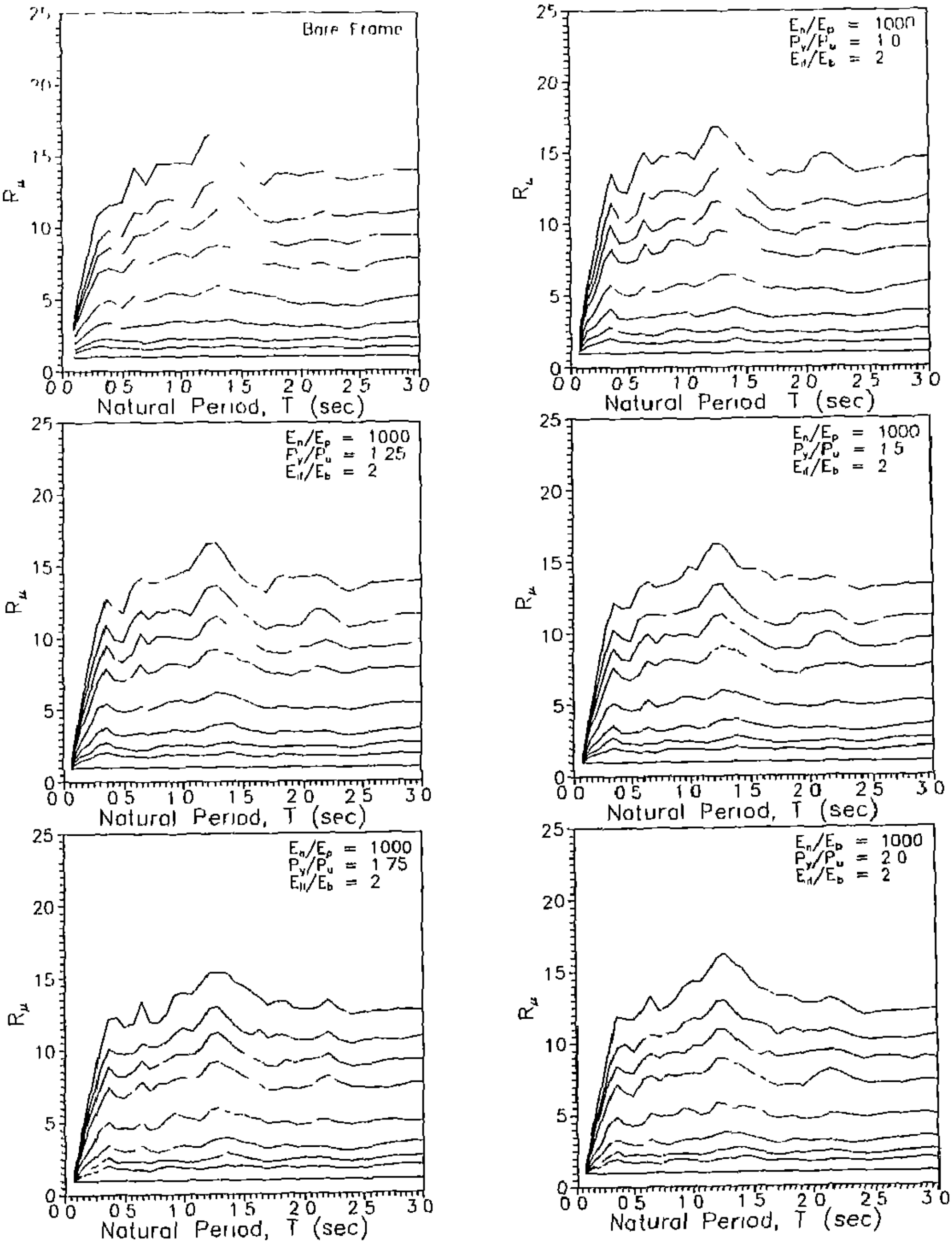

Figure 4.1 . Mean DRF spectra of Uttarkashi earthquake strong motion records, for URM RC infilled frame with stiffness ratio, $\mathcal{K}$ (=E_{if}/E_b)=2, and slope ratio, η (=E_n/E_p)=1000, for different values of strength ratio, σ (=P_y/P_u). Mean DRF spectra of bare frame also shown.

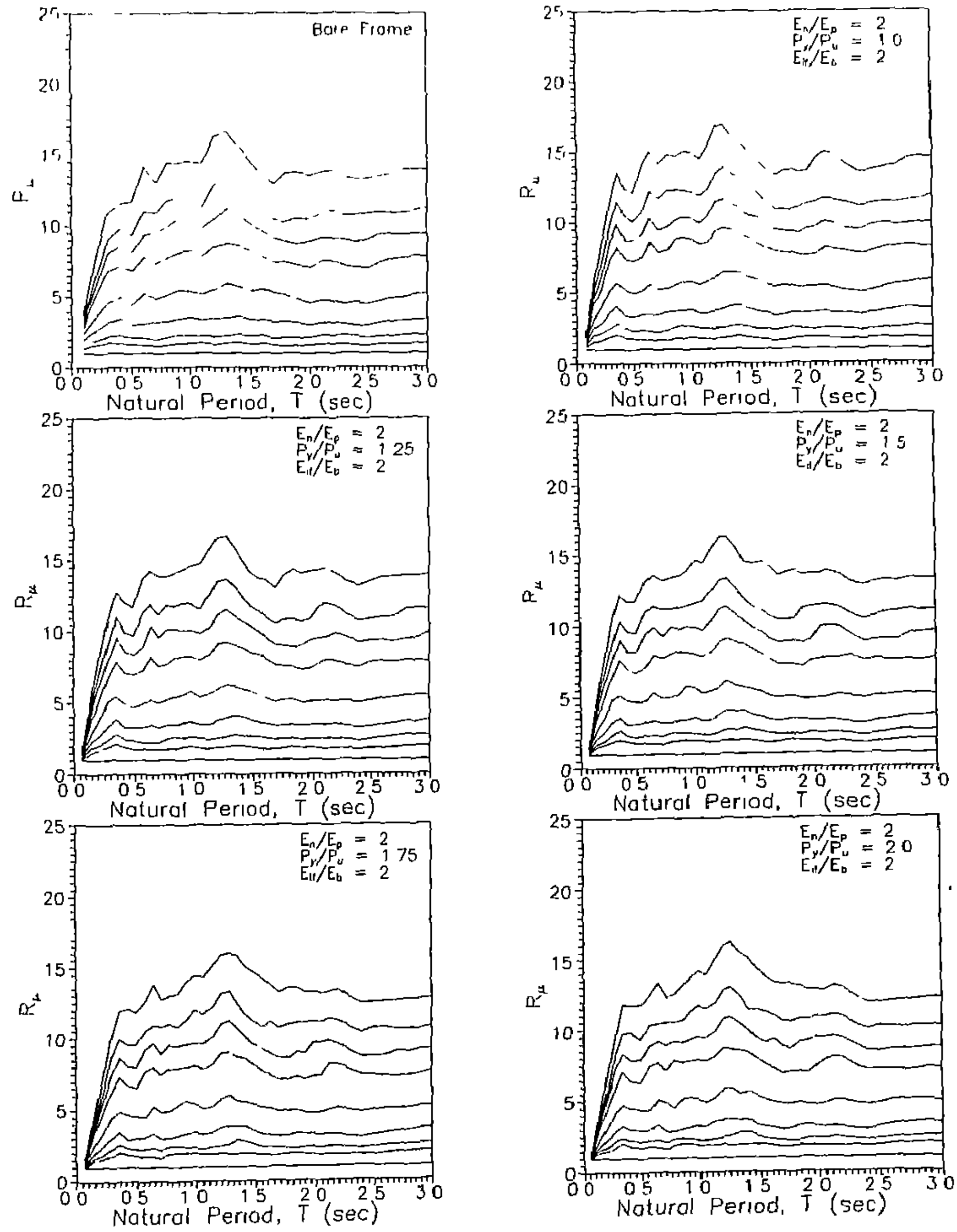

Figure 4.2 . Mean DRF spectra of Uttarkashi earthquake strong motion records, for URM RC infilled frame with stiffness ratio, $\mathcal{K}$ ($=E_{if}/E_b$)=2, and slope ratio, η ($=E_n/E_p$)=2, for different values of strength ratio, σ ($=P_y/P_u$). Mean DRF spectra of bare frame also shown.

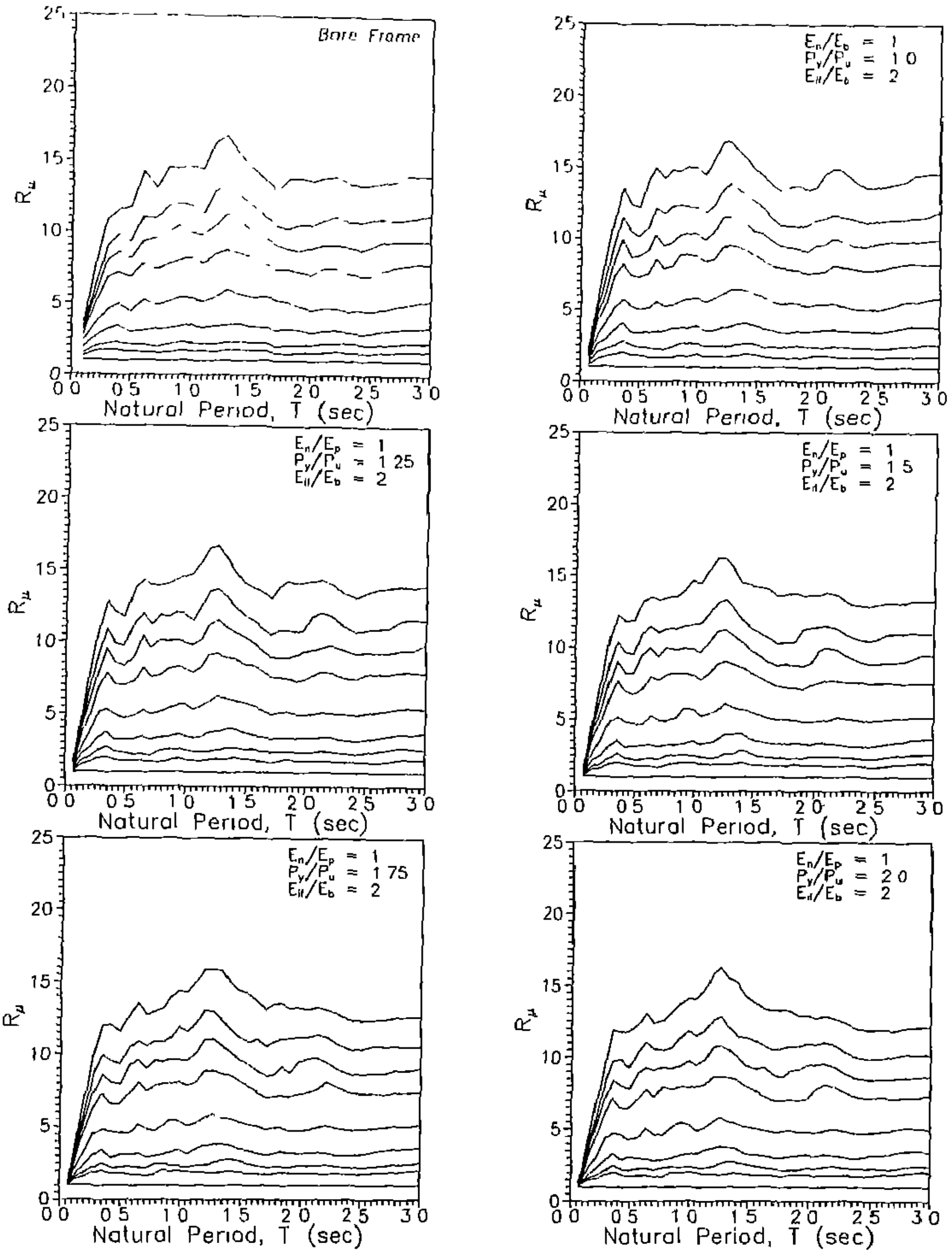

Figure 4.3 : Mean DRF spectra of Uttarkashi earthquake strong motion records, for URM RC infilled frame with stiffness ratio, $\mathcal{K}$ (=E_{if}/E_b)=2, and slope ratio, η (=E_n/E_p)=1, for different values of strength ratio, σ (=P_y/P_u). Mean DRF spectra of bare frame also shown

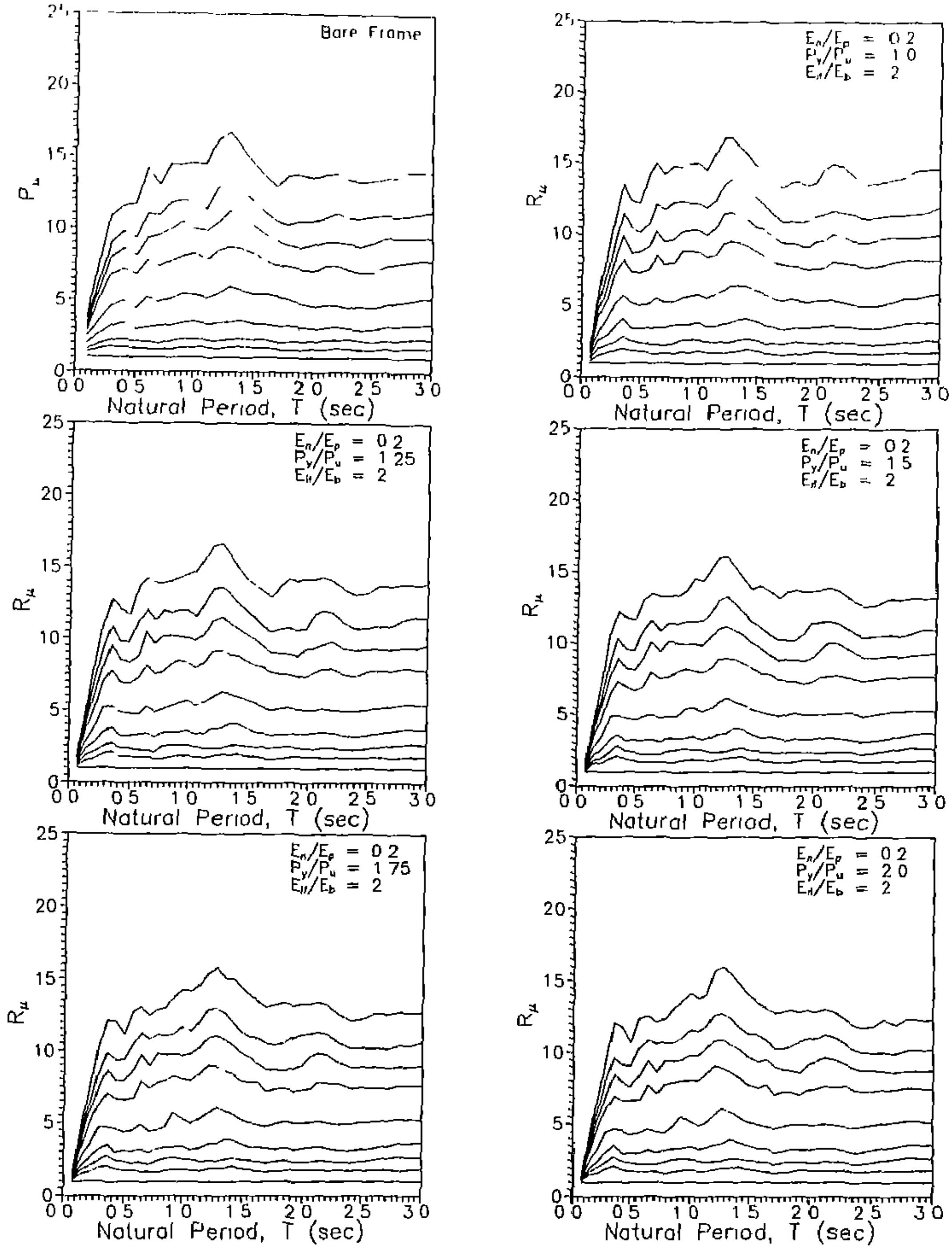

Figure 4.4 : Mean DRF spectra of Uttarkashi earthquake strong motion records, for URM RC infilled frame with stiffness ratio, $\mathcal{K}$ $(=E_{if}/E_b)=2$, and slope ratio, η $(=E_n/E_p)=0.2$, for different values of strength ratio, σ $(=P_y/P_u)$ Mean DRF spectra of bare frame also shown.

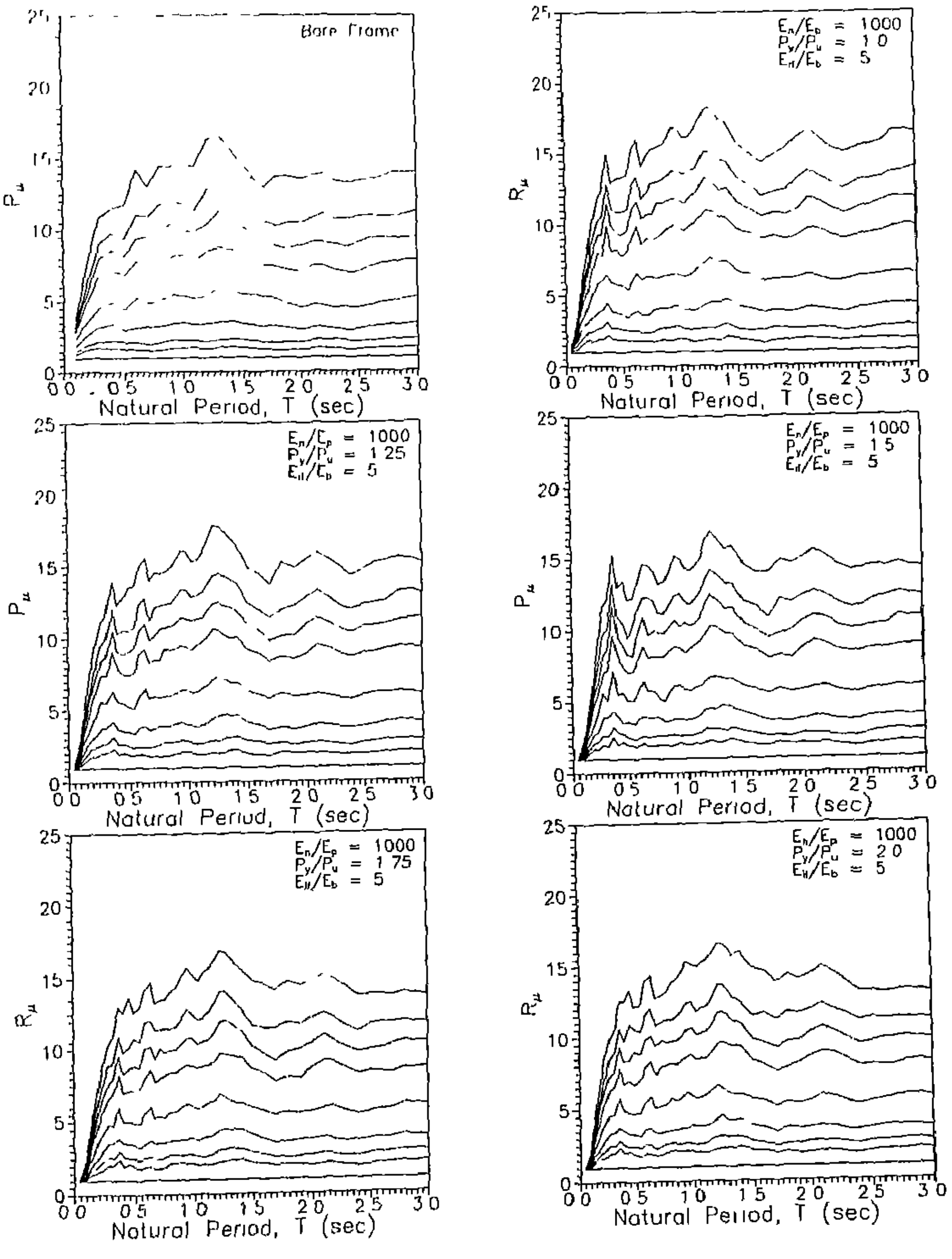

Figure 4.5 : Mean DRF spectra of Uttarkashi earthquake strong motion records, for URM RC infilled frame with stiffness ratio, $\mathcal{K}$ $(=E_{if}/E_b)=5$, and slope ratio, η $(=E_n/E_p)=1000$, for different values of strength ratio, σ $(=P_y/P_u)$. Mean DRF spectra of bare frame also shown.

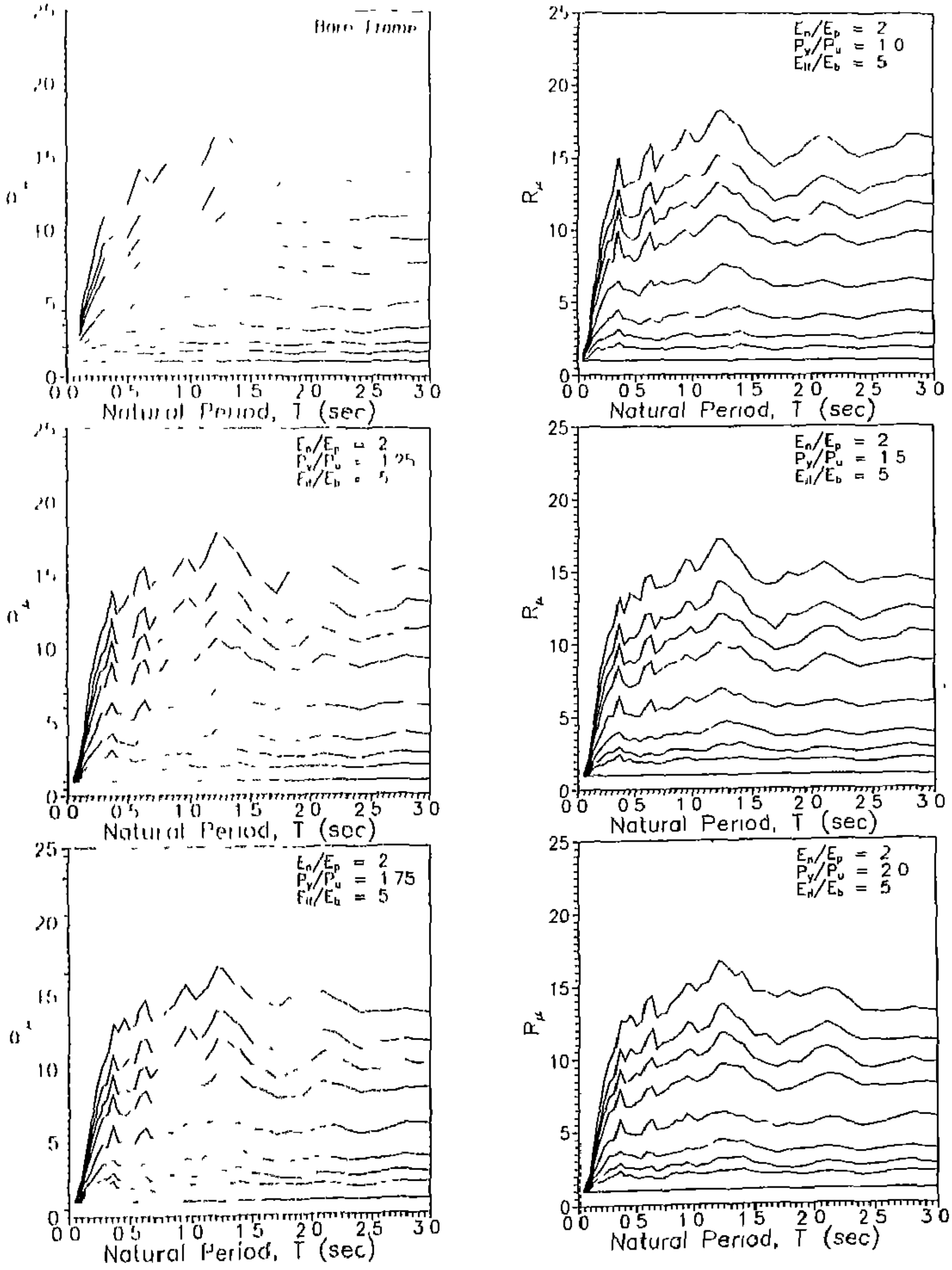

Figure 4.6 : Mean DRF spectra of Uttarkashi earthquake strong motion records, for URM RC infilled frame with stiffness ratio, $\mathcal{K}$ (=E_{if}/E_b)=5, and slope ratio, η (=E_n/E_p)=2, for different values of strength ratio, σ (=P_y/P_u). Mean DRF spectra of bare frame also shown.

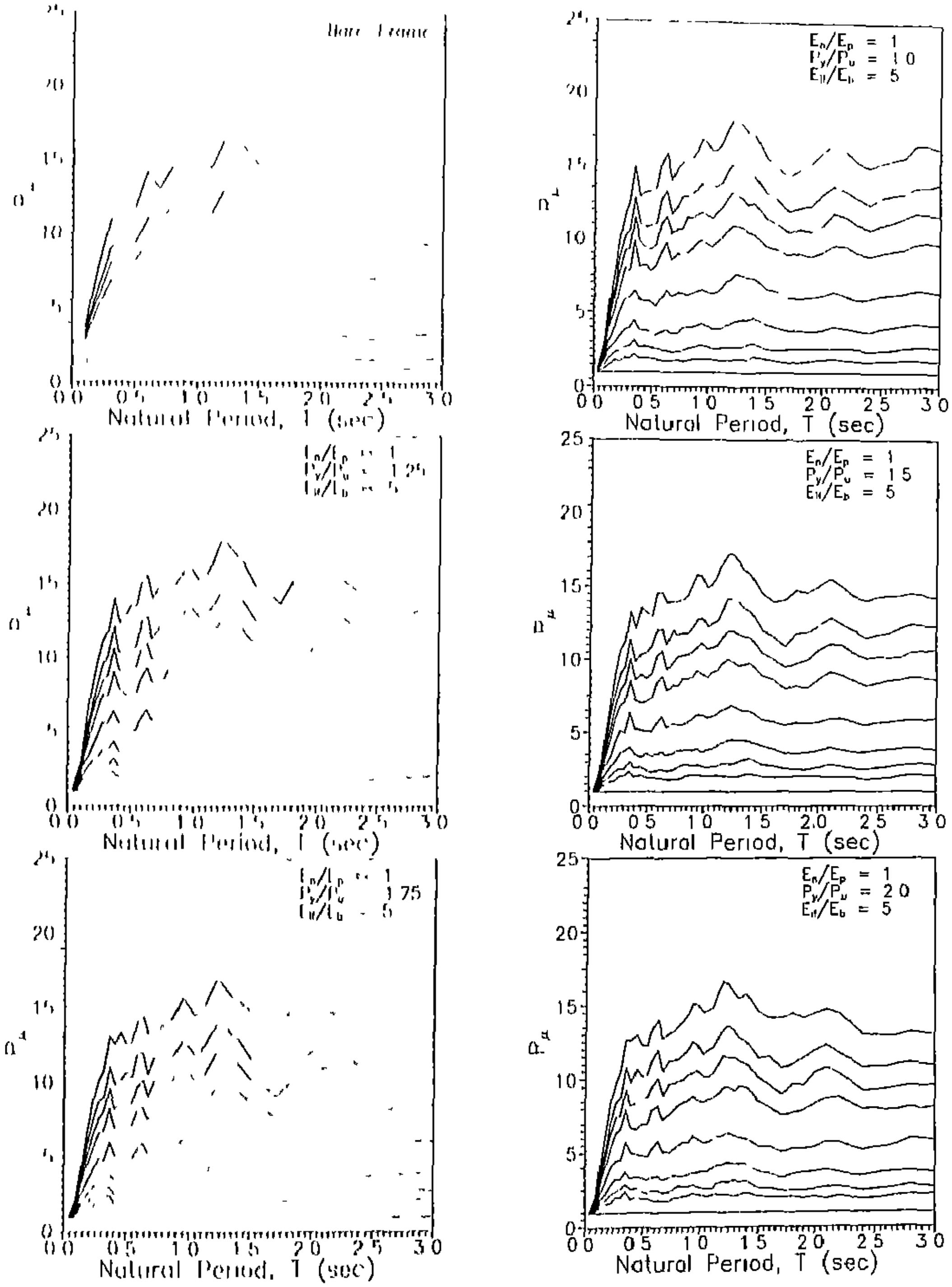

Figure 4.7 : Mean DRF spectra of Uttarkashi earthquake strong motion records, for URM RC infilled frame with stiffness ratio, $\mathcal{K}$ ($=E_{if}/E_b$)=5, and slope ratio, η ($=E_n/E_p$)=1, for different values of strength ratio, σ ($=P_y/P_u$). Mean DRF spectra of bare frame also shown.

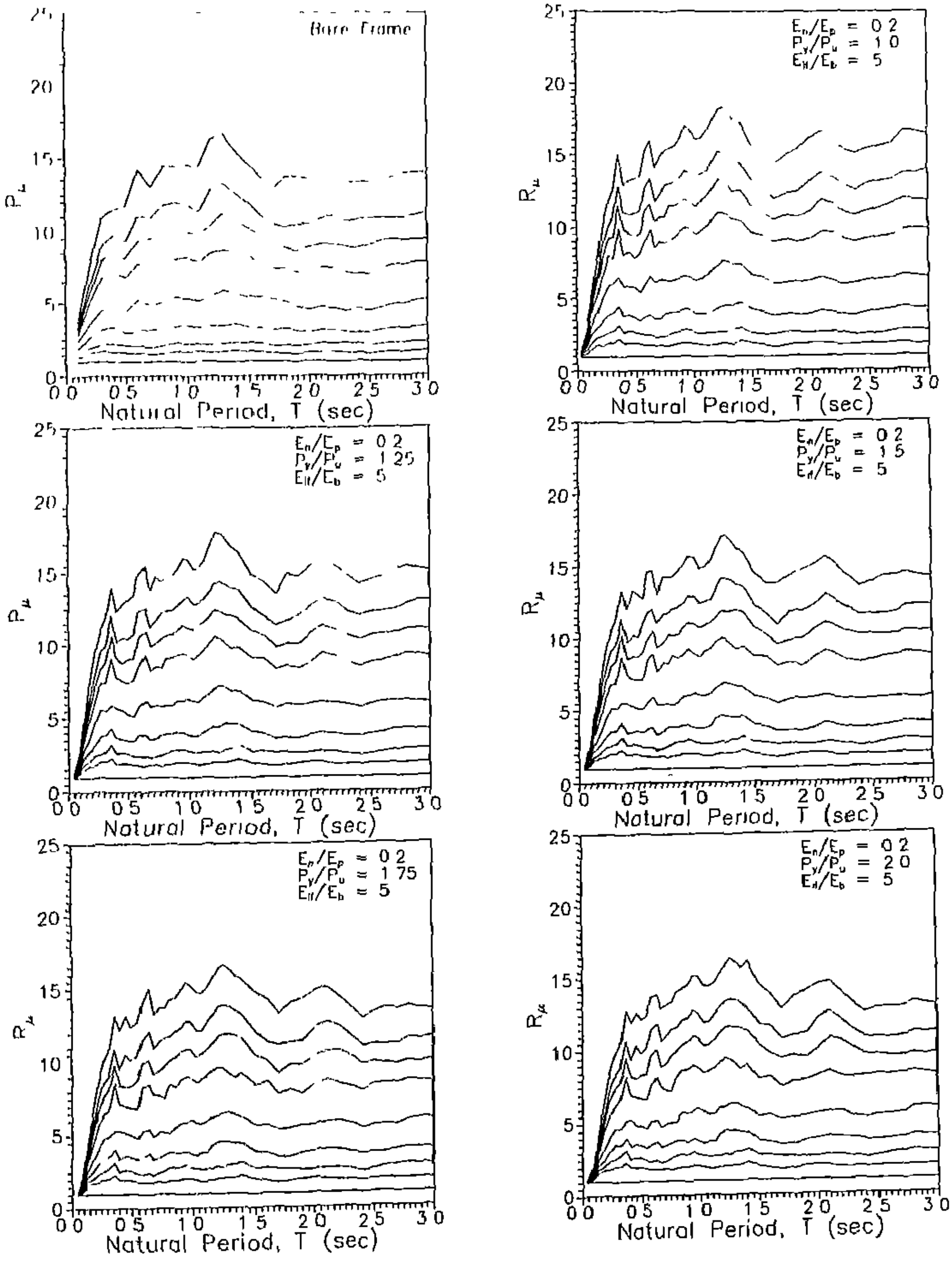

Figure 4.8 : Mean DRF spectra of Uttarkashi earthquake strong motion records, for URM RC infilled frame with stiffness ratio, $\mathcal{K}$ (=E_{if}/E_b)=5, and slope ratio, η (=E_n/E_p)=0.2, for different values of strength ratio, σ (=P_y/P_u) Mean DRF spectra of bare frame also shown.

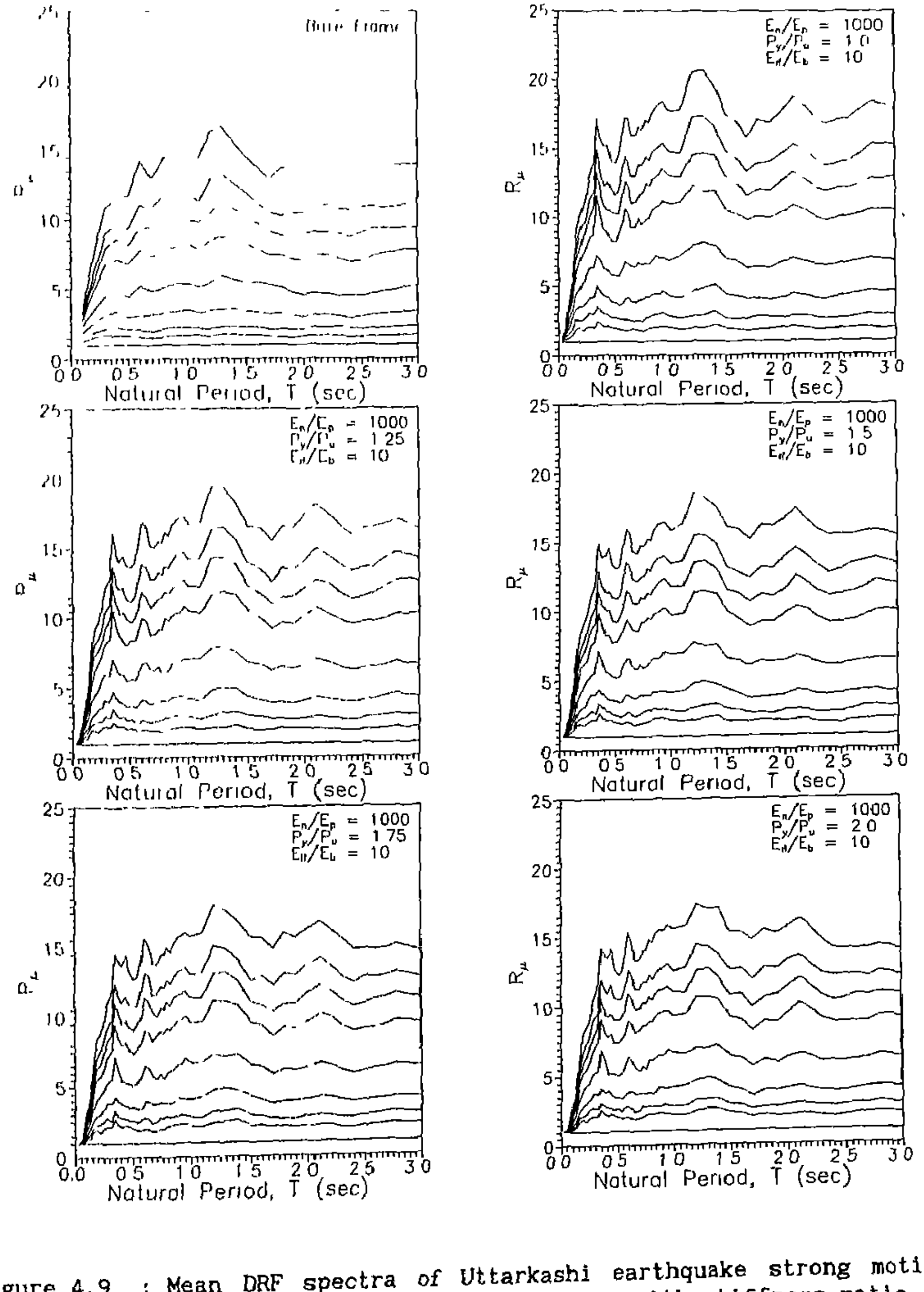

Figure 4.9 : Mean DRF spectra of Uttarkashi earthquake strong motion records, for URM RC infilled frame with stiffness ratio, $\mathcal{K}$ ($=E_{1f}/E_b$)=10, and slope ratio, η ($=E_n/E_p$)=1000, for different values of strength ratio, σ ($=P_y/P_u$). Mean DRF spectra of bare frame also shown.

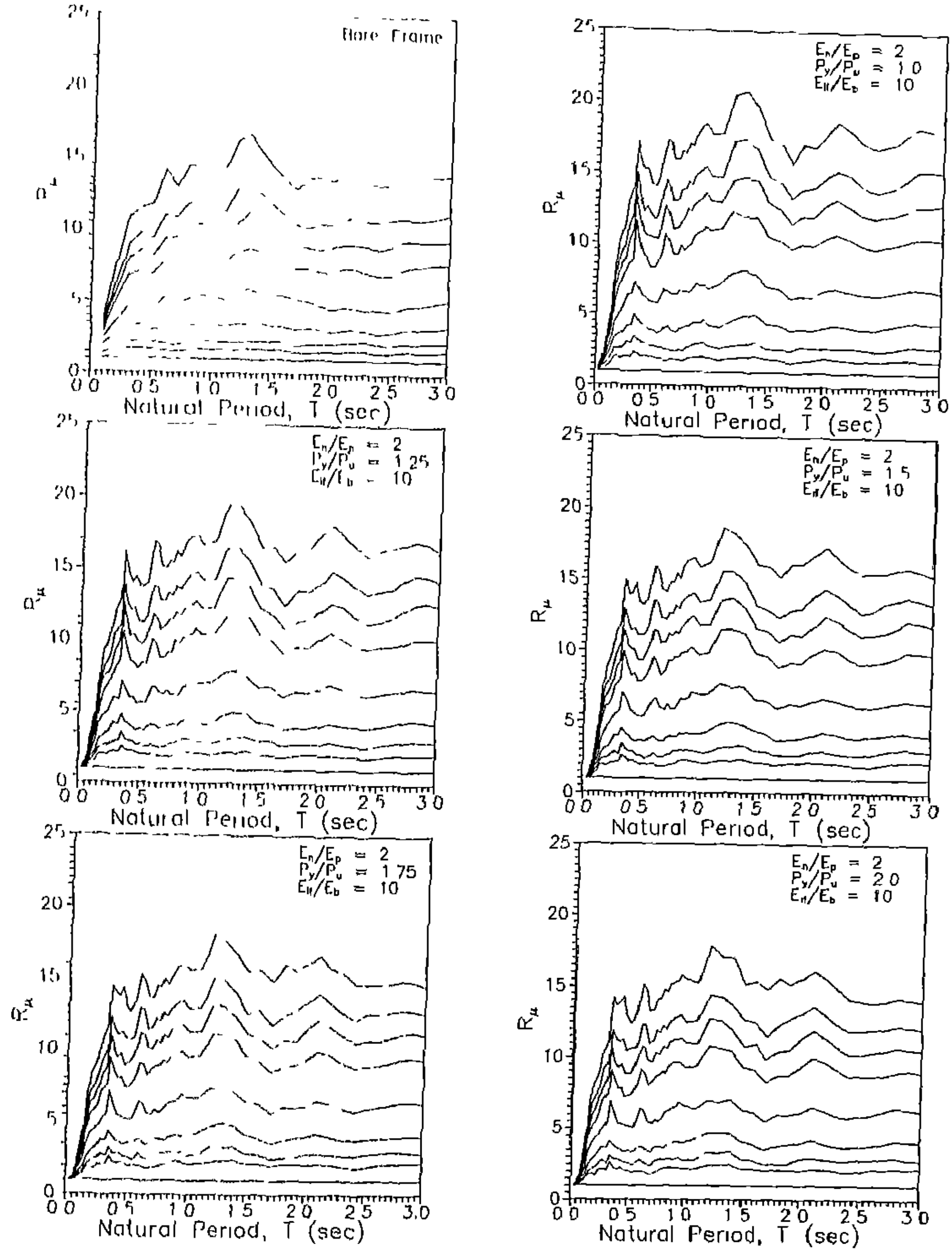

Figure 4.10 : Mean DRF spectra of Uttarkashi earthquake strong motion records, for URM RC infilled frame with stiffness ratio, $\mathcal{K}$ ($=E_{if}/E_b$)=10, and slope ratio, η ($=E_n/E_p$)=2, for different values of strength ratio, σ ($=P_y/P_u$) Mean DRF spectra of bare frame also shown

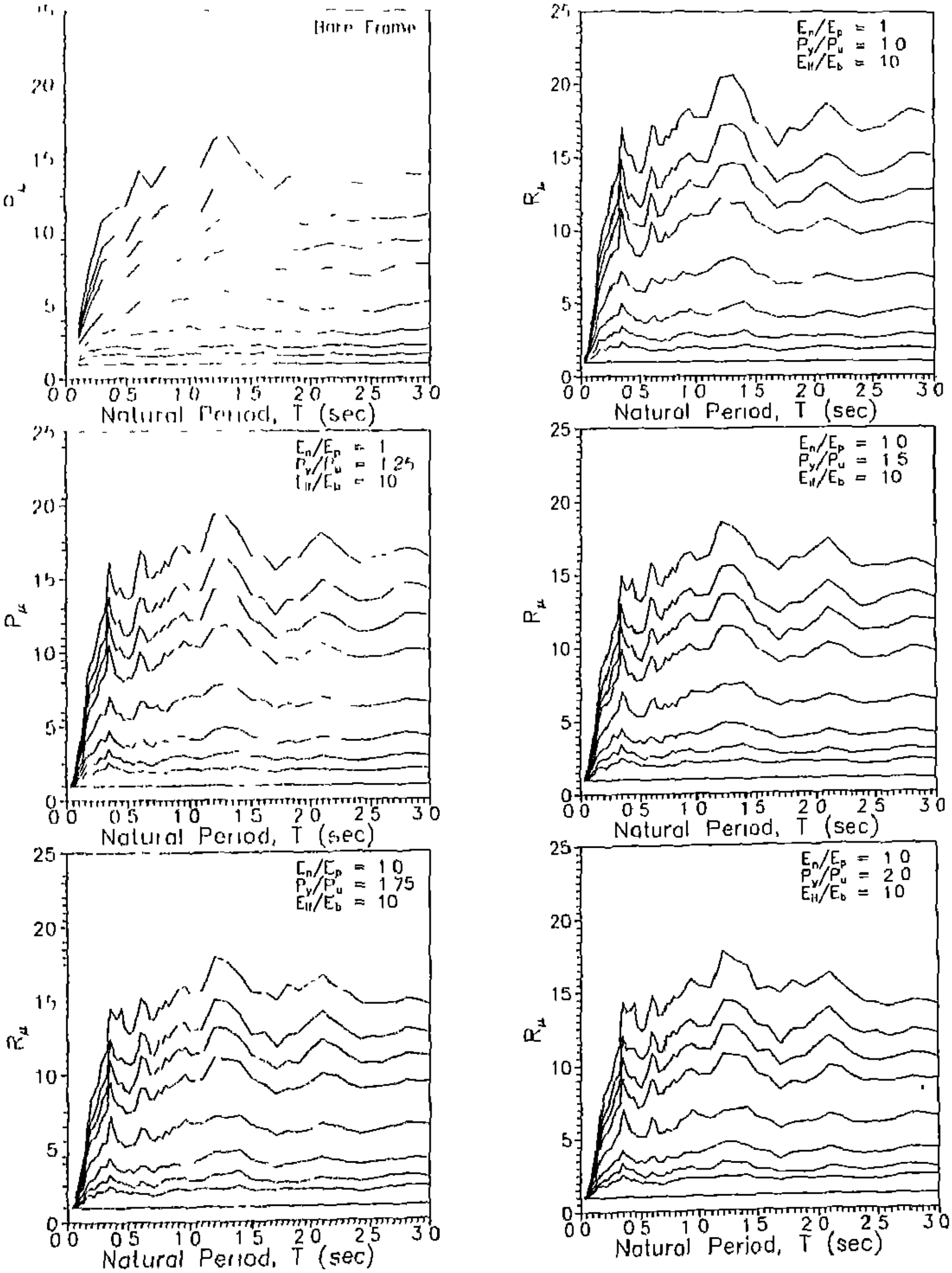

Figure 4.11 : Mean DRF spectra of Uttarkashi earthquake strong motion records, for URM RC infilled frame with stiffness ratio, $\mathcal{K}$ (=E_{if}/E_b)=10, and slope ratio, η (=E_n/E_p)=1, *for different* values of strength ratio, σ (=P_y/P_u). Mean DRF spectra of bare frame also shown

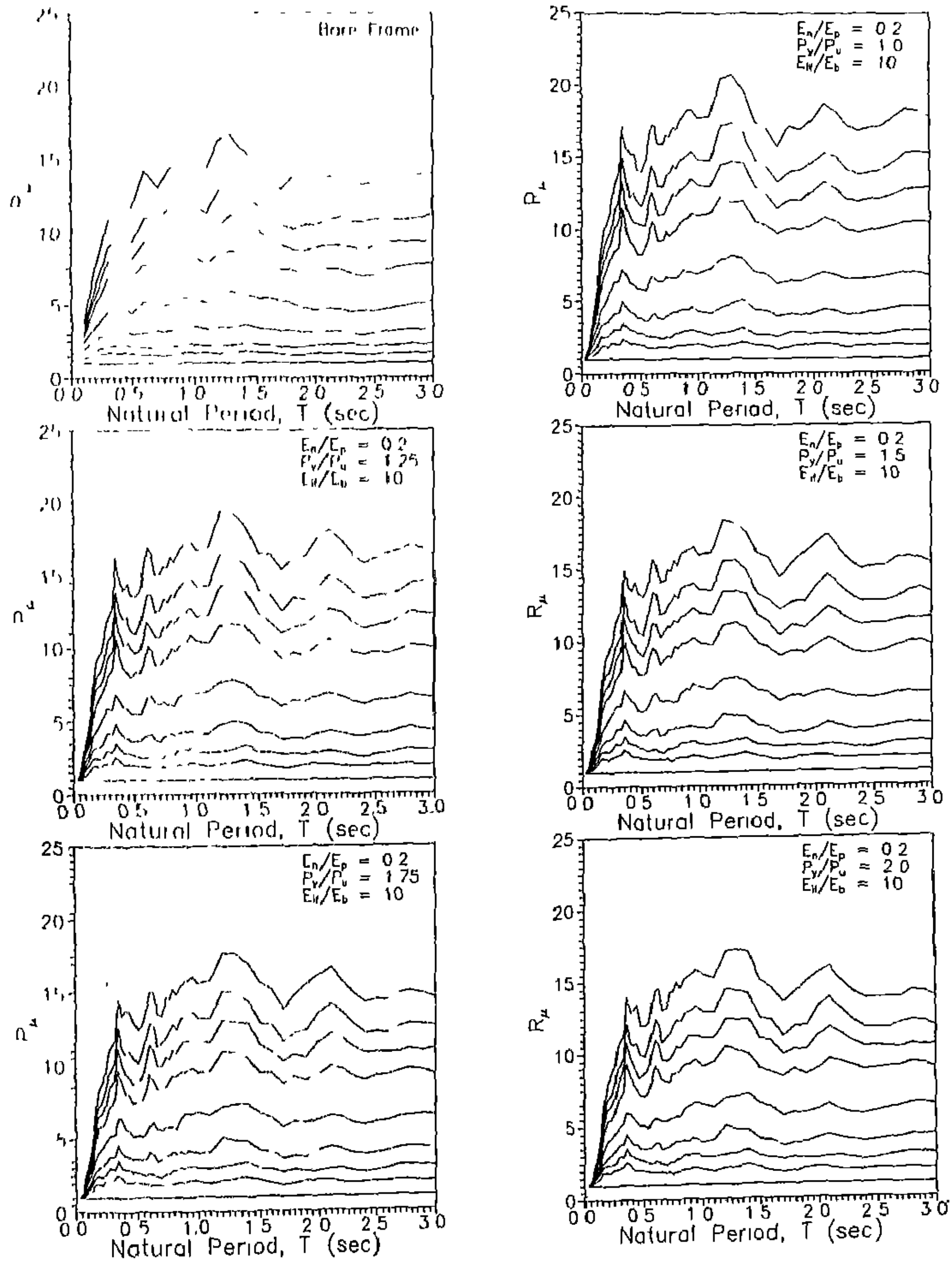

Figure 4.12 : Mean DRF spectra of Uttarkashi earthquake strong motion records, for URM RC infilled frame with stiffness ratio, $\mathcal{K}$ $(=E_{if}/E_b)=10$, and slope ratio, η $(=E_n/E_p)=0.2$, for different values of strength ratio, σ $(=P_y/P_u)$. Mean DRF spectra of bare frame also shown.

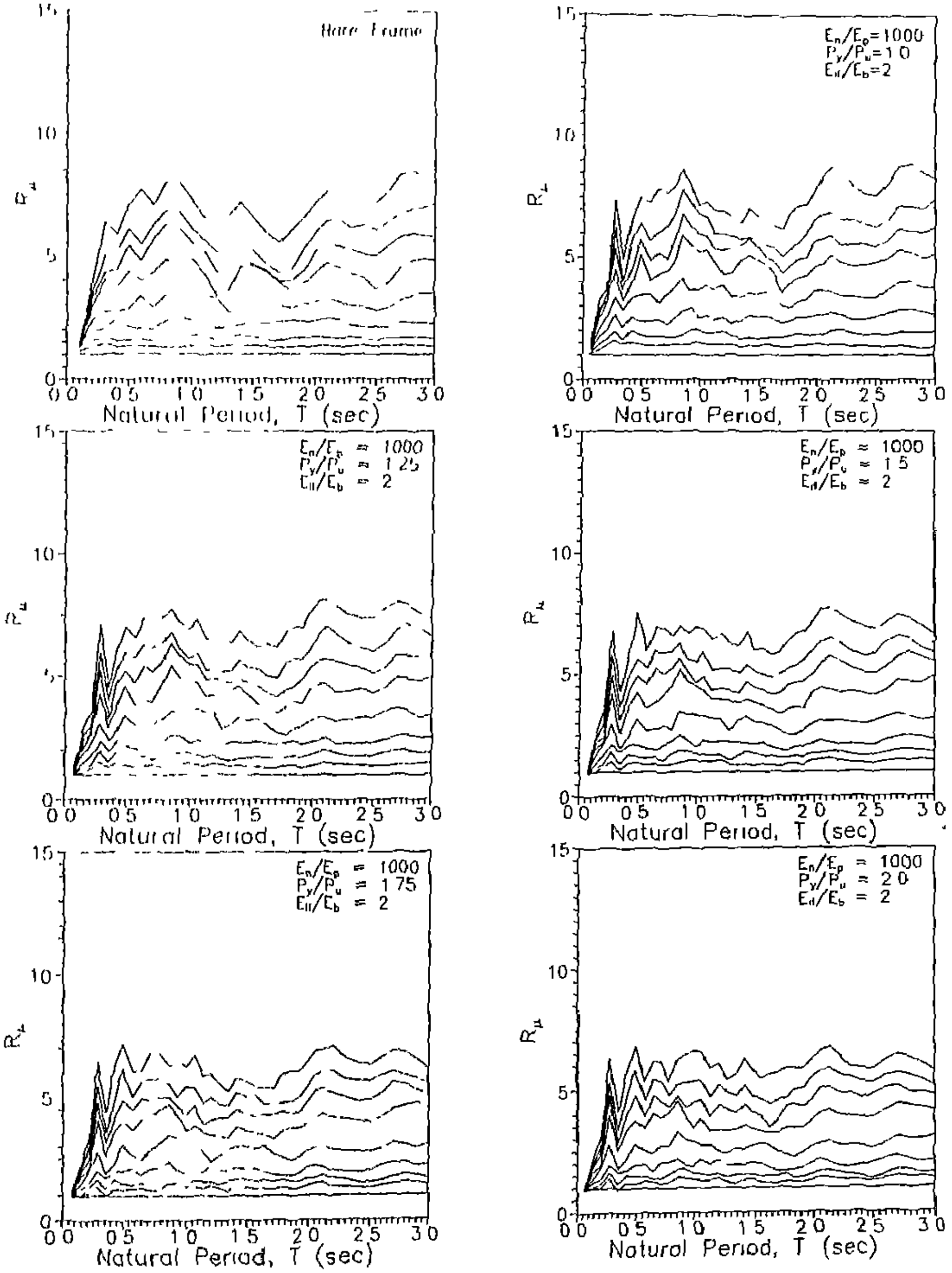

Figure 4.13 : Mean-minus-one standard deviation DRF spectra of Uttarkashi earthquake strong motion records, for URM RC infilled frame with stiffness ratio, $\mathcal{K}$ (=E_{if}/E_b)=2, and slope ratio, η (=E_n/E_p)=1000, for different values of strength ratio, σ (=P_y/P_u). Mean DRF spectra of bare frame also shown.

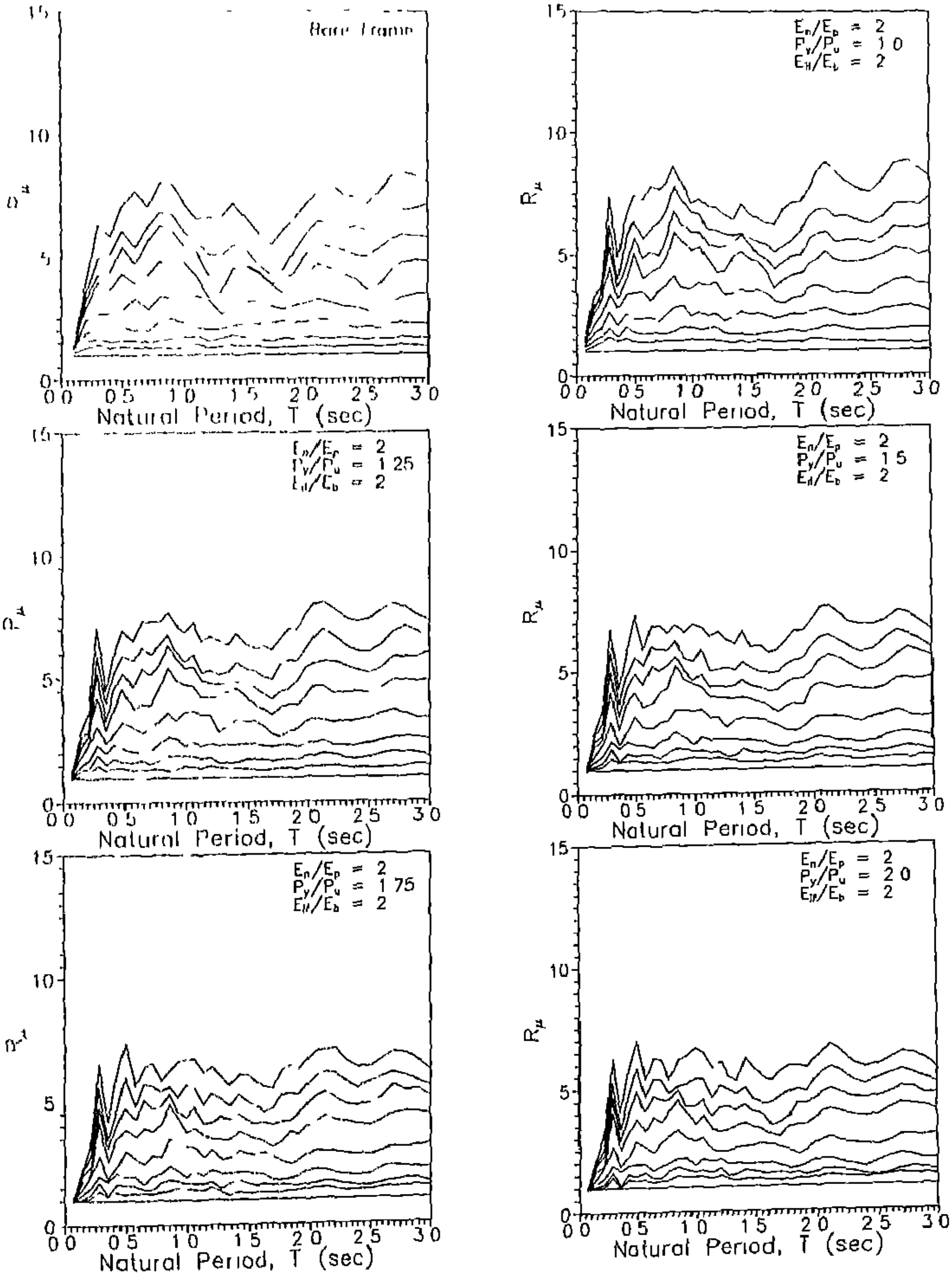

Figure 4.14 : Mean-minus-one standard deviation DRF spectra of Uttarkashi earthquake strong motion records, for URM RC infilled frame with stiffness ratio, $\mathcal{K}$ $(=E_{if}/E_b)=2$, and slope ratio, η $(=E_n/E_p)=2$, *for* different values of strength ratio, σ $(=P_y/P_u)$. Mean DRF spectra of bare frame also shown.

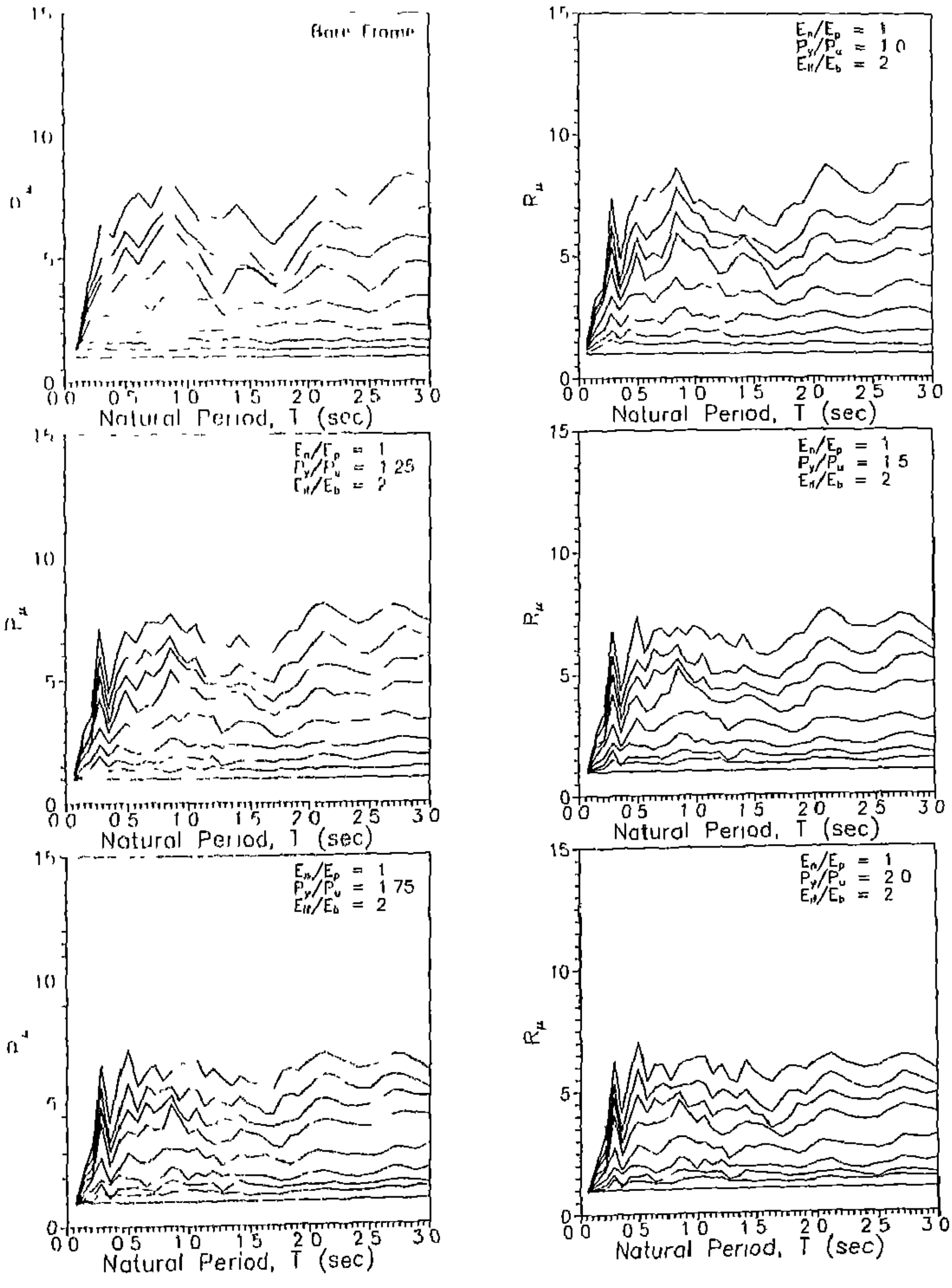

Figure 4.15 : Mean-minus-one standard deviation DRF spectra of Uttarkashi earthquake strong motion records, for URM RC infilled frame with stiffness ratio, $\mathcal{K}$ $(=E_{if}/E_b)=2$, and slope ratio, η $(=E_n/E_p)=1$, for different values of strength ratio, σ $(=P_y/P_u)$. Mean DRF spectra of bare frame also shown.

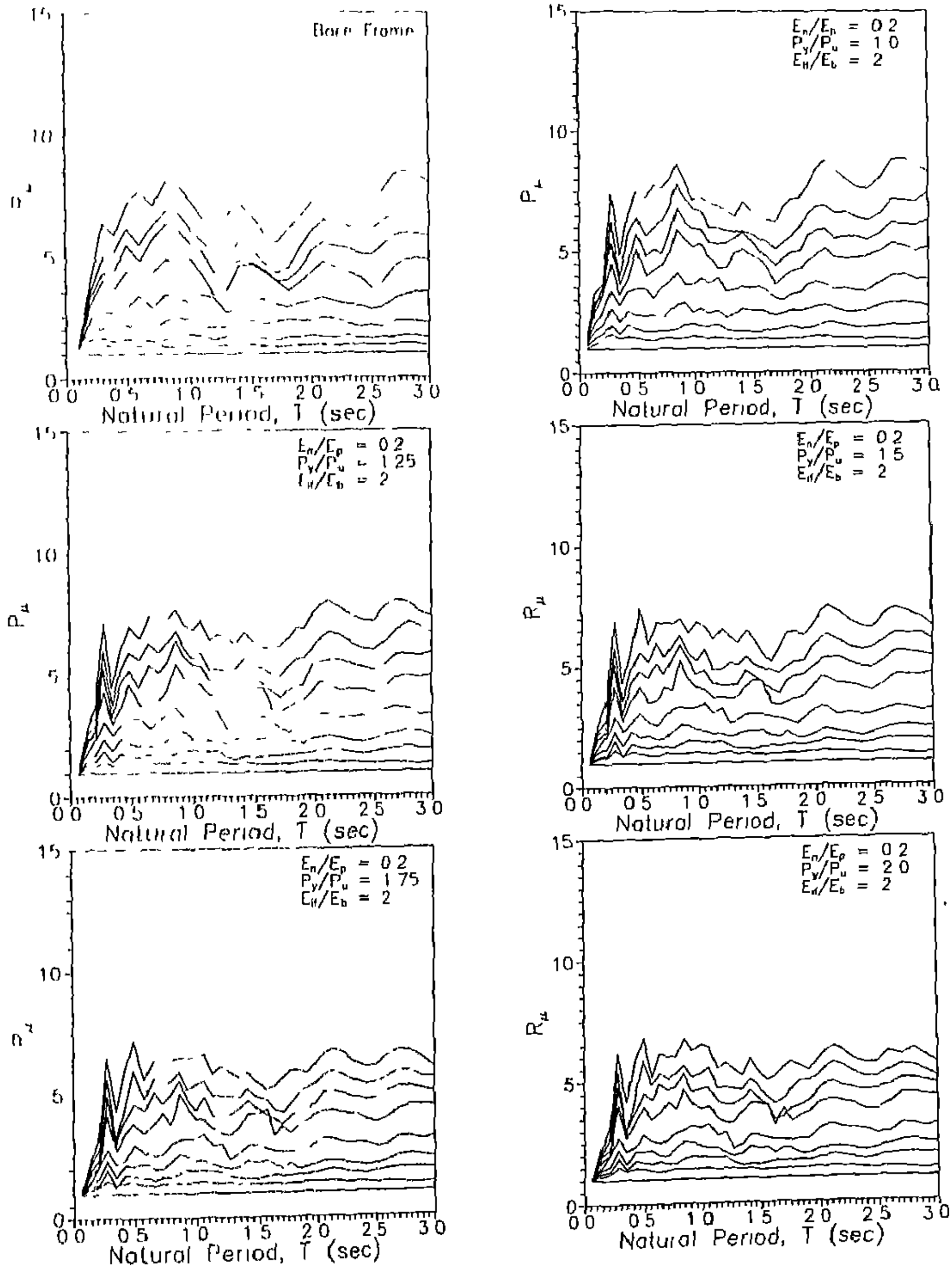

Figure 4.16 : Mean-minus-one standard deviation DRF spectra of Uttarkashi earthquake strong motion records, for URM RC infilled frame with stiffness ratio, K $(=E_{if}/E_b)=2$, and slope ratio, η $(=E_n/E_p)=0.2$, for different values of strength ratio, σ $(=P_y/P_u)$. Mean DRF spectra of bare frame also shown.

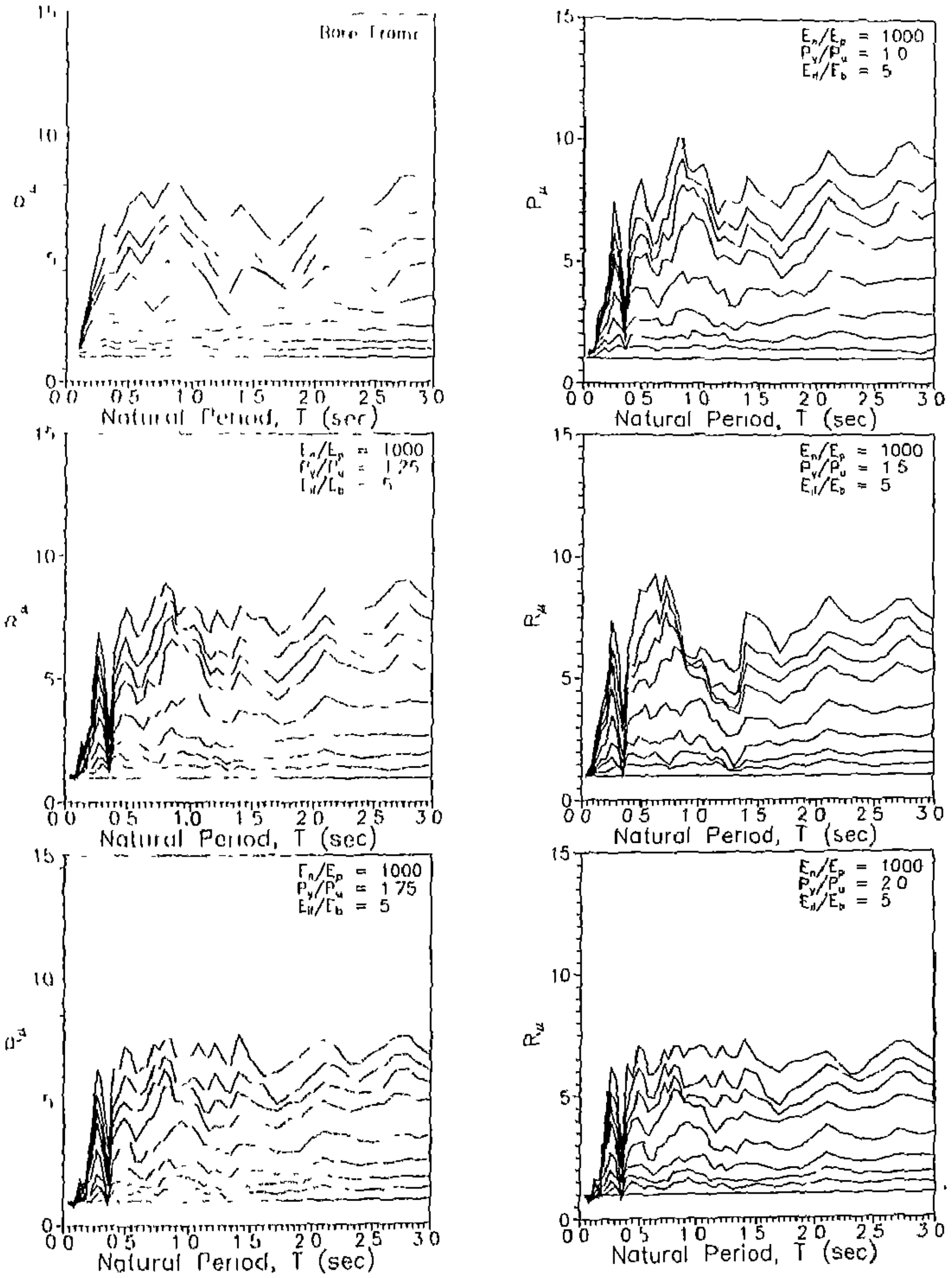

Figure 4.17 : Mean-minus-one standard deviation DRF spectra of Uttarkashi earthquake strong motion records, for URM RC infilled frame with stiffness ratio, κ (=E_{if}/E_b)=5, and slope ratio, η (=E_n/E_p)=1000, for different values of strength ratio, σ (=P_y/P_u). Mean DRF spectra of bare frame also shown.

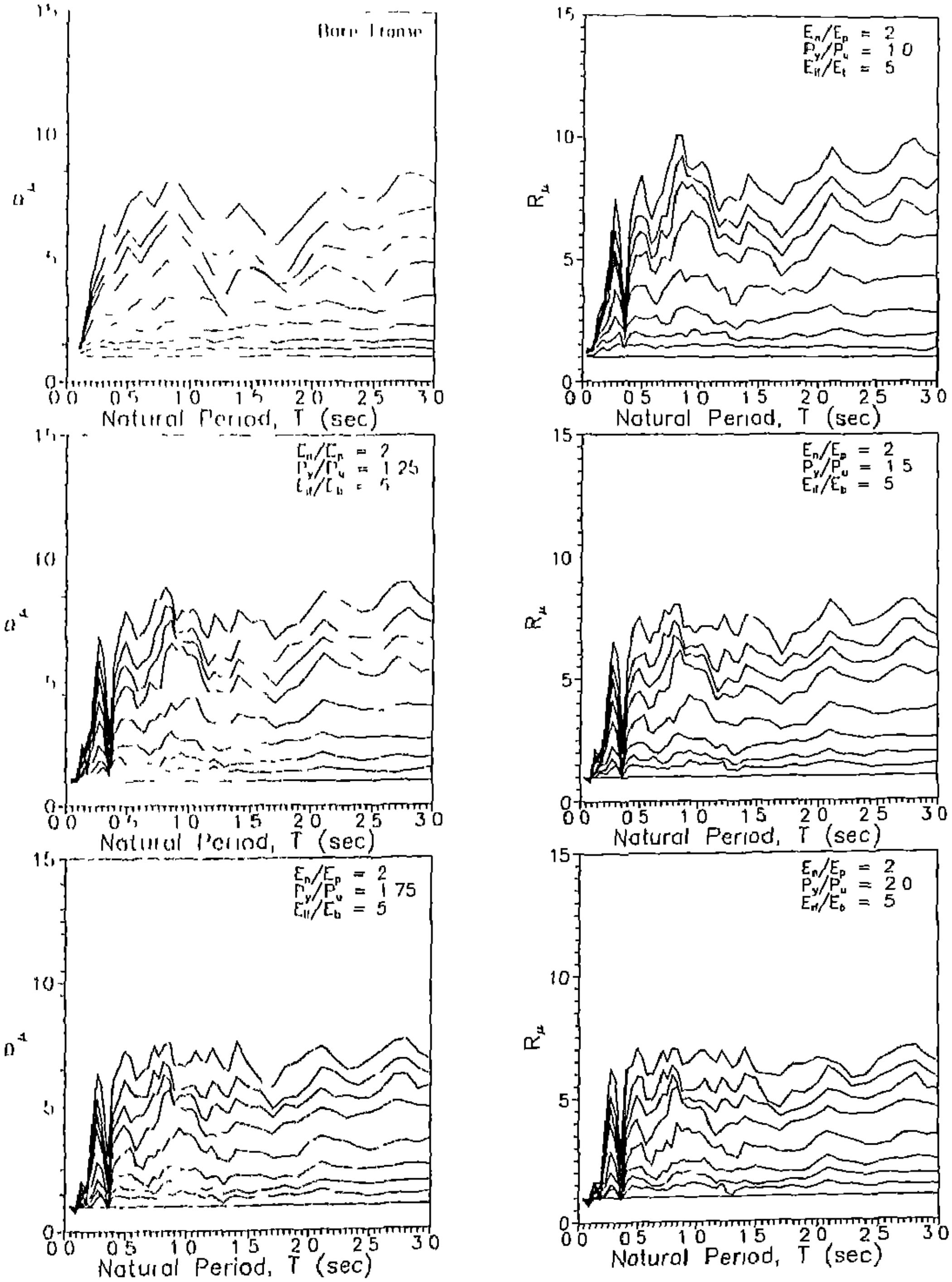

Figure 4.18 : Mean-minus-one standard deviation DRF spectra of Uttarkashi earthquake strong motion records, for URM RC infilled frame with stiffness ratio, $\mathcal{K}$ $(=E_{if}/E_b)=5$, and slope ratio, η $(=E_n/E_p)=2$, for different values of strength ratio, σ $(=P_y/P_u)$. Mean DRF spectra of bare frame also shown.

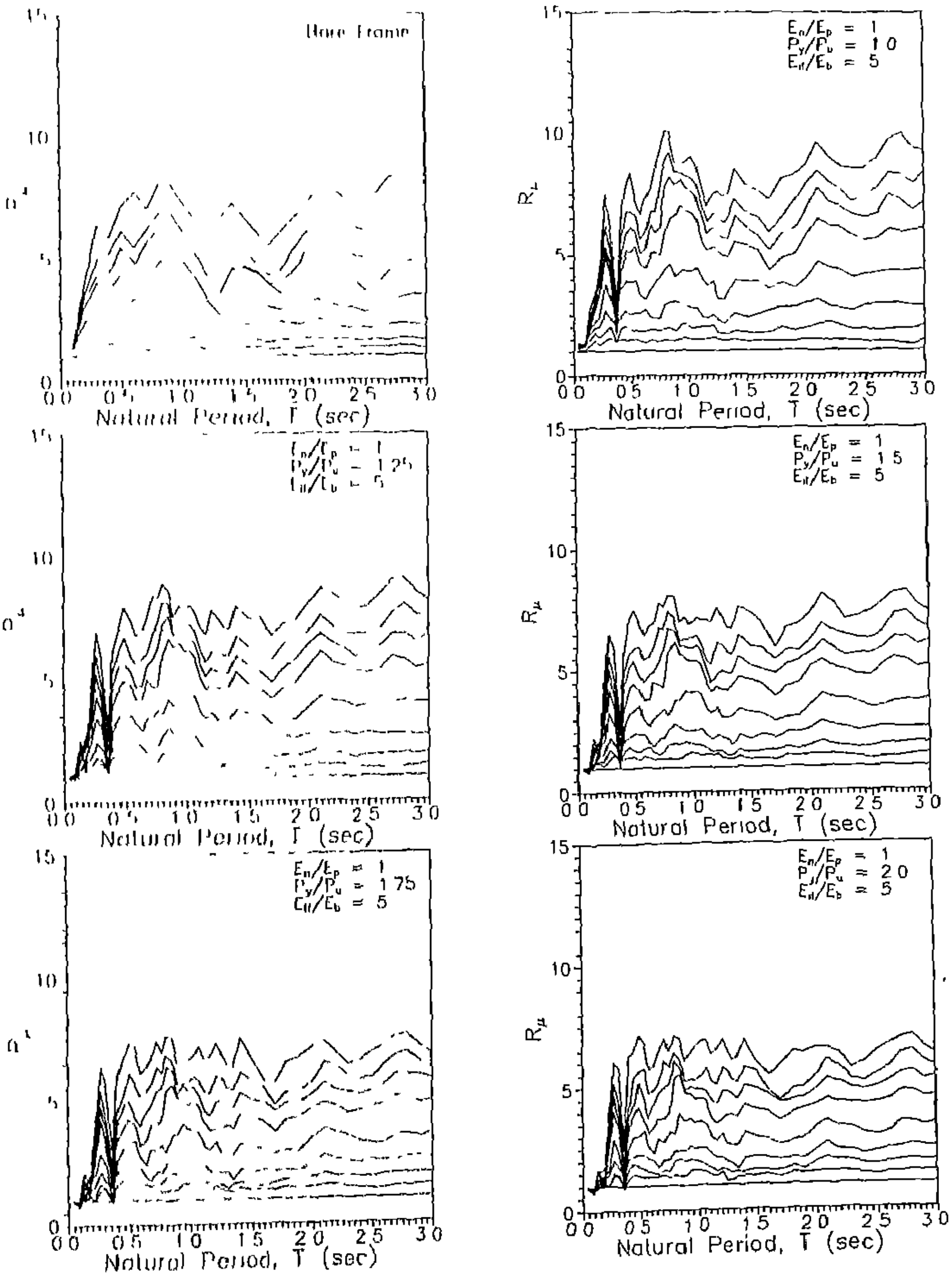

Figure 4.19 : Mean-minus-one standard deviation DRF spectra of Uttarkashi earthquake strong motion records, for URM RC infilled frame with stiffness ratio, $\mathcal{K}$ $(=E_{if}/E_b)=5$, and slope ratio, η $(=E_n/E_p)=1$, for different values of strength ratio, σ $(=P_y/P_u)$. Mean DRF spectra of bare frame also shown.

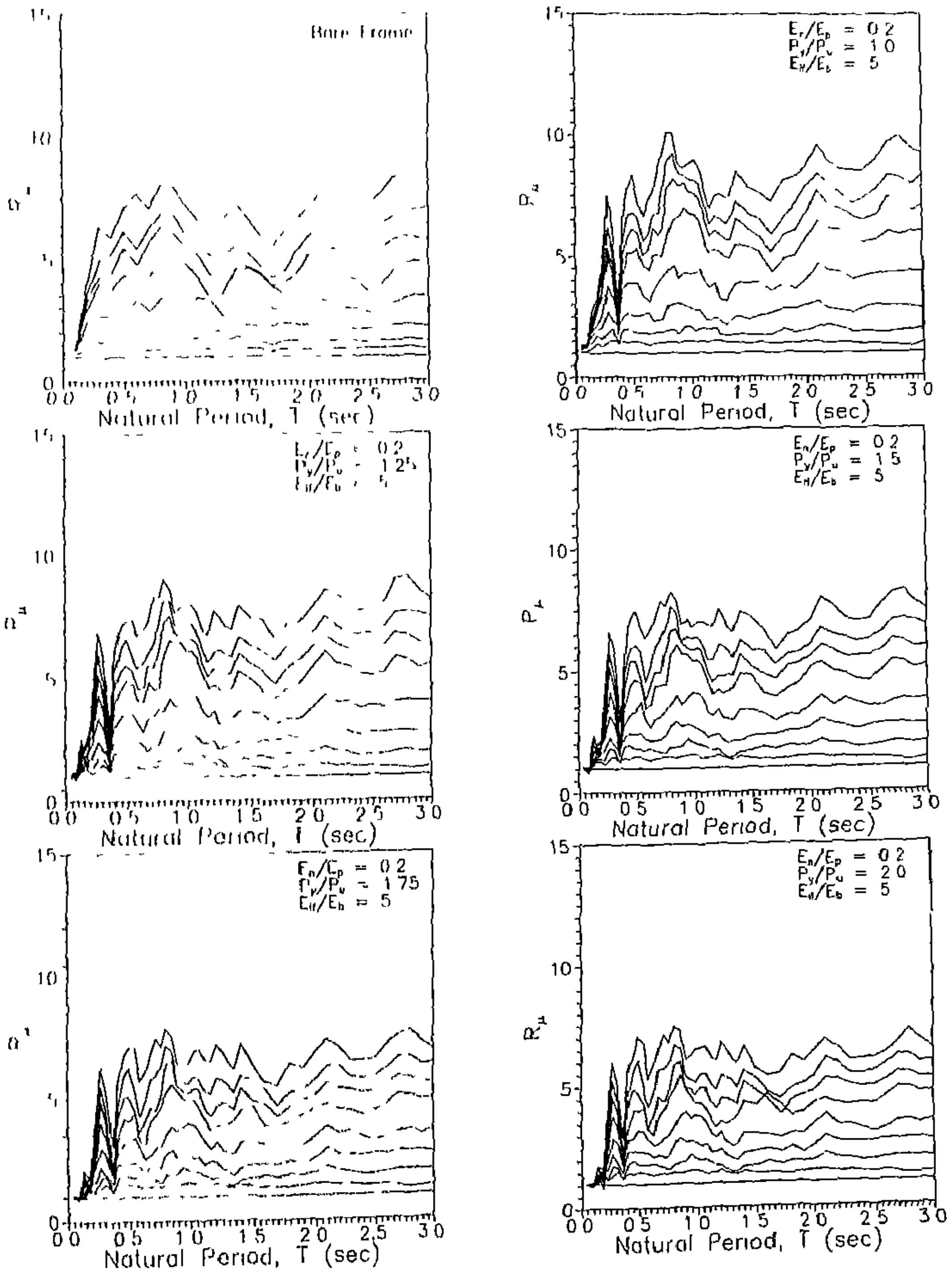

Figure 4.20 : Mean-minus-one standard deviation DRF spectra of Uttarkashi earthquake strong motion records, for URM RC infilled frame with stiffness ratio, $\mathcal{K}$ $(=E_{if}/E_b)=5$, and slope ratio, η $(=E_n/E_p)=0.2$, for different values of strength ratio, σ $(=P_y/P_u)$. Mean DRF spectra of bare frame also shown.

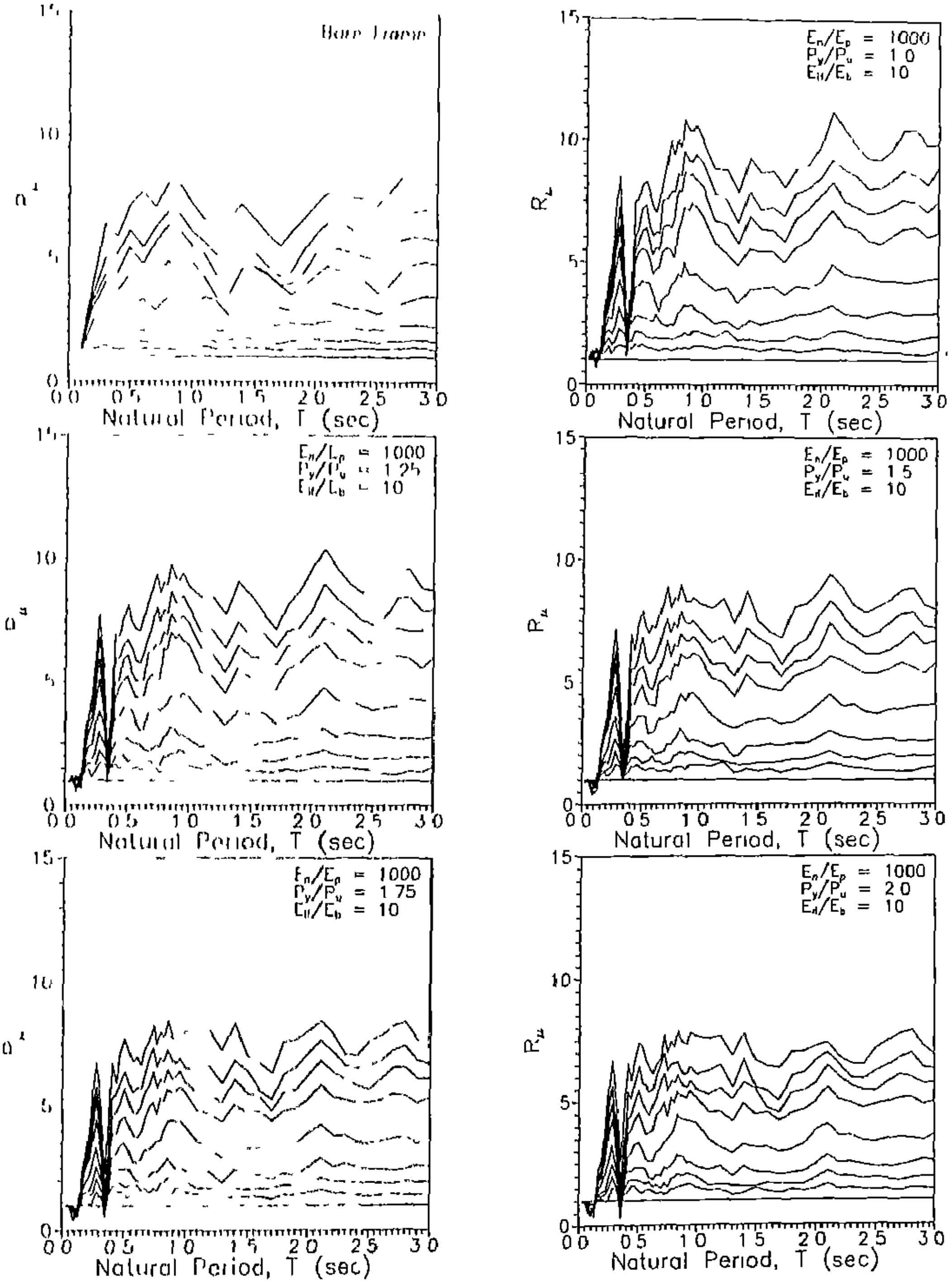

Figure 4.21 : Mean-minus-one standard deviation DRF spectra of Uttarkashi earthquake strong motion records, for URM RC infilled frame with stiffness ratio, $\mathcal{K}$ ($=E_{if}/E_b$)=10, and slope ratio, η ($=E_n/E_p$)=1000, for different values of strength ratio, σ ($=P_y/P_u$). Mean DRF spectra of bare frame also shown.

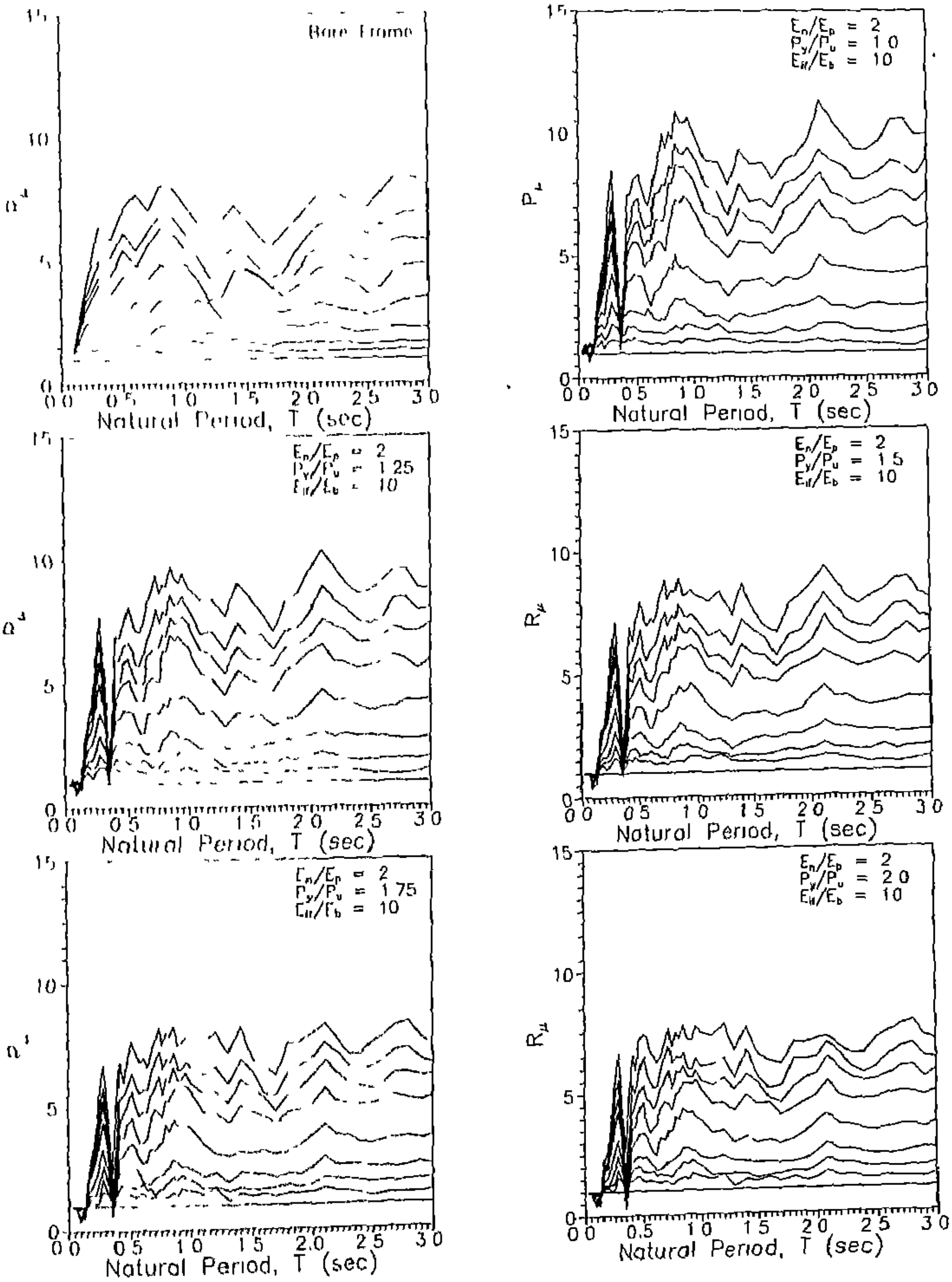

Figure 4.22 : Mean-minus-one standard deviation DRF spectra of Uttarkashi earthquake strong motion records, for URM RC infilled frame with stiffness ratio, $\mathcal{K}$ $(=E_{if}/E_b)=10$, and slope ratio, η $(=E_n/E_p)=2$, for different values of strength ratio, σ $(=P_y/P_u)$. Mean DRF spectra of bare frame also shown.

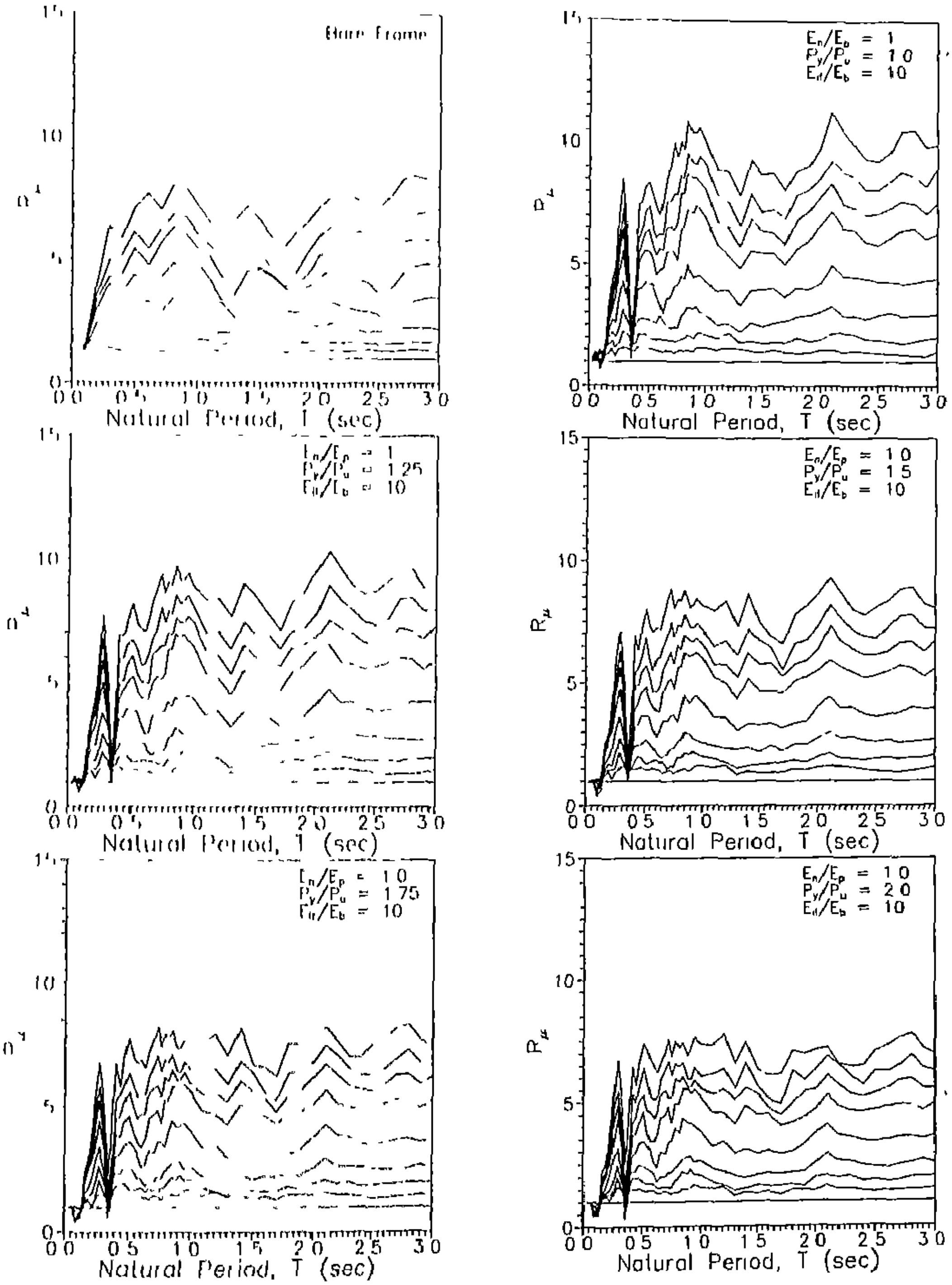

Figure 4.23 : Mean-minus-one standard deviation DRF spectra of Uttarkashi earthquake strong motion records, for URM RC infilled frame with stiffness ratio, K (=E_{if}/E_b)=10; and slope ratio, η (=E_n/E_p)=1, for different values of strength ratio, σ (=P_y/P_u). Mean DRF spectra of bare frame also shown.

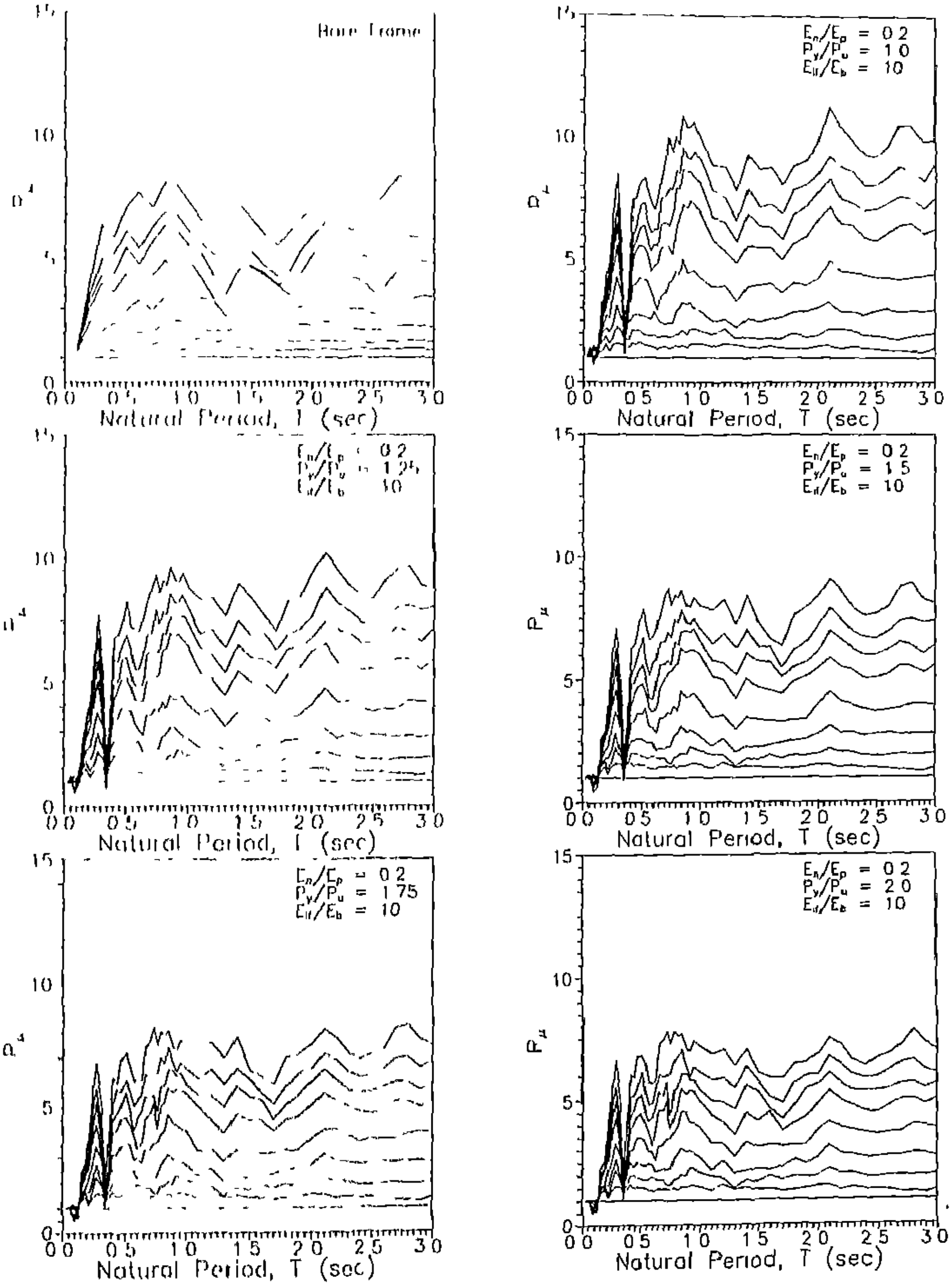

Figure 4.24 : Mean-minus-one standard deviation DRF spectra of Uttarkashi earthquake strong motion records, for URM RC infilled frame with stiffness ratio, $\mathcal{K}$ (=E_{1f}/E_b)=10, and slope ratio, η (=E_n/E_p)=0.2, for different values of strength ratio, σ (=P_y/P_u). Mean DRF spectra of bare frame also shown.

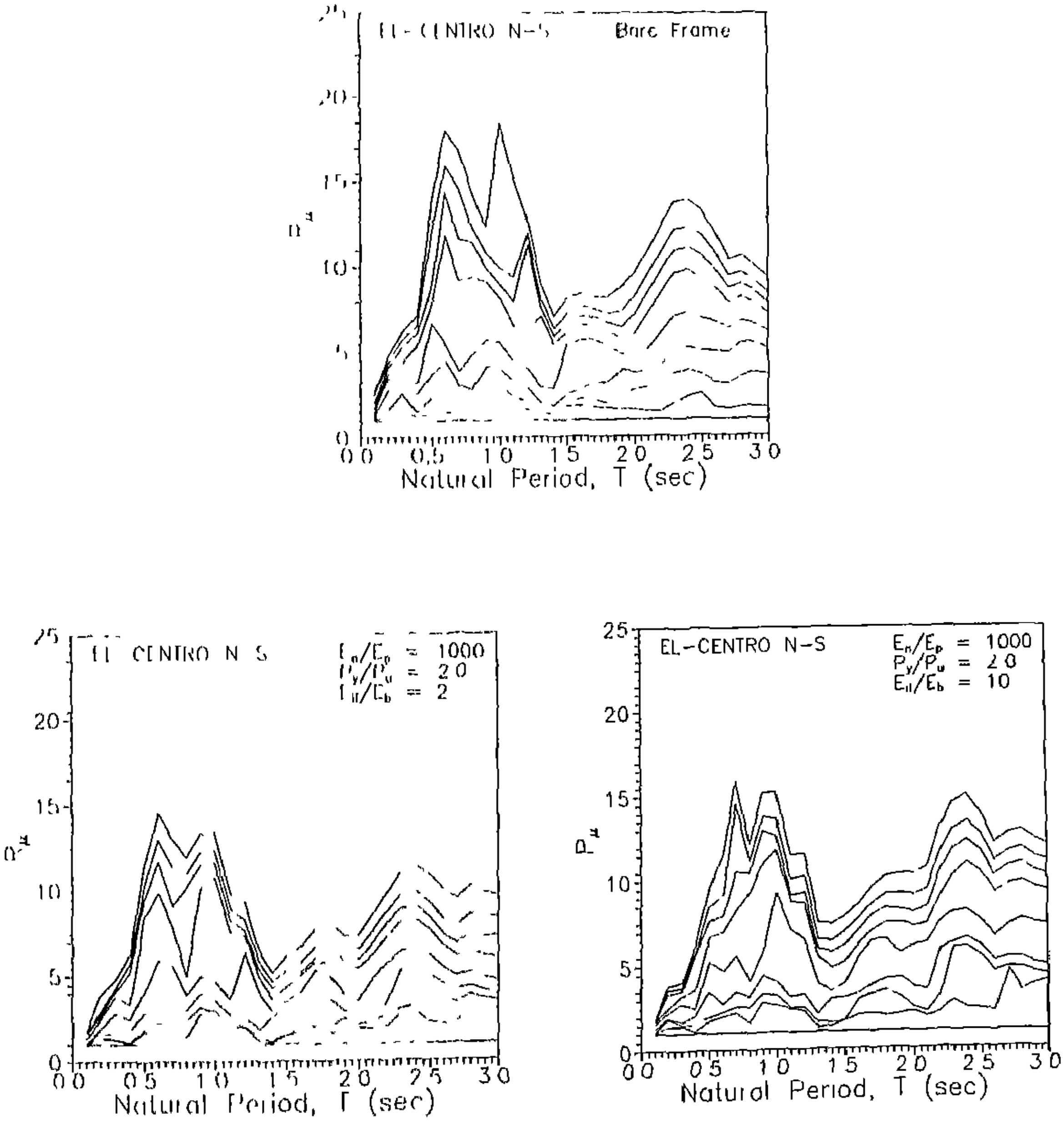

Figure 4.25 : DRF spectra of EL Centro Strong Ground Motion.

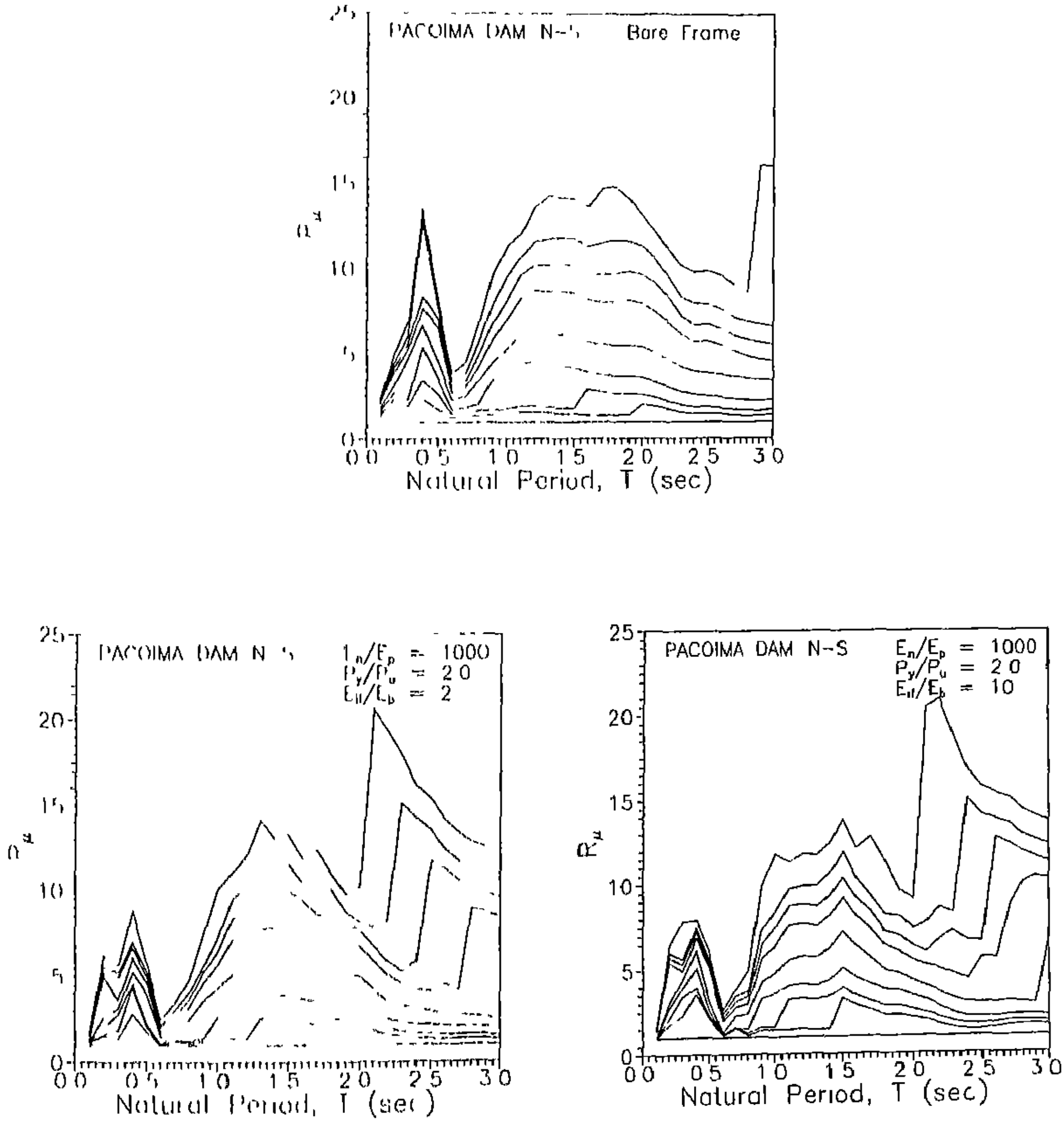

Figure 4.26 : DRF spectra of Pacoima Dam Strong Ground Motion..

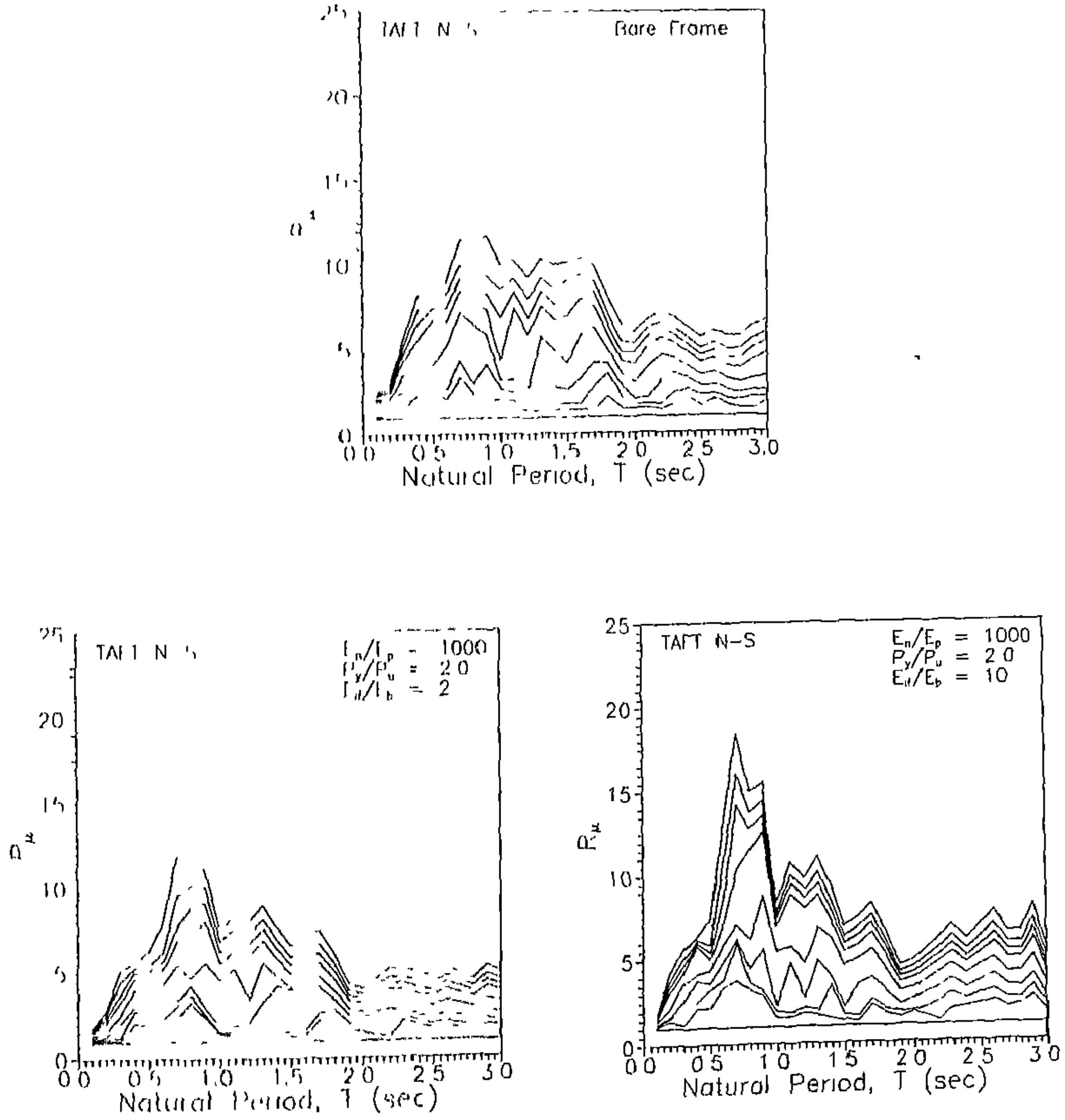

Figure 4.27 : DRF spectra of Taft Strong Ground Motion.

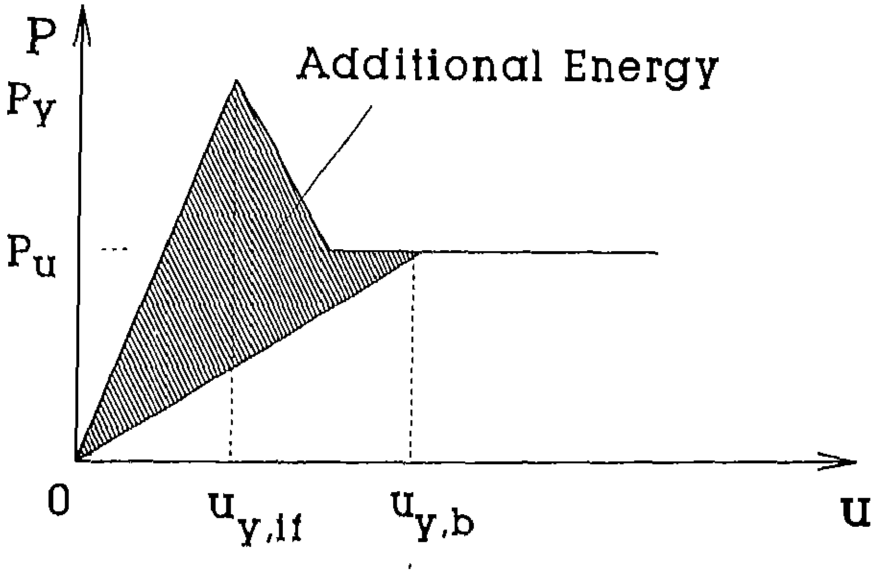

Figure 4.28 : Additional energy dissipated in a URM RC infilled frame from monotonic considerations.

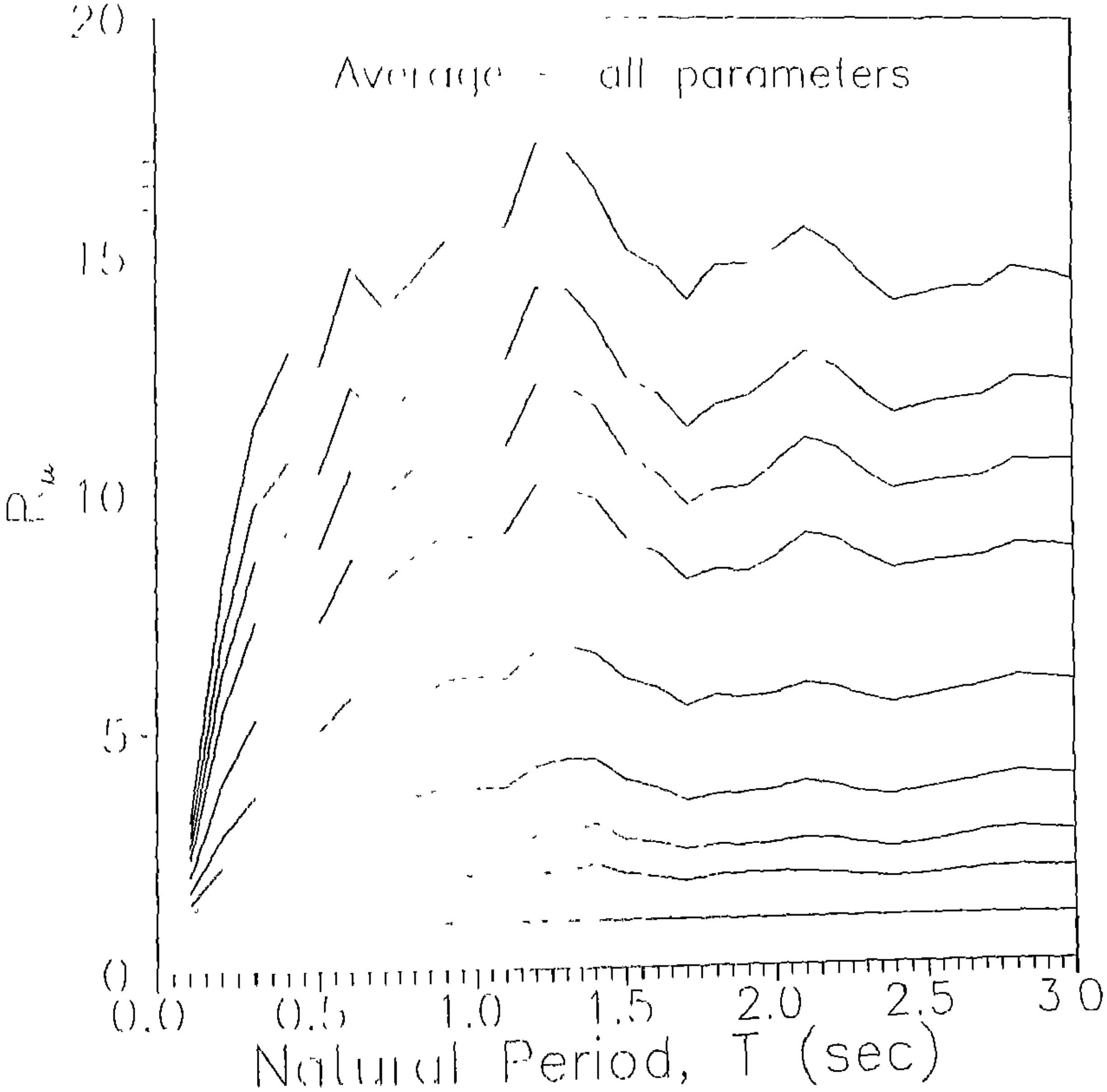

Figure 4.29 : Proposed design DRF spectra for the Himalayan region.

CHAPTER 5

SUMMARY AND CONCLUSIONS

5.1 SUMMARY OF THE STUDY

This thesis attempts to provide a better understanding of the seismic behaviour of unreinforced masonry filled reinforced concrete moment resisting frames The salient contributions of this thesis are summarized below .

(1) The various experimental and analytical studies reported in the literature on RC frames with infills are critically examined. Critical parameters that influence the infill frame behaviour are identified.

(2) A constitutive model is proposed for the hysteretic response of masonry infilled frames. This model, namely the Trilinear Hysteresis Model, incorporates the stiffness and strength contributions of the masonry infill to the overall response of the frame. It also incorporates stiffness deterioration in a limited sense. The simple hysteresis rules on which the model is based are listed. In this thesis, for the first time, the cyclic constitutive modelling of infill frames has been attempted.

(3) A parametric study is conducted to study the effect of various critical parameters on the hysteretic response of masonry infilled frames to seismic excitation. The inelastic response spectra, and from those the ductility reduction factor spectra, are obtained. The results of the parametric study are carefully examined

(4) The implications of the results of this study on the seismic design of RC MRFs with masonry infills are also discussed

(5) Design spectra for the Himalayan region are proposed as the average spectra for all the parameters taken together.

5.2 CONCLUSIONS

The following are the major conclusions of this thesis

(1) The slope ratio η does not have any significant affect on the shape and values of the DRF spectra.

(2) The strength ratio σ also does not seem to significantly influence the DRF spectra.

(3) The stiffness ratio, K, seems to significantly affect the shape and the values of the DRF spectra.

(4) With increase in the stiffness ratio, K, the DRF for infill frames curves for different ductility values converge to a value of unity, at non-zero values of the natural period.

(5) With increase in the K, the mean-minus-one standard deviation curves show a sharp V-notch in the intermediate natural period range, around a value of 0.3-0.4 secs.

(6) It is noticed that the mean-minus-one standard deviation curves show a value less than unity for the short period range.

(7) The DRF spectra for higher values of ductility exhibit a higher standard deviation.

(8) The DRF spectra from ground motions with different spectral characteristics, show the same overall trends. However, the actual

shapes of the spectra are highly sensitive to the ground motions

The following design implications are drawn from the study :

(1) The design provisions are inadequate for short buildings, *i.e.*, buildings with a low natural period value

(2) For infilled frames with high stiffness ratios, the DRF can be slightly increased over that of the corresponding bare frames

(3) The presence of the infill reduces the ductility demand on the frame members.

(4) The initial stiffness of the infill frame buildings governs its overall response, even after the masonry is damaged.

5.3 RECOMMENDATIONS FOR FUTURE WORK

Based upon the conclusions of this work, the following recommendations are made for possible future work in this area .

(1) The basic Trilinear Hysteresis Model proposed in this thesis may be refined to include slip, relaxation, strain-hardening and stiffness deterioration in infilled frames.

(2) Extensive experimental investigations are needed to be carried out to better quantify the stiffness and strength contributions of the URM infills in RC MRFs. Such an exercise is urgently needed to ease the current problems in the analytical modelling of the infilled frames.

(3) The mean and mean-minus-one standard deviation DRF spectra can be further validated by considering more data of the available ground

motions, to arrive at more reliable DRF spectra.

(4) Infilled frame buildings whose natural periods are in the intermediate range, need to be studied in greater details

(5) The Trilinear Hysteresis Model proposed in this study may be used to obtain the time history responses of infilled frames. However, proper quantification of relevant parameters through experiments is needed to render these time history analyses reliable

LIST OF REFERENCES

ATC 3-06, (1978), *Tentative Provisions for the Development of Seismic Regulations*, Applied Technology Council, Palo Alto, CA, USA

Adham,S.A., (1994), "Impact of Infilled Masonry Walls on the Response of Buildings in Moderate Seismic Zones", Proceedings from the NCEER Workshop on Seismic Response of Masonry Infills, **Report No. NCEER-94-0004**, San Francisco, CA, USA.

Ali,S., and Page,A.W., (1987), "Nonlinear Finite Element Analysis of Masonry Subjected to Concentrated Loads", **Proceedings of the Institution of Civil Engineers**, Part 2, Vol.82, pp 815-832.

Altin,S., Ersoy,U., and Tankut,T., (1992), "Hysteretic Response of Reinforced-Concrete Infilled Frames", **Journal of Structural Engineering, ASCE**, Vol.118, No.8, pp 2133-2150.

Bertero,V.V., (1986), "Lessons Learned from Recent Earthquakes and Research and Implications for Earthquake-Resistant Design of Building Structures in the United States", **Earthquake Spectra**, Vol 2, No.4, pp 825-858.

Bhandari,N.M., and Trikha,D.N., (1988), "Analysis of Masonry Buildings Using Proposed Super Masonry Element", **Masonry International**, Vol.2, No.1, pp 30-34.

Brokken,S.T., and Bertero,V.V., (1981), "Studies on Effects of Infills in Seismic Resistant R/C Construction", **Report No. UCB/EERC-81/12**, Earthquake Engineering Research Center, University of California, Berkeley, CA, USA.

Chandak,N.N., and Jain,S.K., (1994), "A Study of Strong Motion Accelerograms from Indian Earthquakes", **Research Report**, Department of Civil Engineering, Indian Institute of Technology, Kanpur.

Chandrasekaran,A.R. and Das,J.D., (1992) "Analysis of Strong Motion Accelerograms of Uttarkashi Earthquake of October 20, 1991," **Bulletin of the Indian Society of Earthquake Technology**, Vol.29, No.1, pp 35-55.

Choubey,U.B., (1990), "Behaviour of Infilled Frames Under Cyclic Loads", **Ph.D. Thesis**, Department of Civil Engineering, Indian Institute of Technology, Delhi.

Chrysostomou,C.Z., Gergely,P., and Abel,J.F., (1992), "Nonlinear Seismic Response of Infilled Steel Frames", **Proceedings of the Tenth World Conference on Earthquake Engineering**, Madrid, Spain, Vol.6, pp 4435-4442.

Dhanasekar,M, and Page,A W., (1986), "The Influence of Brick Masonry Infill Properties on the Behaviour of Infilled Frames", **Proceedings of the Institution of Civil Engineers**, Part 2, Vol.81, pp 593-605.

Flanagan,R.D., Tenbus,M A., and Bennett,R.M., (1994), "Numerical Modelling of Clay Tile Infills", Proceedings from the NCEER Workshop on Seismic Response of Masonry Infills, **Report No. NCEER-94-0004**, San Francisco, CA, USA

Gergely,P., White,R.N., and Mosalam,K.M., (1994), "Evaluation and Modelling of Infilled Frames", Proceedings from the NCEER Workshop on Seismic Response of Masonry Infills, **Report No. NCEER-94-0004**, San Francisco, CA, USA.

Girish,K.B., Achyutha,H., and Radhakrishnan,R., (1992), "Hysteretic and Dynamic Characteristics of Infilled Frames", **Proceedings of the Fourth International Seminar on Structural Masonry for Developing Countries**, Madras, pp 143-149.

Grimm,C T, (1975), "Strength and Related Properties of Brick Masonry", **Journal of the Structural Division, ASCE**, Vol.107, No.1, pp 217-232.

Gupta,A.K., (1990), *Response Spectrum Method in Seismic Analysis and Design of Structures*, Blackwell Scientific Publications

Hudson,D.E., Trifunac,M.D., and Brady,A.G., (1969-1976), "Analysis of Strong-Motion Accelerograms", Vols. I-IV, **Report No. EERL 76-02**, Earthquake Engineering Research Laboratory, California Institute of Technology, Pasadena, CA, USA.

Jagadish,R., Achyutha,H., and Rao,P.S., (1992), "Behaviour of Reinforced Concrete Brick Masonry Infilled Frames with Stiffened Window Opening", **Proceedings of the Fourth International Seminar on Structural Masonry for Developing Countries**, Madras, pp 143-149.

Jain,S.K., and Das,S., (1993), "Analysis of Strong Motion Records from Uttarkashi Earthquake for Assessment of Code Provisions for Different Seismic Zones", **Earthquake Spectra**, Vol.9, No.4, pp 739-754.

Jain,S.K., Saraf,V.K., and Mehrotra,B , (1995), "Experimental Evaluation of Fundamental period of R.C. Frame Buildings with Brick Infills", **Journal of Structural Engineering**, SERC, Madras, Vol.22, No 2 (in press).

Jayakumar,P., (1987), "Modelling and Identification in Structural Dynamics", **Report No. EERL 87-01**, Earthquake Engineering Research Laboratory, California Institute of Technology, Pasadena, CA, USA

King,G.J.W., and Pandey,P C., (1978), "The Analysis of Infilled Frames Using Finite Elements", **Proceedings of the Institution of Civil Engineers**, Part 2, Vol.65, pp 749-760.

Klinger,R.E., and Bertero,V.V , (1976), "Infilled Frames in Earthquake Resistant Construction", **Report No. EERC 76/32**, Earthquake Engineering Research Center, University of California, Berkeley, CA, USA.

Kwan,K.H , Lo,C Q , and Liauw,T.C., (1990), "Large-scale Model Tests and Plastic Analysis of Multibay Infilled Frames", **Proceedings of the Institution of Civil Engineers**, Part 2, Vol.89, pp 261-277

Lai,S.P , and Biggs,J.M., (1980), "Inelastic Response Spectra for Aseismic Building Design", **Journal of the Structural Division, ASCE**, Vol.106, No.ST6, pp 1295-1310.

Liauw,T.C., (1972), "An Approximate Method of Analysis of Infilled Frames With or Without Opening", **Building Science**, Vol.7, pp 233-238.

Liauw,T.C., (1979), "Tests on Multistorey Infilled Frames Subjected to Dynamic Loading", **Journal of the American Concrete Institute**, Title No. 76-26, pp 551-563.

Liauw,T.C., and Kwan,K.H., (1982), "Non-linear Analysis of Multistorey Infilled Frames", **Proceedings of the Institution of Civil Engineers**, Part 2, Vol.73, pp 441-454.

Liauw,T C., and Kwan,K.H., (1984), "Plastic Design of Infilled Frames", **Proceedings of the Institution of Civil Engineers**, Part 2, Vol.77, pp 367-377.

Liauw,T.C., and Lee,S.W., (1977), "On the Behaviour and the Analysis of Multi-storey Infilled Frames Subject to Lateral Loading", **Proceedings of the Institution of Civil Engineers**, Part 2, Vol.63, pp 641-656.

Liauw,T.C., and Lo,C.Q., (1988), "On Multibay Infilled Frames", **Proceedings of the Institution of Civil Engineers**, Part 2, Vol.85, pp 469-483.

Mainstone,R.J., (1971), "On the Stiffness and Strength of Infilled Frames", **Proceedings of the Institution of Civil Engineers**, Part 2, Supplimont (iv), pp 57-90.

Mallick,D.V., and Severn,R.T., (1967), "The Behaviour of Infilled Frames Under Static Loading", **Proceedings of the Institution of Civil Engineers**, Part 2, Vol.38, pp 639-656.

Mallick,D.V., and Severn,R.T., (1968), "Dynamic Characteristics of Infilled Frames", **Proceedings of the Institution of Civil Engineers**, Part 2, Vol.39, pp 261-287

Mallick,D.V., and Garg,R.P., (1971), "Effect of Openings on the Lateral Stiffness of Infilled Frames", **Proceedings of the Institution of Civil Engineers**, Part 2, pp 195-209.

Mehrabi,A.B., and Shing,P.B., (1994), "Performance of Masonry-Infilled R/C Frames Under In-plane Lateral Loads : Analytical Modelling", Proceedings from the NCEER Workshop on Seismic Response of Masonry Infills, **Report No. NCEER-94-0004**, San Francisco, CA, USA

Murty,C.V.R., and Jain,S.K., (1994), "A Proposed Draft for IS:1893 Provisions on Seismic Design of Buildings - Part I : Code", **Journal of Structural Engineering**, SERC, Madras, Vol.22, No.1 (in press).

Newmark,N.M., and Hall,W.J., (1982), *Earthquake Spectra and Design*, Earthquake Engineering Research Institute, Berkeley, CA, USA.

Paulay,T., and Priestley,M.J.N., (1992), *Seismic Design of Reinforced Concrete and Masonry Buildings*, Wiley Interscience

Pires,F., and Carvalho,E.C., (1992), "The Behaviour of Infilled Reinforced Concrete Frames Under Horizontal Cyclic Loading", **Proceedings of the Tenth World Conference on Earthquake Engineering**, Madrid, Spain, Vol.6, pp 3419-3422.

Polyakov,S.V., (1952), "On the Strength and Deformation of Stone Masonry Filling in Framed Walls Under Shearing Loads", **Building Industry**, No.3, Moscow.

Rahman,S.S., and Reddy,G.V.B.S., (1992), "Effect of Size of Infill Panels on the Behaviour of Infilled Frames with Openings", **Proceedings of the Fourth International Seminar on Structural Masonry for Developing Countries**, Madras, pp 143-149.

Rashad,G.E., (1993), "A Ductility and Displacement Based Design Procedure for Seismic Design of Reinforced Concrete Frames", **PhD. Thesis**, Department of Civil Engineering, Indian Institute of Technology, Kanpur.

Riddell,R., Hidalgo,P., and Cruz,E., (1989), "Response Modification Factors for Eathquake Resistant Design of Short Period Buildings", **Earthquake Spectra**, Vol.5, No.3, pp 571-590.

Riddell,R., and Newmark,N.M., (1979), Statistical Analysis of the Response of Nonlinear Systems Subjected to Earthquakes, **Report No. UILU-ENG 79-2016**, Department of Civil Engineering, University of Illinois at Urbana-Champaign, Urbana, Illinois, USA.

Riddington, J.R., (1984), "The Influence of Initial Gaps on Infilled Frame Behaviour", **Proceedings of the Institution of Civil Engineers**, Part 2, Vol.77, pp 295-310.

Riddington, J.R., and Smith, B.S., (1977), "Analysis of Infilled Frames Subjected to Racking Loads with Design Recommendations", **The Structural Engineer**, Vol.155, No.6, pp 263-268.

Samarasinghe, W., and Hendry, A.W., (1982), "A Finite Element Model for the In-plane Behaviour of Brickwork", **Proceedings of the Institution of Civil Engineers**, Part 2, Vol.73, pp 171-178.

Sawko, F., and Rouf, M.A., (1984), "On the Stiffness Properties of Masonry", **Proceedings of the Institution of Civil Engineers**, Part 2, Vol.77, pp 1-12.

Schuller, M., Mehrabi, A.B., Noland, J.L., and Shing, P.B., (1994), "Performance of Masonry-Infilled R/C Frames Under In-plane Lateral Loads : Experiments", Proceedings from the NCEER Workshop on Seismic Response of Masonry Infills, **Report No. NCEER-94-0004**, San Francisco, CA, USA.

Smith, B.S., (1962), "Lateral Stiffness of Infilled Frames", **Journal of the Structural Division, ASCE**, ST6, pp 183-199.

Smith, B.S., (1966), "Behaviour of Square Infilled Frames", **Journal of the Structural Division, ASCE**, pp 381-403.

Smith, B.S., and Carter, C., (1969), "A Method of Analysis for Infilled Frames", **Proceedings of the Institution of Civil Engineers**, Part 2, Vol.44, pp 31-48.

Tomaževič, M., and Sheppard, P., (1987), "Mathematical Modelling of Masonry Buildings for Earthquake Resistance Analysis", *Engineering Aspects of Earthquake Phenomena*, Koridze, A., (Ed.), INEEC, Omega Scientific, pp 121-135.

UBC-1994, *Uniform Building Code*, International Conference of Building Officials, Whitter, CA.

Youssef, N., (1994), "The Influence of Modelling Assumptions on the Pedicted Behaviour of Unreinforced Masonry Infill Structures", Proceedings from the NCEER Workshop on Seismic Response of Masonry Infills, **Report No. NCEER-94-0004**, San Francisco, CA, USA

CE-1995-M-NAG-MOD.

A121353